



2015

# LAYERED, FLEXIBLE DRUG DELIVERY FILMS FOR THE PREVENTION OF FIBROTIC SCAR TISSUE FORMATION

Cheryl L. Rabek

University of Kentucky, [cheryl.rabek@gmail.com](mailto:cheryl.rabek@gmail.com)

## Recommended Citation

Rabek, Cheryl L., "LAYERED, FLEXIBLE DRUG DELIVERY FILMS FOR THE PREVENTION OF FIBROTIC SCAR TISSUE FORMATION" (2015). *Theses and Dissertations--Biomedical Engineering*. 31.  
[http://uknowledge.uky.edu/cbme\\_etds/31](http://uknowledge.uky.edu/cbme_etds/31)

This Doctoral Dissertation is brought to you for free and open access by the Biomedical Engineering at UKnowledge. It has been accepted for inclusion in Theses and Dissertations--Biomedical Engineering by an authorized administrator of UKnowledge. For more information, please contact [UKnowledge@lsv.uky.edu](mailto:UKnowledge@lsv.uky.edu).

## **STUDENT AGREEMENT:**

I represent that my thesis or dissertation and abstract are my original work. Proper attribution has been given to all outside sources. I understand that I am solely responsible for obtaining any needed copyright permissions. I have obtained needed written permission statement(s) from the owner(s) of each third-party copyrighted matter to be included in my work, allowing electronic distribution (if such use is not permitted by the fair use doctrine) which will be submitted to UKnowledge as Additional File.

I hereby grant to The University of Kentucky and its agents the irrevocable, non-exclusive, and royalty-free license to archive and make accessible my work in whole or in part in all forms of media, now or hereafter known. I agree that the document mentioned above may be made available immediately for worldwide access unless an embargo applies.

I retain all other ownership rights to the copyright of my work. I also retain the right to use in future works (such as articles or books) all or part of my work. I understand that I am free to register the copyright to my work.

## **REVIEW, APPROVAL AND ACCEPTANCE**

The document mentioned above has been reviewed and accepted by the student's advisor, on behalf of the advisory committee, and by the Director of Graduate Studies (DGS), on behalf of the program; we verify that this is the final, approved version of the student's thesis including all changes required by the advisory committee. The undersigned agree to abide by the statements above.

Cheryl L. Rabek, Student

Dr. David Puleo, Major Professor

Dr. Abhijit Patwardhan, Director of Graduate Studies

LAYERED, FLEXIBLE DRUG DELIVERY FILMS FOR THE  
PREVENTION OF FIBROTIC SCAR TISSUE FORMATION

---

DISSERTATION

---

A dissertation submitted in partial fulfillment of the  
requirements for the degree of Doctor of Philosophy in the  
College of Engineering  
at the University of Kentucky

By  
Cheryl Lynn Rabek

Lexington, Kentucky

Director: Dr. David Puleo, Professor of Biomedical Engineering

Lexington, Kentucky

2015

Copyright © Cheryl Lynn Rabek 2015

## ABSTRACT OF DISSERTATION

### LAYERED, FLEXIBLE DRUG DELIVERY FILMS FOR THE PREVENTION OF FIBROTIC SCAR TISSUE FORMATION

Open wounds account for about 50% of military injuries and 10% of non-fatal traffic injuries. Scar tissue formation in these wounds may be reduced or prevented if treated with a combination of molecules whose release is tuned to the healing phases. The goal of this research was to develop flexible, layered drug delivery films for sequential, localized release of anti-inflammatory, anti-oxidant, and anti-fibrotic molecules to soft tissue.

Films were composed of cellulose acetate phthalate (CAP) and Pluronic F-127 (Pluronic). To impart flexibility, plasticizers, triethyl citrate (TEC) or tributyl citrate (TBC), were added. Mechanical analysis was performed on films as prepared and following phosphate-buffered saline incubation to determine property changes after implantation. Tensile tests revealed higher plasticizer content increased film elongation but decreased elastic modulus and ultimate tensile strength. TEC films elongated twice as much as those with TBC. After incubation, properties increased because plasticizer leached from films. Micro computerized tomography and scanning electron microscopy determined how erosion and plasticizer leaching affected the film's structures before and after incubation. Porosity increased as plasticizer content increased; however, plasticizer content did not significantly affect erosion rates.

Next, effects of drugs with plasticizers on film erosion, release, and mechanical properties were investigated. Films were loaded with quercetin, an anti-oxidant, or pirfenidone, an anti-fibrotic, and plasticized with TEC or TBC. TEC-plasticized films containing quercetin released drug at a slower rate than TBC films. Pirfenidone-loaded films released drug at a faster rate than erosion occurred for both plasticizers. Increased pirfenidone loading resulted in significantly higher modulus and decreased elongation, an anti-plasticizer effect. Increasing quercetin loading significantly increased elongation. Size, solubility, and structure differences between quercetin and pirfenidone affected drug interaction with the films and the consequent mechanical and release properties.

Cell studies found TBC to be toxic even in low concentrations. Consequently, only TEC was further analyzed. Layered devices containing two drugs demonstrated

sequential release regardless of drug order. Plasticizer concentration did not significantly affect the release profiles. Lastly, *in vitro* and *in vivo* 9-layered device studies sequentially released drugs confirming the research objective: sequential, local release of anti-inflammatory, anti-oxidant, and anti-fibrotic molecules from CAP-Pluronic films.

KEYWORDS: Drug delivery, mechanical properties, plasticizer, cellulose acetate phthalate, Pluronic F-127.

Cheryl Lynn Rabek

Student's Signature

April 22, 2015

Date

LAYERED, FLEXIBLE DRUG DELIVERY FILMS FOR THE  
PREVENTION OF FIBROTIC SCAR TISSUE FORMATION

By

Cheryl Lynn Rabek

Dr. David A. Puleo

Director of Dissertation

Dr. Abhijit Patwardhan

Director of Graduate Studies

April 22, 2015

Date

## Acknowledgements

First and foremost, thank you to my advisors, Dr. David Puleo and Dr. Thomas Dziubla, for their support, understanding, and flexibility throughout my doctoral research. I met Dr. Puleo in my first semester freshman year. I asked him the best path to earn a graduate degree in Biomedical Engineering and he suggested earning a bachelor's degree in Materials Engineering so that is what I did. My senior year I worked on a collaborative project with him and later chose to work in his lab for my doctoral research. Dr. Dziubla was my thermodynamics professor in undergrad and the first person to discuss the IGERT program with me. He highly encouraged that I consider the fellowship and a few years later I was awarded IGERT funding that supported my research and me throughout graduate school. The last two years of my doctoral research, I worked in industry full time; I very much appreciate the early morning meetings Dr. Puleo, Dr. Dziubla, and I had that allowed me to keep making progress on my project. They have both impacted my life more than they know and I am so grateful.

I would like to thank Dr. Hainsworth Shin, Dr. Kimberly Anderson, and Dr. Todd Milbrandt for serving on my committee and being a positive part of my graduate experience. I want to give Dr. Mark Thomas, who passed away before I defended, a special thank you for being such an involved and encouraging committee member during my first few years as a graduate student and during my qualifying exam.

I would also like to express gratitude to my lab and class mates, specifically Dr. Matthew Brown and Dr. Megan Phillips, who were such an integral part of my graduate life. We created a bond that will last forever.

Lastly, I would like to thank my parents, Dr. Richard and Karen Rabek, and my fiancé, John Jennings, for the overwhelming support every step of this journey. I truly appreciate your unwavering confidence in me.

This work was possible through funding by the National Institutes of Health, DE019645 and AR060964. I was supported separately by the National Science Foundation Integrated Graduate Education and Research Traineeship (DGE-0653710).



## Table of Contents

Acknowledgements.....	iii
Table of Contents.....	v
List of Tables.....	viii
List of Figures.....	ix
Chapter 1 Introduction.....	1
Chapter 2 Background and Significance.....	4
2.1 Clinical Need.....	4
2.2 Wound Healing.....	3
2.3 Current Treatments.....	7
2.4 Current Research.....	9
2.4.1 Scarless Wound Healing.....	9
2.4.2 Growth Factors and Wound Healing.....	10
2.4.3 Wound Healing Devices.....	12
2.5 Proposed System.....	13
2.5.1 CAP-Pluronic.....	13
2.5.2 Plasticizers.....	14
2.5.3 Anti-inflammatory Drugs.....	14
2.5.4 Anti-oxidant Drugs.....	15
2.5.5 Anti-fibrotic Drugs.....	15
2.6 Significance.....	16
Chapter 3 The Effect of Plasticizers on the Erosion and Mechanical Properties of Polymer Films.....	18
3.1 Introduction.....	18
3.2. Materials and Methods.....	20
3.2.1 Film Production.....	20
3.2.2 Erosion Studies.....	21
3.2.3 Mechanical Properties.....	21
3.2.4 Scanning Electron Microscopy.....	22
3.2.5 Microcomputerized Tomography.....	22
3.2.6 Mass Spectroscopy.....	23
3.2.7 Statistical Analysis.....	23
3.3 Results.....	24
3.3.1 Films.....	24
3.3.2 Erosion Studies.....	24
3.3.3 Mechanical Properties as Prepared.....	28
3.3.4 Mechanical Properties After Incubation.....	32
3.3.5 Morphology.....	34

3.4 Discussion.....	40
3.5 Conclusion.....	43
Chapter 4 The Combined Effects of Drugs and Plasticizers on the Properties of Drug Delivery Films.....	45
4.1 Introduction.....	45
4.2 Materials and Methods.....	47
4.2.1 Film Fabrication.....	47
4.2.2 Erosion and Drug Release Studies.....	48
4.2.3 Mechanical Properties.....	48
4.2.4 Statistics.....	49
4.3 Results.....	49
4.3.1 Erosion and Release Studies.....	49
4.3.2 Mechanical Properties.....	55
4.4 Discussion.....	57
4.5 Conclusions.....	61
Chapter 5 Sequential Release of Multiple Drugs from Flexible Drug Delivery Films .....	63
5.1 Introduction.....	63
5.2 Materials and Methods.....	65
5.2.1 Cytotoxicity Studies. ....	65
5.2.2 Film and Device Fabrication.....	66
5.2.3 Drug Release Studies.....	68
5.2.4 Erosion Studies.....	69
5.2.5 Mechanical Properties.....	69
5.2.6 Statistics.....	69
5.3 Results.....	70
5.3.1 Cytotoxicity Studies.....	70
5.3.2 Mechanical Properties.....	71
5.3.3 Four-Layered Device Studies.....	73
5.3.4 Nine-Layered Device Studies.....	78
5.4 Discussion.....	83
5.5 Conclusions.....	86
Chapter 6 Comparison of In vitro and In vivo Erosion and Release.....	87
6.1 Introduction.....	87
6.2. Materials and Methods.....	89
6.2.1 CAP-Pluronic Film Fabrication.....	89
6.2.2 EVA Film Fabrication.....	90
6.2.3 Device Fabrication.....	90
6.2.4 Animal Methodology and Procedure.....	93
6.3 Results.....	94
6.4 Discussion.....	96
6.5 Conclusion.....	99
Chapter 7 Conclusion.....	100

References.....	102
VITA.....	118

## List of Tables

Table 4.1: Standard deviations of (a) elastic modulus and (b) elongation for pirfenidone or quercetin loaded films.....	57
Table 6.1: Device fabrication information for animal trials.....	91
Table 6.2: Fabrication of devices used for the third trial .....	92
Table 6.3: Initial and final weights of <i>in vivo</i> device components for third study.....	95

## List of Figures

- Figure 3.1:** Chemical structures of Pluronic F127 (a), cellulose acetate phthalate (b), triethyl citrate (c), and tributyl citrate (d).....20
- Figure 3.2:** A) Unplasticized inflexible CAP-Pluronic film and B) plasticized CAP-Pluronic film able to conform to any shape.....24
- Figure 3.3:** Example of typical degradation curves. Data are mean  $\pm$  standard deviation (n=3).....26
- Figure 3.4:** Remaining mass after 16 hours of incubation in PBS at 37°C. Data are mean  $\pm$  standard deviation (n=3). No differences were statistically significant.....27
- Figure 3.5:** Absorbance at 630 nm of supernatants from TEC and TBC films after 2 hours of incubation compared to PBS. Data are mean  $\pm$  standard deviation (n=3). Inset: Images showing appearance of supernatants from TEC (above) and TBC (below) films..28
- Figure 3.6:** A) UTS of TBC and TEC films. 0 and 20 TEC were statistically different,  $p < 0.001$ . 0 and 20 TBC were statistically different,  $p < 0.01$ . B) Elastic modulus of TBC and TEC films. 0, 10, and 20 TBC were all statistically different from each other,  $p < 0.01$ . Both 10 and 20 TEC were statistically different from 0 TEC,  $p < 0.001$  but 10 and 20 TEC were statistically the same. C) Elongation of TBC and TEC films normalized by the cross-sectional areas (CSA). 0 samples are statistically different from 20 TBC samples,  $p < 0.05$ . 0 was statistically different from 10 TEC,  $p < 0.05$ . 20 TEC was statistically different from both 0 and 10 TEC,  $p < 0.001$ . Data are mean  $\pm$  standard deviation (n=3).....30

**Figure 3.7:** A) UTS of dry films and films incubated in PBS for 2 hours. Dry values compared to degraded values were all significantly different,  $p < 0.001$ . B) Elastic modulus of dry films and films incubated in PBS for 2 hours. 0 films were statistically different than their degraded counterparts,  $p < 0.05$ . 20 TBC was statically different from its wet counterpart,  $p < 0.05$ . C) Elongation of dry films and films incubated in PBS for 2 hours. Dry 0 and 10 TBC and TEC films were statistically different from their wet counterparts,  $p < 0.001$ . Data are mean  $\pm$  standard deviation ( $n=3$ ).....33

**Figure 3.8:** Scanning electron micrographs of the as-prepared surface (top left) and the surface (top right) and cross-section (bottom) of films incubated in PBS for 2 hours. A) 0, B) 10, and C) 20 wt% films.....36

**Figure 3.9:** Micro CT images showing A) 0, B) 10, and C) 20 wt% films incubated in PBS for 2 hours.....38

**Figure 3.10:** Porosity measurements for as-prepared films and films incubated in PBS for 2 hours. A) TEC-containing films. 20 TEC was statistically different than 0 TEC,  $p < 0.05$ . B) TBC-containing films. No statistical difference between incubated samples, and no statistical difference between non-incubated samples.....39

**Figure 4.1:** Chemical structures of quercetin (a) and pirfenidone (b).....47

**Figure 4.2:** Release and erosion of TEC films loaded with 10 mg quercetin (a), 6.1 mg pirfenidone (c), 100 mg quercetin (e), and 61 mg pirfenidone (g). Release versus erosion of TEC films loaded with 10 mg quercetin (b), 6.1 mg pirfenidone (d), 100 mg quercetin (f), 61 mg pirfenidone (h). Data are mean  $\pm$  standard deviation ( $n=3$ ).....52

<b>Figure 4.3:</b> Release and erosion of TBC films loaded with 10 mg quercetin (a), 6.1 mg pirfenidone (c), 100 mg quercetin (e), and 61 mg pirfenidone (g). Release versus erosion of TBC films loaded with 10 mg quercetin (b), 6.1 mg pirfenidone (d), 100 mg quercetin (f), 61 mg pirfenidone (h). Data are mean $\pm$ standard deviation (n=3).....	54
<b>Figure 4.4:</b> Elastic modulus of pirfenidone-loaded films (a) and quercetin-loaded films (b). Percent elongation normalized by the cross-sectional area of pirfenidone loaded films (c) and quercetin loaded films (d). Data are mean (n=3).....	56
<b>Figure 5.1:</b> Wound healing stages and the planned drug targets.....	64
<b>Figure 5.2:</b> Chemical structures of drugs (a) quercetin, (b) ketoprofen, and (c) pirfenidone, and plasticizers, (d) triethyl citrate and (e) tributyl citrate.....	65
<b>Figure 5.3:</b> “Forward” (left) and “reverse” (right) device types.....	67
<b>Figure 5.4:</b> Nine layered device.....	68
<b>Figure 5.5:</b> Cell viability after plasticizer exposure. Data are mean $\pm$ standard deviation (n=3).....	70
<b>Figure 5.6:</b> Mechanical properties of 4-layered devices: (a) % elongation, (b) ultimate tensile strength, and (c) elastic modulus. Data are mean $\pm$ standard error (n=3).....	71
<b>Figure 5.7:</b> Release from “forward” 4-layered devices plasticized with (a) 0 TEC, (b) 10 TEC, and (c) 20 TEC. Data are mean $\pm$ standard error (n=3).....	73
<b>Figure 5.8:</b> Area under the curves during ketoprofen and pirfenidone overlap release from 4-layered “forward” devices. Data are mean $\pm$ standard error (n=3).....	75

**Figure 5.9:** Release from “reverse” 4-layered devices plasticized with (a) 0 TEC, (b) 10 TEC, and (c) 20 TEC. Data are mean  $\pm$  standard error (n=3).....76

**Figure 5.10:** Area under the curves during ketoprofen and pirfenidone overlap release from 4-layered “reverse” devices. Data are mean  $\pm$  standard error (n=3).....78

**Figure 5.11:** Instantaneous release from 9-layered devices plasticized with (a) 0 TEC, (b) 10 TEC, and (c) 20 TEC. Cumulative release from 9-layered devices plasticized with (d) 0 TEC, (e) 10 TEC, and (f) 20 TEC. Data are mean  $\pm$  standard error (n=3).....79

**Figure 5.12:** Mass loss of 9-layered devices. Data are mean  $\pm$  standard error (n=3).....83

**Figure 6.1:** Chemical structures of (a) meloxicam, (b) ketoprofen, (c) quercetin, and (d) pirfenidone.....89

**Figure 6.2:** Eight layered devices for animal study.....92

**Figure 6.3:** Images of animal procedure: (a) implant in surgical site and (b) wound closure.....93

**Figure 6.4:** Study 3 *in vivo* CAP-Pluronic mass loss over time.....96



## Chapter 1

### Introduction

Open wounds accounted for 10.3% of the 5.3 million non-fatal injuries from traffic collisions in the U.S. in 2000, and about 50% of all military injuries involve musculoskeletal wounds to the extremities (1, 2). Chronic inflammation in these types of soft tissue defects can result in scars that have functional and aesthetic consequences. Fibrotic scar formation in these wounds may be reduced or prevented if treated with a combination of anti-inflammatory, anti-oxidant, and anti-fibrotic molecules targeted to the different healing phases. As such, the objective of this research was to develop and characterize flexible, layered drug delivery films for sequential, localized release of the aforementioned molecules to soft tissue.

Chapter 2, provides a review of the current state of the art on treatments for large soft tissue defects and a critical analysis of their shortcomings and potential areas of development. Scarless healing is examined and ongoing research in wound healing and drug delivery devices are discussed. To work towards developing a soft tissue wound healing device, mechanical and erosion properties of the system were evaluated (Chapter 3), drug release mechanisms were determined (Chapter 4), the cellular impact and capability of sequential release were assessed (Chapter 5), and finally in vivo studies were performed (Chapter 6). The films examined in this research are composed of two polymers, cellulose acetate phthalate (CAP) and Pluronic F-127 (Pluronic). Along the

films are rigid. Since every wound has its own geometry and topography, the films need to be flexible and able to contour to the shape of any wound. To impart flexibility, plasticizers, triethyl citrate (TEC) or tributyl citrate (TBC), were added. In the third chapter, mechanical analysis was performed on plasticized films as prepared and following phosphate-buffered saline incubation to determine property changes after implantation. Micro computerized tomography and scanning electron microscopy determined how erosion and plasticizer leaching affected the film's structures before and after incubation.

The combined effects of drugs with plasticizers on film erosion, release, and mechanical properties were investigated in Chapter 4. Films were loaded with quercetin, an anti-oxidant, or pirfenidone, an anti-fibrotic, and plasticized with TEC or TBC. Size, solubility, and structure differences between quercetin and pirfenidone were determined to affect how the drugs interacted with the films and the consequent mechanical and release properties.

In Chapter 5, cell studies were performed to evaluate the cytotoxicity of the TEC and TBC. The effect the plasticizers had on the mechanical properties of the films and the cytotoxicity results narrowed down the plasticizer choice for multi-layered devices. Two different multi-layered device types were evaluated, 4-layered devices and 9-layered devices. Both types demonstrated sequential drug release. Again, the differences in the drugs were found to affect the resulting release profiles. Pilot animal trials were performed to evaluate the devices in vivo and compare against in vitro

results in Chapter 6. Lastly, Chapter 7 is an assessment and conclusion of the developed and characterized devices against the objectives.

Copyright © Cheryl Lynn Rabek 2015

## Chapter 2

### Background and Significance

#### 2.1 Clinical Need

With soft tissue defects accounting for over 10% wounds inflicted from motor vehicle accidents, over half a million car accident victims every year could benefit from wound healing films (1). Additionally, wounds caused during war, industrial accidents, or surgeries could also heal faster and with less scarring by the proposed drug delivery films.

#### 2.2 Wound Healing

There are two categories of wound repair: primary unions and secondary unions (3). An example of a primary union wound is a surgical incision. The wound is narrow and clean and a limited number of epithelial and tissue cells die. Secondary unions are wounds in which a large mass of tissue has been destroyed and the wound cannot be neatly sewn together with sutures (4, 5). The healing steps are the same for secondary union and primary union wounds, but with secondary union wounds the process is longer, more complex, and the wound experiences more inflammation ultimately resulting in excessive scar tissue formation (6). Specifically, secondary union wound healing is the target of this research.

Wound healing is a complex process involving four main phases: hemostasis, inflammation, proliferation, and remodeling (7, 8). After the initial injury to tissues, the body undergoes hemostasis to stop blood loss (7, 9). During this phase, blood vessel walls have been damaged and platelets adhere to the collagen fibers present at the ruptured vessel walls. The platelets degranulate releasing adenosine diphosphate (ADP), calcium, and serotonin (10). These biomolecules or tissue damage initiates the plasma coagulation cascade. Incoming platelets exposed to ADP begin aggregating and start forming a platelet plug (11). The platelets degranulate further causing additional aggregation of platelets. Fibrinogen present in blood plasma is converted to fibrin which strengthens the clot.

Once blood loss is successfully controlled, the wound site undergoes inflammation (12). The signs of inflammation are redness, swelling, heat, pain, and sometimes loss of function. Preexisting chemical mediators, including histamine and serotonin, are released from local platelets and mast cells (3, 13, 14). These chemical mediators cause the surrounding vasculature to become leaky, predominately by endothelial cell retraction which causes a widening of the intercellular junctions (15, 16). The leaky vasculature allows an influx of fluid and cells into the injured tissue. Increased blood flow and fluid cause the previously mentioned signs of inflammation. Chemokines, chemotactic cytokines, are released by proximate cells and which causes recruitment of more cells to the area (17). The majority of the cells to enter the injured tissue are neutrophils and monocytes (10). They synthesize and release additional

chemical mediators, including arachidonic acid metabolites: prostaglandins and leukotrienes, cytokines, and nitric oxide (3). Nitric oxide and prostaglandins cause vasodilation allowing for the influx of more cells and extracellular fluid (18). The cytokines and leukotrienes activate other leukocytes to perform their inflammatory roles. Neutrophils protect against invading pathogens. Monocytes can differentiate into macrophages, which break down dead or invading cells and impurities through phagocytosis. Macrophages can congregate into one larger foreign body giant cell (FBGC) and remove larger debris (10). In normal healing, inflammation is a self-limiting process and the release of inflammatory mediators will reduce and cells will retract as the threat is resolved (19, 20). In chronic healing, the chemical mediators exacerbate the inflammation.

The next phase, the proliferation phase, replaces lost or damaged tissue. Angiogenesis occurs from surrounding blood vessels (21, 22). Macrophages present in the wound secrete epidermal growth factor (EGF) and vascular endothelial growth factor (VEGF). These cause endothelial cells in the blood vessels to bud and branch towards the wound, allowing for the exchange of nutrients and waste. Within a couple days, fibroblasts migrate to the injured tissue (23). The fibroblasts proliferate and create the proteoglycans and proteoglycan aggregates in the extracellular matrix (24). They repair the damaged tissue by forming a collagen matrix. If inflammation is not reduced, chemotaxis recruits excess fibroblasts to the newly formed granulation tissue. Growth factors, including platelet-derived growth factor (PDGF), fibroblast growth

factor (FGF), and transforming growth factor (TGF), cause fibroblasts to differentiate into proto-myofibroblasts (25-27). Then the proto-myofibroblasts differentiate into myofibroblasts which are responsible for expression of smooth muscle actin and create the contractile forces in the tissue (28).

Remodeling is the maturation of the scar tissue (3, 7, 12). This is the longest phase of all four since it can last for months. If inflammation continues during remodeling, cytokines and growth factors stimulate secretion of collagenases that breakdown the newly formed scar tissue (29). The collagen fibers will continue to be realigned, which can cause the contractile forces to become greater over time (30-32). These forces can cause disfiguration and malfunction around the injury site leading to the development of contracture, hypertrophic, or keloid scars (33-35).

### **2.3 Current Treatments**

Secondary union wounds often contain bacteria (36). Either the object that severed the skin was unclean or the wound becomes susceptible to bacteria because of the large amount of exposed soft tissue (37). These wounds may also contain foreign materials. The first step to treating secondary union wounds is debridement, the process of removing foreign debris and dead tissue (6). There are five main types of debridement: surgical, mechanical, enzymatic, biosurgery, and autolytic (38, 39). In surgical debridement, necrotic tissue is surgically cut away and debris is removed with sterile tools. Saline irrigation, vacuum-assisted closure, ultra sound, and wound

redressing are types of mechanical debridement (39, 40). Pharmaceutically manufactured proteolytic enzymes are used applied to wounds in enzyme debridement. Collagenase is one of the most common enzymatic debridement methods because it selectively breakdowns triple helical collagen and disregards other proteins (29). In biosurgery debridement, sterilely grown maggots are applied to the wound to remove necrotic tissue (39, 40). Autolytic debridement naturally occurs through cellular responses. Macrophages and FBGCs phagocytose debris and necrotic tissue (41). Phagocytosis occurs on the micron scale so some material can be too large or resistant for macrophages and FBGCs to break down (41, 42). If the debris is not removed a fibrous capsule will form around it (10). If a wound is infected, bacteria can create necrotic tissue faster than the macrophages and FBGCs can eliminate it. Depending on the severity of the wound, intravenous or oral antibiotics may also given prophylactically to kill any present bacteria (43).

Once the wound is cleaned, bandages are applied. Bandages are typically redressed every couple days (37). If a wound is too large for epithelium to fill in the defect, a skin graft may be required for the wound to close (6). There are a two different categories of skin grafts: split-thickness skin grafts (STSG) and full-thickness skin grafts (FTSG) (44). Several factors must be considered before selecting a donor site, including contour, color, and vascularity. If a wound has not responded to traditional wound treatment, negative pressure wound therapy (NPWT) or vacuum-assisted closure



can also be used (45). NPWT creates a physical barrier, removes excess fluid, allows the wound to stay moist, and increases perfusion and granulation tissue formation (39).

Even though the treatment is more or less the same for all secondary union wounds, the healing time is not. Healing rates of chronic wounds are negatively affected by increased age of the individual wounded, increased size and decreased perfusion of the wound, and by reduced nutrition and health of the patient (3, 6, 46). Ischemia, diabetes, edema, and infection can also cause adverse healing (8). If inflammation continued through the remodeling phase, keloid, contracture, or hypertrophic scars are likely to develop (35). Once formed, treatments of these scars include surgical removal, cryotherapy, laser resurfacing, and steroid injections (47-50). If these treatments are utilized, the healing process of that location will occur again. Secondary union wounds often cause fibrotic scar tissue with aesthetic and functional consequences. There is much room and need for improvement upon current treatments.

## **2.4 Current Research**

### **2.4.1 Scarless Wound Healing**

During early development, human fetuses heal without any evidence of a scar (51-54). Fetal skin experiences a very minimal inflammation process during wound healing, which is related to the levels of cytokines and growth factors present (52). Transforming growth factors  $\beta_1$  and  $\beta_2$  have been shown to play a large role in the

development of a fibrotic scar experimentally. In fetal wounds, these are exhibited at very low levels (52). Interleukins (IL) 6 and 8 are found in low levels in fetal wounds and are much higher in adult wounds, while IL-10, a known anti-inflammatory biomolecule, is found in higher concentrations in fetuses than in adults. As discussed earlier, myofibroblasts mediate fibrotic tissue formation in adults; myofibroblasts are not even present in fetal flesh wounds until late gestation (52, 55). Knowledge gained through experiments with fetal wound healing can give insight into effective strategies to combat scar tissue formation in adult wounds.

#### **2.4.2. Growth Factors and Wound Healing**

As described above, the levels of growth factors present in a wound play a direct role in wound closure and scar formation. Hence, research is being conducted to better understand the effects of growth factors, including TGF, PDGF, FGF, and EGF, on wound healing (27, 56, 57). The effect of (EGF) on cutaneous scar formation in mice revealed that daily treatment, 100 µg, resulted in a third faster healing rate as compared to the saline treated control (58). The average scar size of the control group was 1.44 times as large as the average scar of the EGF treated group and the number of inflammatory cells present in the histological samples and the expression of TGF-β<sub>1</sub> were much less for the EGF treated group (58). The concentration of EGF was found to be inversely proportional to the degree of scarring.

To study the effect of fibroblast growth factor (FGF) on wound healing, full-thickness dermal wounds were created in a rodent model (59). Chitosan films loaded with FGF were placed on the cutaneous wounds. There were three groups of experimental mice. One group's films were loaded with 0.6  $\mu\text{g}$  of FGF, another with 2.0  $\mu\text{g}$  of FGF, and another with 6.0  $\mu\text{g}$  of FGF. Another group of mice received an unloaded chitosan films on their wounds and the control group received only saline on their wounds. The FGF loaded chitosan films reduced the wound size and sped up the healing rate in a dose-dependent way (59). Histology revealed that the control group didn't receive as high of an influx of macrophages and fibroblasts that the other groups did, nor did they experience as high a degree of angiogenesis in the healing wounds. In addition, FGF treated mice had more granulation tissue at the wound site as compared to the control.

Ischemic wounds often have adverse healing with excess inflammation (60, 61). PDGF and VEGF are growth factors that promote angiogenesis and correct an ischemic wound. Ischemia was inflicted on the hind limbs of mice (62). Immediately following surgery and again 5 days later, the experimental mice were treated with either PDGF, VEGF, or both PDGF and VEGF. Twenty one days after ischemia, the limbs treated with PDGF or both PDGF and VEGF had over 1.5 times the blood flow than the VEGF treated group or the control implying that PDGF is more important to ischemic wounds than VEGF (62).

### 2.4.3 Wound Healing Devices

Many different materials are being explored for drug delivery devices for wound healing applications including alginate (63-65), carboxymethylcellulose (66, 67), chitosan (68-71), collagen (72), dextran (73), hydrogels (65, 74-78), hydroxypropylmethylcellulose (HPMC) (79, 80), poly(vinyl alcohol) (PVA) (70, 81, 82), polycaprolactone (PCL) (83-85), poly(lactic-co-glycolic acid) (86-88), polyurethane (80, 89), and silk (86, 90, 91). Although all of these materials have been well studied for a variety of applications, very few are being evaluated as implantable wound healing devices. Instead, their effectiveness as topical dressings has been explored.

Porous gelatin and hyaluronic acid scaffolds were investigated as wound healing devices (92). When placed over split thickness wounds in a rat model, wound closure was accelerated and collagen deposition increased compared to the control which was no treatment. Electrospun wound dressings composed of PLGA and silk fibroin were shown to have a significant effect on wound closure in rats compared to PLGA dressings alone and the positive and negative controls after 15 days (86). Although the gelatin and hyaluronic scaffolds and PLGA fibroin wound dressings demonstrated an improvement to the control, they were replaced on the wounds every 24 and 48 hours, respectively, which is not possible with an implantable system.

Another challenge for implantable systems is coordinating the rates of drug release and erosion of the device. In topical wound dressings, that does not have to be considered. Films composed of electrospun PVA and PCL fibers and loaded with

caffeine, used as a model drug, were analyzed as potential flexible wound healing devices (93). These PVA and PCL films release drug on the order of hours and degrade on the order of weeks limiting the films to only dermal applications (84, 94). If these devices were implanted, they would leave behind material to cause an inflammatory response for far longer than the duration of the treatment (93). Hydrogels crosslinked with glutaraldehyde and loaded with gentamicin sulfate or norfloxacin were explored as an antimicrobial wound dressing (74). A full thickness dorsal wound was created in rats and the hydrogel was applied. Histology performed after 21 days revealed that the glutaraldehyde cross-linked hydrogels were found to have broken down into fragments and elicited an inflammatory response that interfered with the wound healing process (74) highlighting another challenge of the development of wound healing devices.

## **2.5 Proposed System**

### **2.5.1 CAP-Pluronic**

For over 20 years cellulose acetate phthalate combined with Pluronic F127 has been known to be a surface eroding drug delivery system (95). CAP and Pluronic can be easily fabricated into films, cylinders, or microspheres that can release a variety of different drugs (95-100). When loaded with drug in layers, devices were shown to release the drugs in a pulsatile manner (97, 100). Erosion and release rates of the system can be adjusted by changing the ratio of CAP:Pluronic; increasing Pluronic content increases the erosion and release rates while increasing CAP content decreases

the rates (95). The release mechanism from CAP-Pluronic devices is pH dependent. In neutral and basic conditions release is controlled through surface erosion and in acidic conditions, release is diffusion controlled (95). Previous studies have proven the system to be capable of releasing multiple drugs over several days, which is why it was chosen for this evaluation as a wound healing device.

### **2.5.2 Plasticizers**

The CAP-Pluronic system alone is rigid. To allow a CAP-Pluronic film to contour to the varying geometries of a wound, plasticizers need to be added (101). There are several different families of plasticizers that are commonly used in medical and pharmaceutical applications (102-104). Glycols, citrates, sebacates in particular are frequently used to plasticize cellulose acetate (104). Phthalates were also commonly used to plasticize CAP, but in recent years, long term phthalate exposure has proven to have an adverse impact on health and development (105, 106). Triethyl citrate and tributyl citrate were chosen for the wound healing device developed because of their lower effect on erosion rates as compared to other plasticizers in addition to their biocompatibility.

### **2.5.3 Anti-inflammatory Drugs**

There are two classes of anti-inflammatory drugs: steroidal and non-steroidal. Steroidal anti-inflammatory drugs typically require prescriptions and side effects can be

severe (107). Non-steroidal anti-inflammatory drugs (NSAIDs) act by inhibiting formation of prostaglandins by inhibiting the cyclooxygenase (COX) pathways that create them (108). There are two types of cyclooxygenase enzymes, COX-1 and COX-2. COX-1 is a common enzyme in healthy tissue and the inhibition of it can lead to gastrointestinal damage (109). Unselective NSAIDs inhibit prostaglandin synthesis by blocking both COX enzymes where selective NSAIDs preferentially inhibit either COX-1 or COX-2 enzymes (110). There are many different NSAIDs on the market including ibuprofen, acetaminophen, and aspirin. The drug delivery devices were evaluated in rodents first. NSAIDs approved for use in rodents include ketoprofen and meloxicam, so they were chosen for the device (108).

#### **2.5.4 Anti-oxidant Drugs**

There are two types of anti-oxidants: enzymatic and non-enzymatic. Of the non-enzymatic anti-oxidants, many different families exist: carotenoids, minerals, phenols, thiols, and vitamins (111, 112). They all reduce oxidative stress through a variety of mechanisms (113). Quercetin, a highly abundant dietary phenol, was chosen as the anti-oxidant drug for the device. Quercetin decreases superoxide activity of leukocytes and acts as a pro-inflammatory mediator (114-116).

### 2.5.5 Anti-fibrotic Drugs

Pirfenidone was the anti-fibrotic drug chosen for the wound healing film. Through several double blind studies, pirfenidone has proven to be an effective treatment for fibrotic diseases (117, 118). Pirfenidone reduces scar tissue formation by down-regulating cytokines and growth factors, including interleukin 1 $\beta$  and transforming growth factor- $\beta$ 1 (119-123). Other drugs, including imatinib mesylate and rosiglitazone, were developed as therapies for different conditions but inhibit pathways that create fibrosis. Imatinib mesylate inhibits growth factor receptors on mast and stem cells and rosiglitazone reduces inflammation that leads to fibrosis by reducing the inflammatory signally molecule, nuclear factor kappa-B (124-130).

### 2.6 Significance

Little research is currently being conducted on wound healing systems with the distinct aim of reducing fibrotic scar tissue formation. For an implantable drug delivery device to be effective at preventing scar tissue, it needs to be capable of altering the mechanisms of fibrotic tissue formation by providing therapeutic molecules over an extended period of time. The device also needs to erode as it delivers drug or be biologically inert, so the remaining vehicle does not perpetuate an inflammatory response (131, 132). Although research on topical wound dressings or treatments are promising, they require application of the therapeutic molecules on a daily basis over several weeks and cannot be implanted, only treat on one healing front by releasing



only one molecule, or leave behind a polymer vehicle in the wound that could cause adverse healing. There is a need for devices that are applied or implanted once, are capable of sequential release of multiple molecules to heal on multiple fronts, and erode as drug is released. This research was focused on the development and characterization of CAP-Pluronic films loaded with anti-inflammatory, anti-oxidant, and anti-fibrotic drugs for local delivery to soft tissue defects, with the ultimate goal of preventing or reducing fibrotic scar tissue formation and encouraging proper wound healing.

Copyright © Cheryl Lynn Rabek 2015

## Chapter 3

### The Effect of Plasticizers on the Erosion and Mechanical Properties of Polymer Films

This chapter reproduced from a published manuscript, “Rabek C. L., Van Stelle R., Dziubla T.D., and Puleo D.A. , The Effect of Plasticizers on the Erosion and Mechanical Properties of Polymer Films. Journal of Biomaterials Applications. 2014; 28(5): p. 779-89.”

#### 3.1 Introduction

While convenient, medications taken orally must make a long journey, traveling from the intestines, through the portal vein, into the liver, through the bloodstream until finally reaching their intended therapeutic target. During this convoluted process, many drug molecules are eliminated from circulation by the liver and kidneys, metabolized and excreted from the body (133-136). Because of this, oftentimes drugs must be given at doses far exceeding what the target site needs for treatment. This excessive concentration coupled with presence of the drug throughout all of the body systems results in a scenario where systemic side effects are guaranteed (137-139).

As a result, there is a need for a degradable, localized, drug delivery system capable of delivering drug to soft tissue so unnecessary sites are not medicated, reducing the risk of side effects, and drug is not wasted during clearance. Most of the current drug delivery systems are composed of slowly eroding polymer networks,

including Eudragit and poly(sebacic anhydride), from which drug diffuses out to provide therapy (140-145). This kind of device leaves behind material that may cause a foreign body reaction or cause inflammation from the byproducts as it slowly degrades. Also, many of the other currently researched systems are composed of rigid polymers, such as chitosan and Eudragit, that cannot contour to the shape of the treated site (145-147). The rigidity or stiffness of materials is related to their elastic modulus (148). Rigid polymers implanted in soft tissue will cause discomfort and possible fibrous capsule formation (10, 149, 150).

Plasticizers can be added to polymers to make them more flexible (102, 104). Plasticizers are small lubricating molecules that can change polymer properties and processability (104). In this study, the effect of plasticizers on the mechanical properties of an association polymer was explored. The system formed from cellulose acetate phthalate (CAP) and Pluronic F-127 has been proven to be a surface-eroding system that would release drug as the device eroded so no material would be left behind to cause an inflammatory reaction (95, 96, 151). Without plasticizer, however, the polymer is rigid and cannot be readily contoured. Two plasticizers, triethyl citrate (TEC) and tributyl citrate (TBC), have been included, and the system as a whole has been evaluated through mechanical analysis and degradation studies. Because these materials are ultimately intended to be implanted, their properties and structure when wet were also determined (152, 153).

## 3.2. Materials and Methods

### 3.2.1 Film Production

Films were made with a 70:30 weight percent ratio of cellulose acetate phthalate (CAP; Sigma-Aldrich, St. Louis, MO) and Pluronic F-127 (Sigma-Aldrich), respectively (Figure 3.1). Plasticizer, either tributyl citrate (Sigma-Aldrich) or triethyl citrate (Sigma-Aldrich), was added to the CAP-Pluronic mixture at either 0, 10, or 20 wt%. Acetone was added to make a 25% (w/v) solution. After vortexing the solution to ensure homogeneity, it was cast into Teflon dishes and then let stand in a 10°C refrigerator overnight. Films were desiccated overnight before testing.

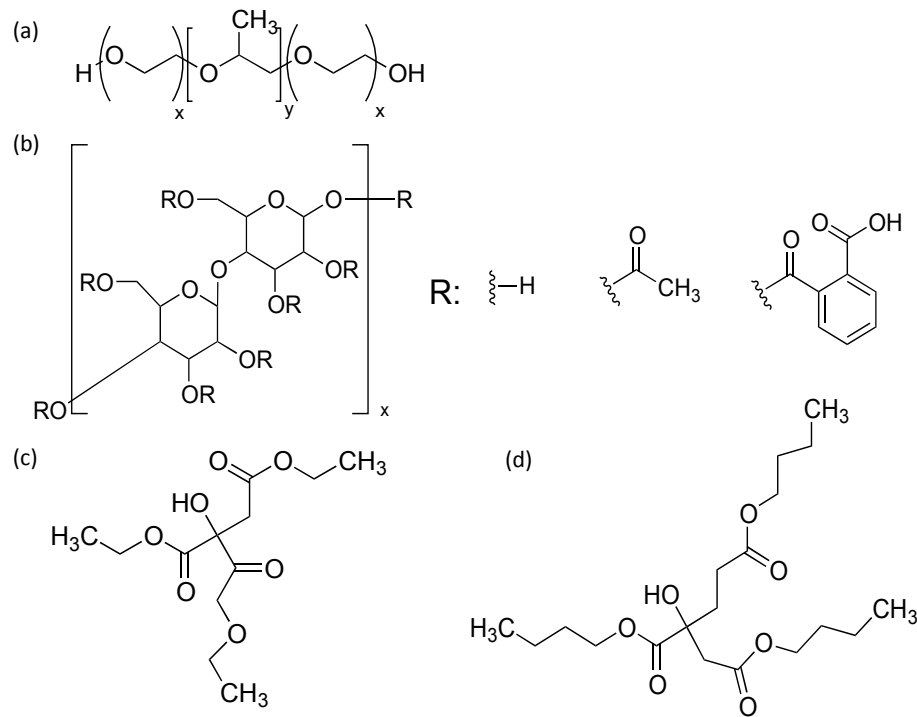


**Figure 3.1:** Chemical structures of Pluronic F127 (a), cellulose acetate phthalate (b), triethyl citrate (c), and tributyl citrate (d).

### 3.2.2 Erosion Studies

Films were cut into discs using a circular punch measuring 5 mm in diameter. After determining their initial mass, samples were placed individually in a 24-well plate, and 1.85 ml of phosphate-buffered saline (PBS), pH 7.4, was added to each well. Plates were incubated on an orbital shaker plate 37°C. Half of the supernatant was replaced with fresh PBS every 12 hours. Three samples were collected and dried at different time points ranging from every 3 to 5 hours. Dried samples were weighed to determine final mass. The average mass loss was determined. The erosion rates were found by calculating the slope of average mass loss with time. Supernatants were collected from both TEC and TBC films after being incubated in PBS for 2 hours. The supernatants were pipetted into a 96-well plate and UV absorbance was measured at 630 nm using the BioTek PowerWave HT and Gen5 software to determine the opacity. PBS was used as a control.

### 3.2.3 Mechanical Properties

Films were cut to make microtensile test samples using a dog bone die (ASTM D 1708). Wet samples were incubated in 4 ml of PBS for two hours. Cross-sectional areas were measured for each film, both wet and dry, using calipers. Samples were mechanically tested to failure in tensile mode using the BOSE ELF 3300 with a ramp at a displacement rate of 0.5 mm/sec. Stress and strain were calculated, and elastic modulus (E), percent elongation, and ultimate tensile strength (UTS) were determined.

The percent elongation was normalized by the cross-sectional area so this value would not be influenced by thickness variations in the cast films.

### **3.2.4 Scanning Electron Microscopy**

After dog bones were incubated in PBS for two hours, they were lyophilized and frozen at -80°F for 30 min. Samples were then fractured so the cross-sectional area could be analyzed using a model S-3200-N Hitachi scanning electron microscope. The samples were coated with gold, and the microscope was operated at 20 kV and digital images were collected.

### **3.2.5 Microcomputerized Tomography (MicroCT)**

To determine the interior porosity, microCT scans were performed using the SCANCO Medical AG  $\mu$ CT 40. Samples were cut to fit 12.3 mm tubes and were batch scanned. Scans were run in high resolution having 1000 projections with 2048 samples, a current of 177  $\mu$ A, a potential of 70 kVp, and a 0° angle. Samples were contoured and evaluated with a program that distinguished between the polymer material and vacancies. The uniformly biased lower threshold was set to 20 so any part of the scan with a density below that was considered a void. The slices were reconstructed into a 3-dimensional representation of the scanned samples, from which the total volume, porosity volume, average pore size, and average spacing between pores were calculated

using a morphometry script. Samples were scanned before and after being incubated in PBS for two hours.

### **3.2.6 Mass Spectroscopy**

Mass spectra were acquired by the University of Kentucky Mass Spectrometry Facility. Supernatants from erosion studies were mixed an equal volume of acetonitrile before analysis. Electrospray ionization mass spectra were obtained on a ThermoFinnigan LTQ (ion trap mass spectrometer), with sample introduction by direct infusion at 3uL/min. Full scan mass spectra were recorded in positive ion mode. Instrument parameters included spray voltage: 3.5kV, capillary temperature: 185C, capillary voltage: 50V, and tube lens voltage: 80V

### **3.2.7 Statistical analysis**

Statistical analysis was performed using InStat (GraphPad Software). All of the samples with the same weight percentage of plasticizer or the same type of plasticizer were compared against each other. Results were analyzed using two-way ANOVA, and a p-value < 0.05 was considered statistically significant.

### 3.3 Results

#### 3.3.1 Films

Plasticized films increased in flexibility as plasticizer content increased, while the unplasticized films remained rigid and could not be plastically deformed without failure (Figure 3.2). Qualitatively, films plasticized with TEC were more flexible than those plasticized with TBC at an equivalent weight percentage.

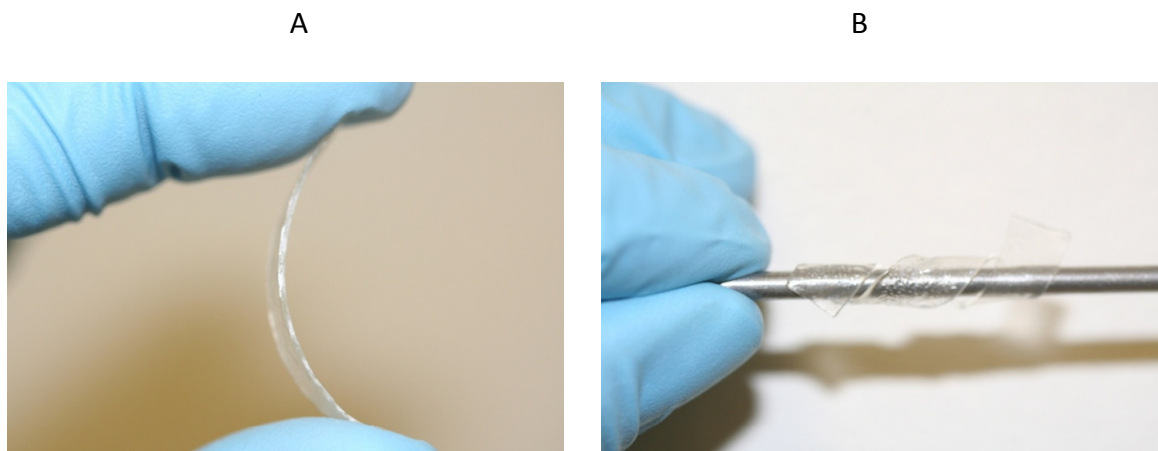


**Figure 3.2:** A) Unplasticized inflexible CAP-Pluronic film and B) plasticized CAP-Pluronic film able to conform to any shape.

#### 3.3.2 Erosion Studies

Figure 3.3 shows typical mass loss curves for the control (unplasticized) and plasticized films. The addition of plasticizer did not significantly affect the erosion of the films. As the weight percentage of plasticizer increased, the magnitude of rate of erosion slightly increased from 2.2 wt% to 2.4 wt% per hour but the differences



between the three rates were not significant (Figure 3). As the films eroded, collecting the residual polymer to measure mass loss became a challenge so samples were only collected for the first 24 hours. The remaining mass of all of the films, plasticized with either TEC or TBC, after 16 hours was also statistically the same (Figure 3.4). Sixteen hours was chosen because at that point the initial mass loss due to plasticizer leaching had already occurred and the supernatant had been replenished with fresh PBS resulting in close to sink conditions. As TBC films eroded, the PBS became milky in appearance, whereas the supernatant remained transparent as TEC films eroded (Figure 3.5). Quantitatively, the opacity of the supernatant from the TBC sample was over 10 times as high as the TEC sample. The supernatant from the TEC sample was the same as PBS alone. Supernatants were analyzed by mass spectroscopy and after two hours the mass-to-charge ratios corresponding to TEC and TBC had a higher relative abundance than any other peak.

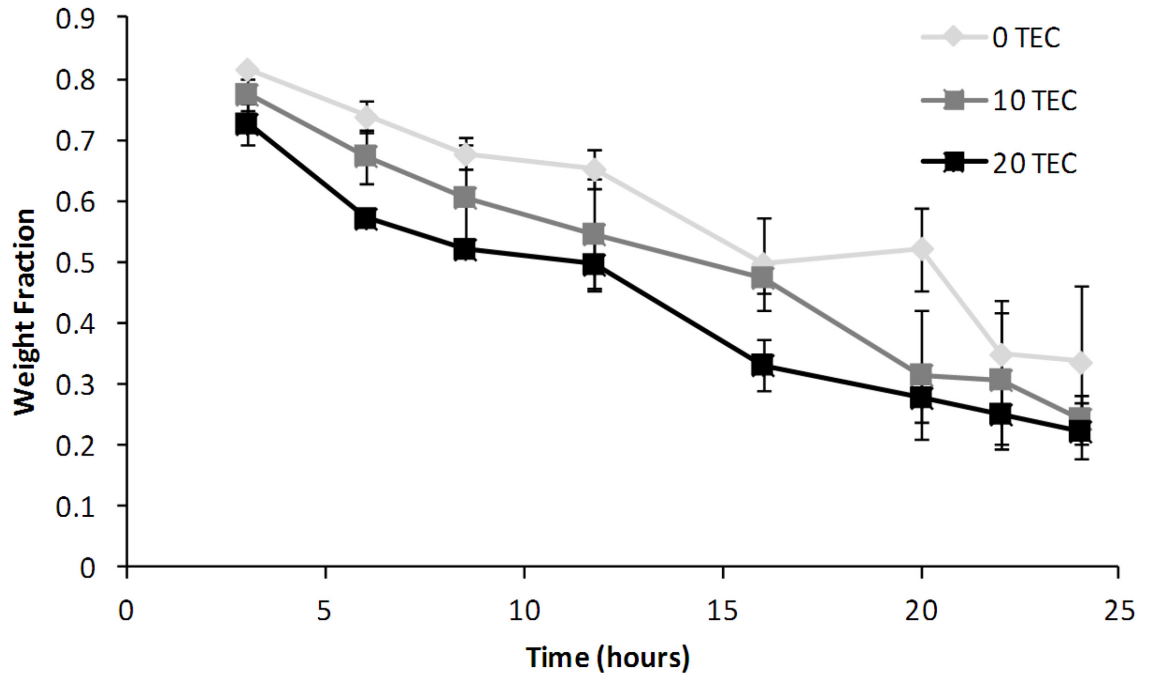


**Figure 3.3:** Example of typical degradation curves. Data are mean  $\pm$  standard deviation (n=3).

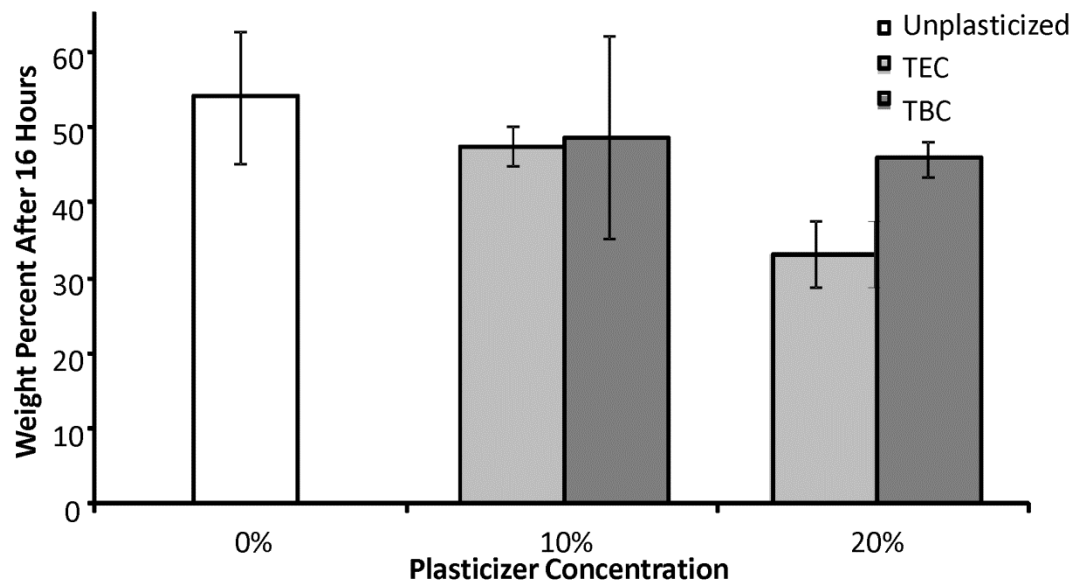


**Figure 3.4:** Remaining mass after 16 hours of incubation in PBS at 37°C. Data are mean  $\pm$  standard deviation (n=3). No differences were statistically significant.

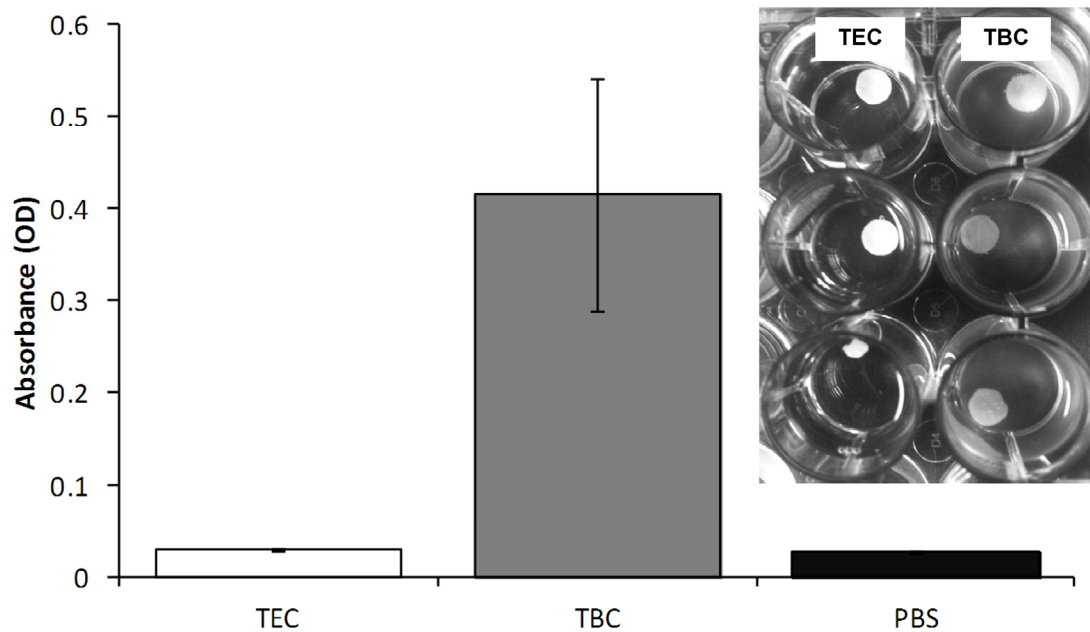


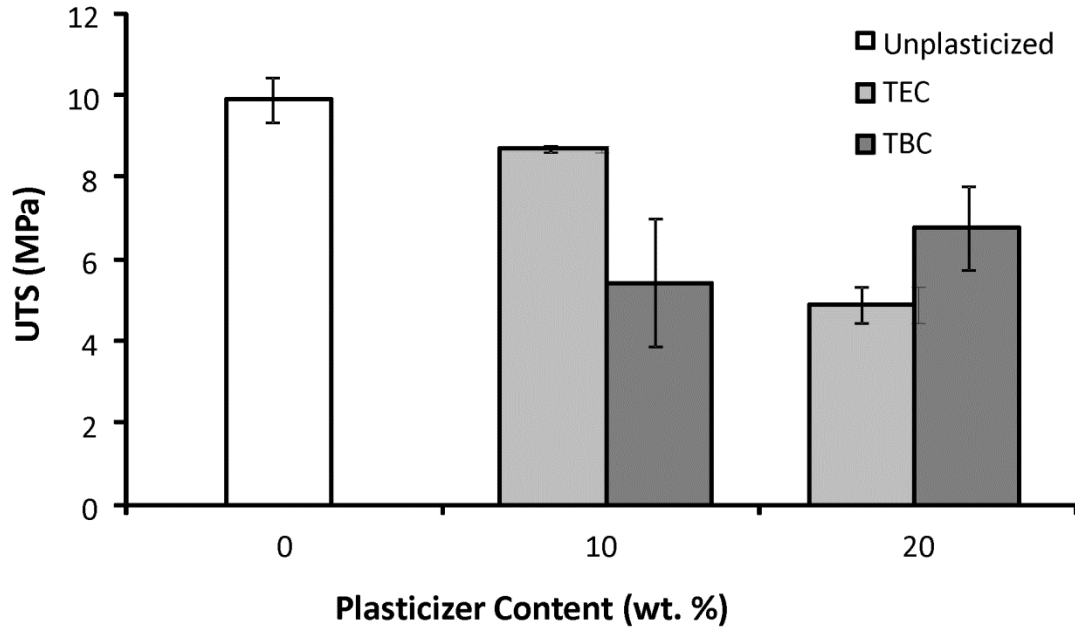
**Figure 3.5:** Absorbance at 630 nm of supernatants from TEC and TBC films after 2 hours of incubation compared to PBS. Data are mean  $\pm$  standard deviation (n=3). Inset: Images showing appearance of supernatants from TEC (above) and TBC (below) films.

### 3.3.3 Mechanical Properties as Prepared

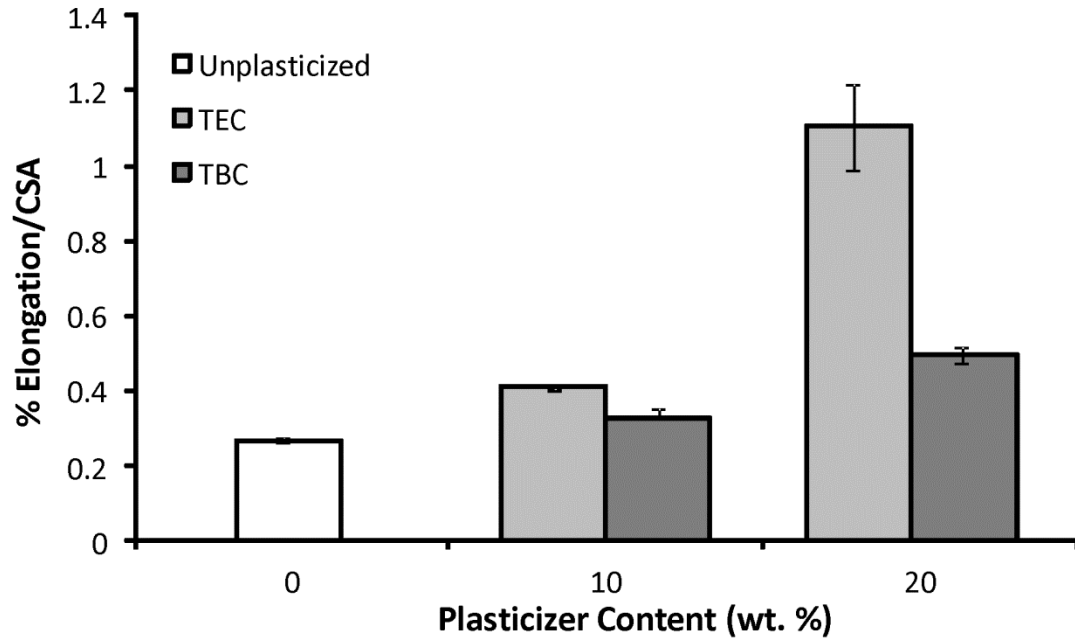
Increasing the plasticizer content increased the effects on the mechanical properties; more plasticizer decreased the E and UTS and increased the percent elongation. Compared to unplasticized films, the 20 wt% samples plasticized with TEC had a lower E and UTS (Figures 3.6a and 3.6b), by about half, but had a 5 times higher percent elongation (Figure 3.6c). Addition of TEC to the films always significantly ( $p \leq 0.05$ ) affected the mechanical properties except between the ultimate tensile strength

of the 10 wt% TEC and unplasticized samples. Adding 10 wt% TBC to the films decreased the UTS by roughly half, but addition of more TBC did not further affect the UTS. The 0 wt% TBC films had an elongation that was statistically the same as the 10 wt% TBC films, which had an elongation that was comparable to that of the 20 wt% TBC films. However, 0 and 20 wt% TBC films had elongations significantly ( $p \leq 0.05$ ) different from each other. The elastic modulus did significantly ( $p \leq 0.001$ ) decrease as more TBC was added to the films. For the concentrations examined, as plasticizer increased, the UTS of the TEC films decreased. With the TBC films, increasing plasticizer concentration past 10 wt% did not significantly affect the UTS. For similar plasticizer content, TEC caused greater changes to elongation, UTS, and E. For the 20 wt% samples, the TEC and TBC films had statistically similar UTS and E values, but their elongations were statistically different ( $p < 0.001$ ), with and the 20 wt% TEC films plastically deforming over twice as much as the TBC films.

(a)



(b)



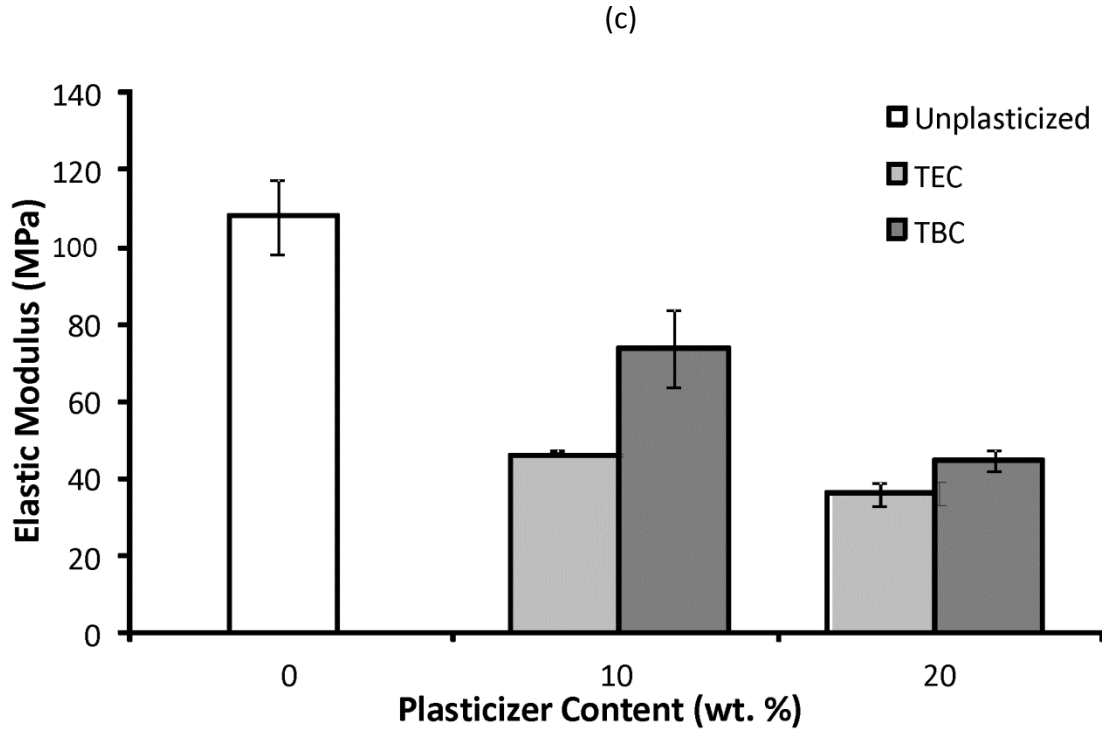
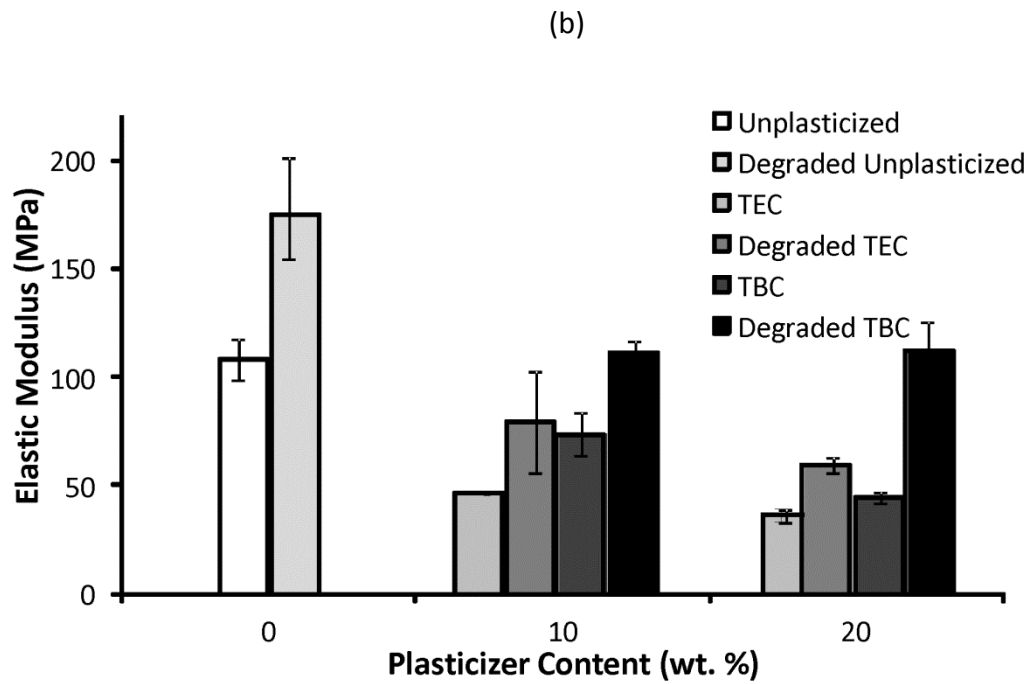
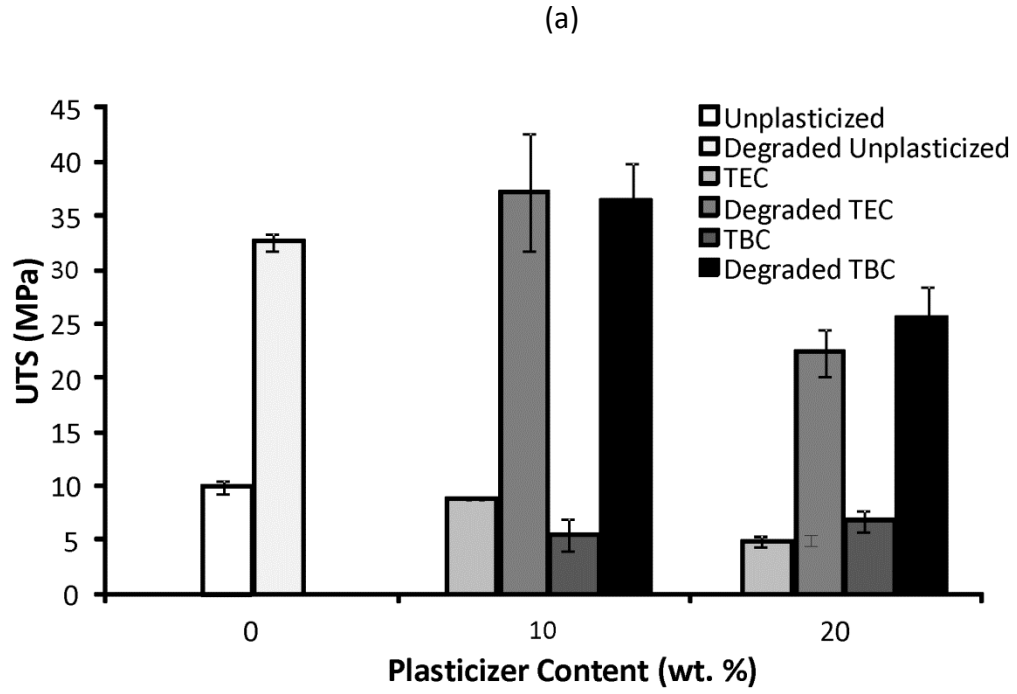


**Figure 3.6:** A) UTS of TBC and TEC films. 0 and 20 TEC were statistically different,  $p < 0.001$ . 0 and 20 TBC were statistically different,  $p < 0.01$ . B) Elastic modulus of TBC and TEC films. 0, 10, and 20 TBC were all statistically different from each other,  $p < 0.01$ . Both 10 and 20 TEC were statistically different from 0 TEC,  $p < 0.001$  but 10 and 20 TEC were statistically the same. C) Elongation of TBC and TEC films normalized by the cross-sectional areas (CSA). 0 samples are statistically different from 20 TBC samples,  $p < 0.05$ . 0 was statistically different from 10 TEC,  $p < 0.05$ . 20 TEC was statistically different from both 0 and 10 TEC,  $p < 0.001$ . Data are mean  $\pm$  standard deviation ( $n=3$ ).

### 3.3.4 Mechanical Properties After Incubation

Allowing the films to soak in PBS for 2 hours drastically changed their properties, with the magnitude of some properties being five times different from those of the dry samples. With both TEC and TBC films, the UTS, E, and elongation (except for the 20 wt% TEC film) all increased after films soaked in PBS for 2 hours. When comparing the dry samples to their wet counterparts, the differences were always significant ( $p < 0.001$ ) for all UTS data for both TEC and TBC samples (Figure 3.7a). The elongation significantly decreased for 0 and 10 wt% TEC samples when they became wet, but the 20 wt% had an elongation that was the same when wet or dry (Figure 3.7c). For the TEC samples, the elastic modulus was significantly ( $p < 0.05$ ) affected by the duration in PBS for only the 0 wt% films (Figure 3.7b). Elastic moduli for the 0 and 20 wt% TBC films were significantly ( $p < 0.05$ ) higher after incubation in PBS. For both TEC and TBC films, the elongation increased ( $p < 0.001$ ) for 0 wt% and 10 wt% films, but not 20 wt%.





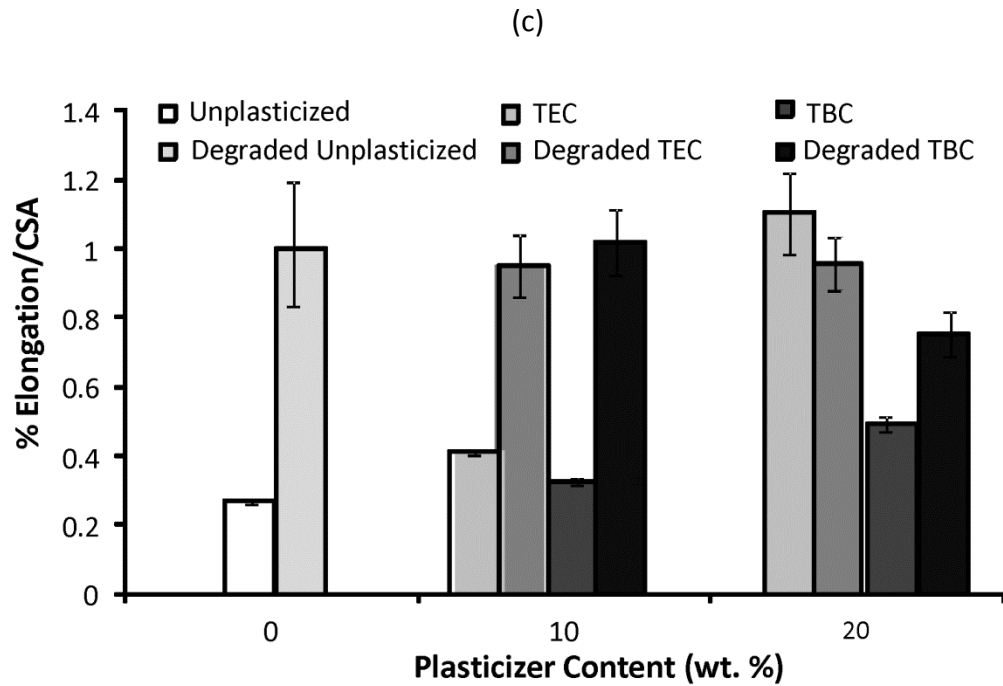


**Figure 3.7:** A) UTS of dry films and films incubated in PBS for 2 hours. Dry values compared to degraded values were all significantly different,  $p < 0.001$ . B) Elastic modulus of dry films and films incubated in PBS for 2 hours. 0 films were statistically different than their degraded counterparts,  $p < 0.05$ . 20 TBC was statically different from its wet counterpart,  $p < 0.05$ . C) Elongation of dry films and films incubated in PBS for 2 hours. Dry 0 and 10 TBC and TEC films were statistically different from their wet counterparts,  $p < 0.001$ . Data are mean  $\pm$  standard deviation ( $n=3$ ).

### 3.3.5 Morphology

Figure 3.8 shows representative SEM images of dry film surfaces and surfaces and cross-sectional areas after incubation in PBS for two hours. Samples appeared

smooth and had no porosity present before incubation. All of the samples had begun eroding after incubating in PBS for two hours. Porosity was seen both on the surfaces and in the cross-sections. As plasticizer content increased, more erosion occurred both on the exterior and interior of the film, resulting in increased porosity.

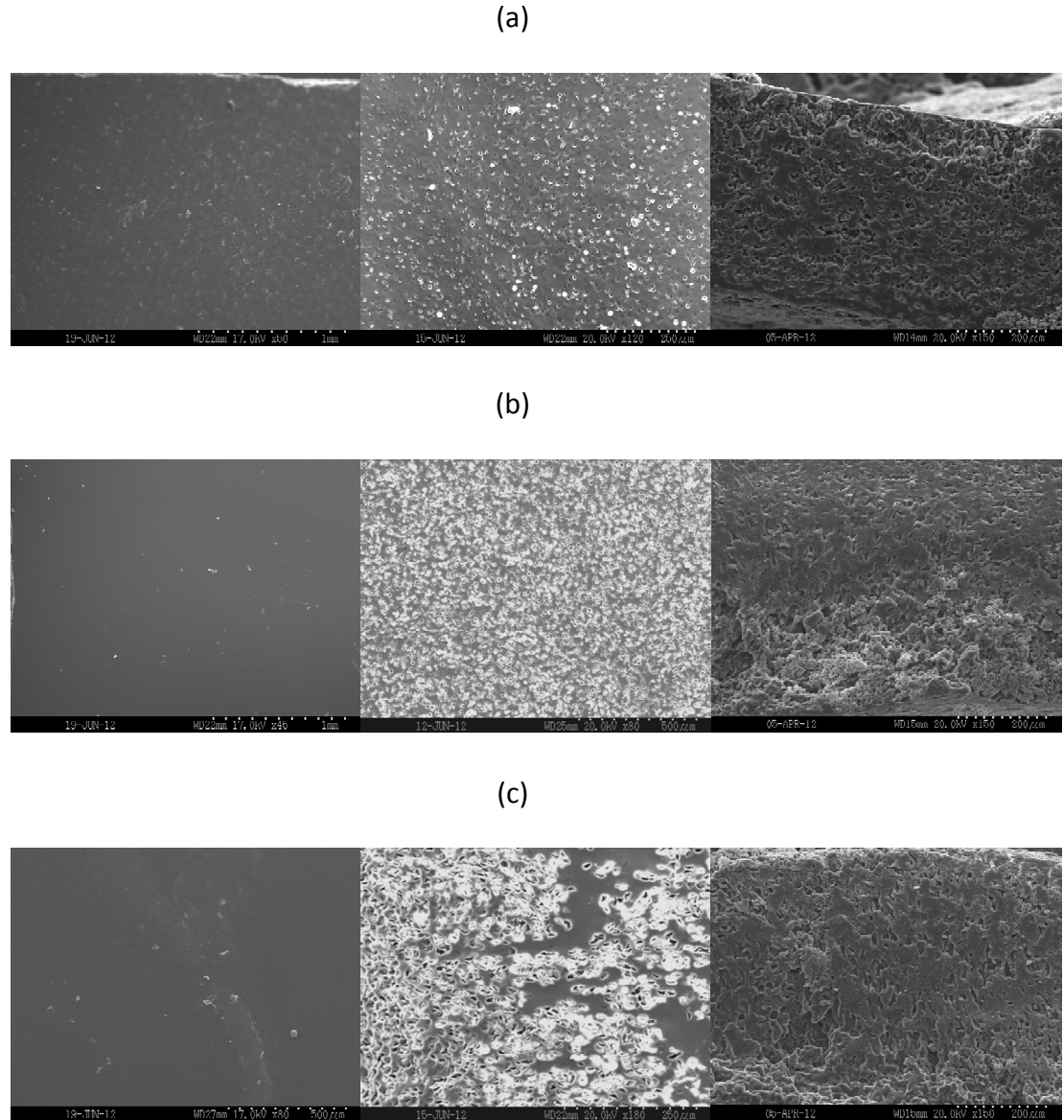
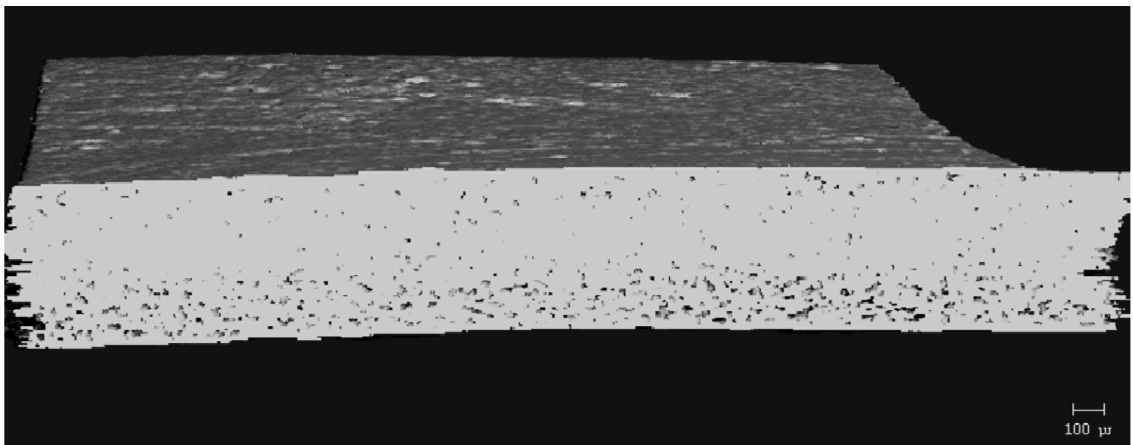


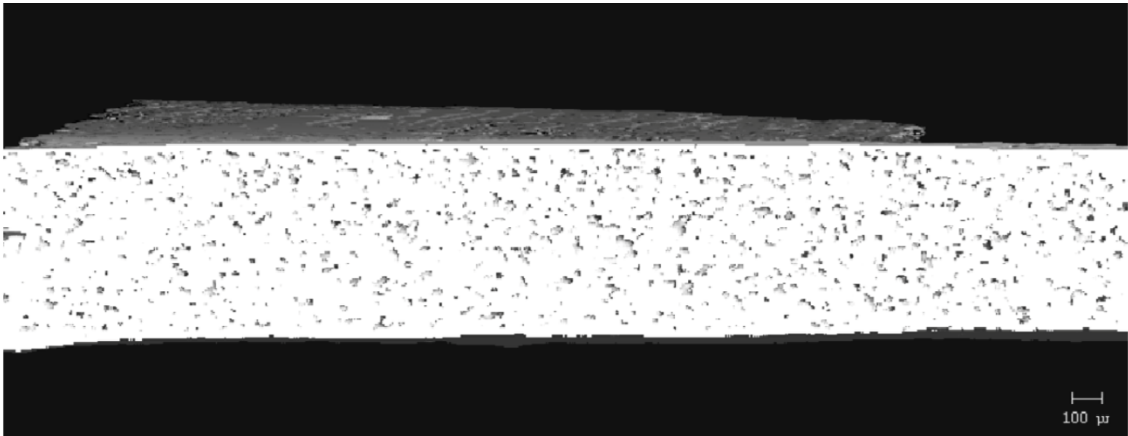
**Figure 3.8:** Scanning electron micrographs of the as-prepared surface (top left) and the surface (top right) and cross-section (bottom) of films incubated in PBS for 2 hours. A) 0, B) 10, and C) 20 wt% films.

MicroCT analysis quantitatively confirmed what was seen in the SEM images. Figure 3.9 shows cross-sectional slices of representative films before and after two hours in PBS, and the porosity of each film type is plotted in Figure 3.10. For TEC films, as plasticizer content increased, so did the porosity. The 20 wt% films increased to 17% porosity during incubation. The incubated samples were always statistically ( $p \leq 0.05$ ) different from their dry counterparts. Incubated 0 and 10 wt% samples were statistically the same, but both were significantly ( $p < 0.001$ ) different than the porosity measured in the 20 wt% films. With TBC films, plasticizer content did not affect the porosity after 2 hours in PBS. Porosity increased uniformly to just under 1%. Pore sizes for both TEC and TBC films were found to be as small as  $6 \mu\text{m}$ . The majority of the accessible volume in the films after erosion was from pores with a diameter of less than  $20 \mu\text{m}$ . There were almost no pores present that were larger than  $40 \mu\text{m}$  in either TBC or TBC plasticized films.

(a)



(b)



(c)

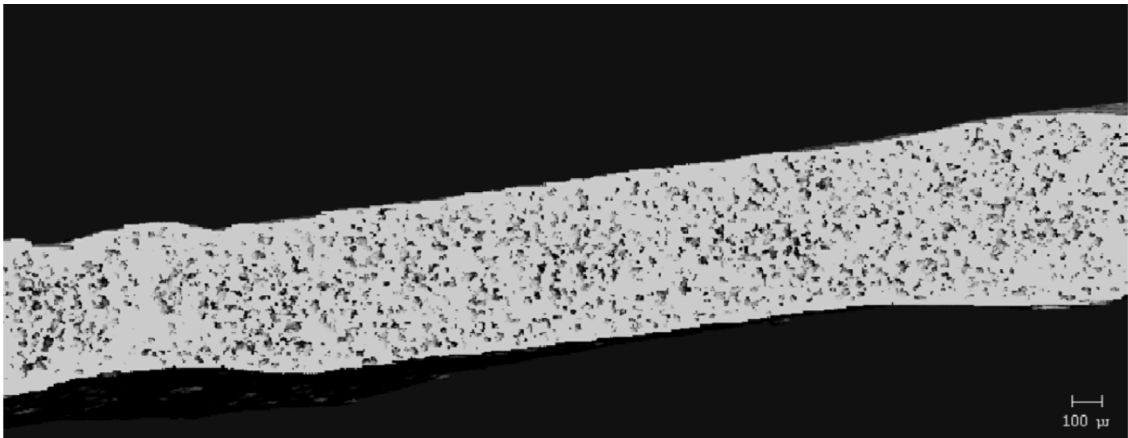


**Figure 3.9:** Micro CT images showing A) 0, B) 10, and C) 20 wt% films incubated in PBS for 2 hours.

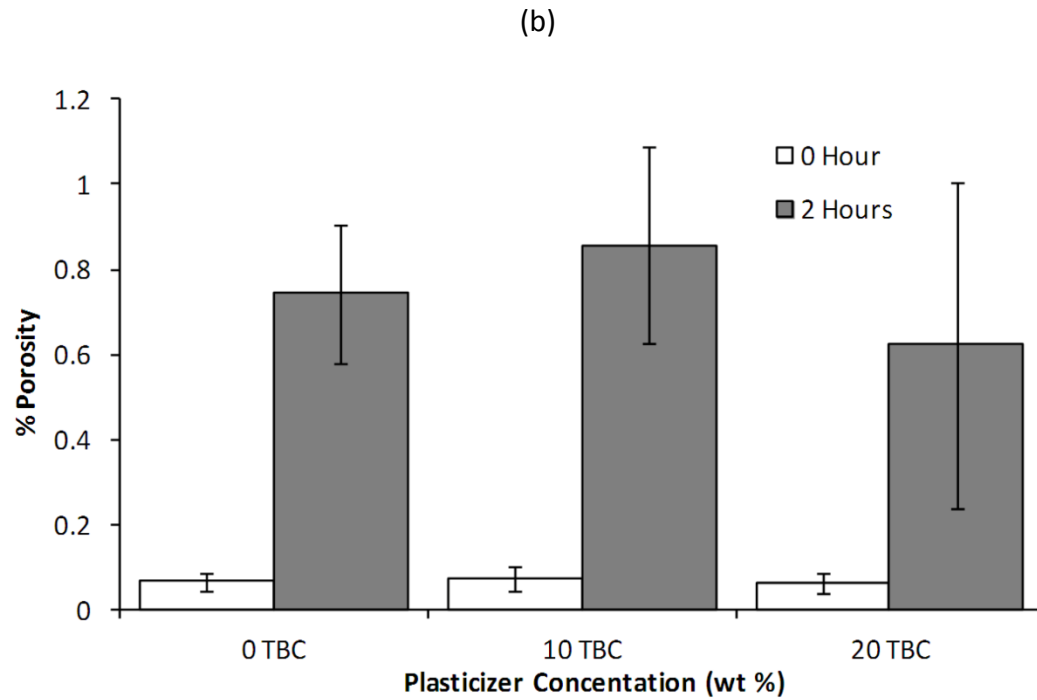
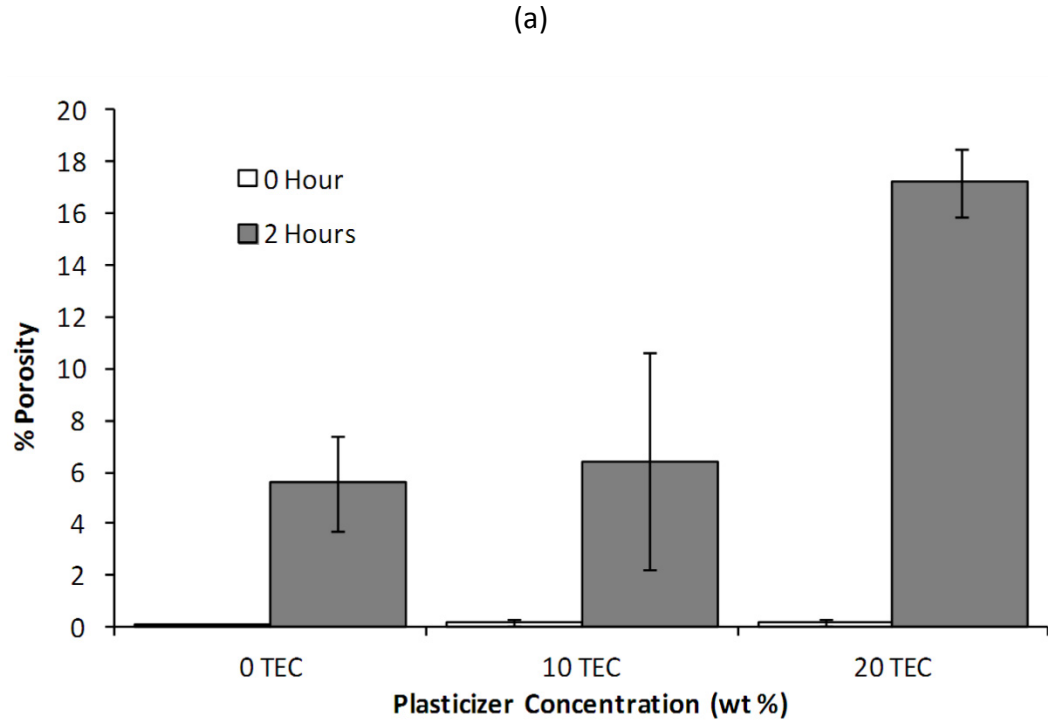


**Figure 3.10:** Porosity measurements for as-prepared films and films incubated in PBS for 2 hours. A) TEC-containing films. 20 TEC was statistically different than 0 TEC, p

< 0.05. B) TBC-containing films. No statistical difference between incubated samples, and no statistical difference between non-incubated samples.

### 3.4 Discussion

CAP-Pluronic films are rigid and unable to conform to the varying topology of soft tissue defects that may occur in motor vehicle accidents or war wounds. In order to aid in placement of the films, imparting flexibility and allowing the films to contour to any shape, plasticizers were added. With the aim of making the FDA approval process quicker, plasticizers that were already deemed safe were chosen for the CAP-Pluronic films. Both triethyl citrate and tributyl citrate are common plasticizers used in pharmaceutical and biomedical devices (102, 103, 154, 155). The United States Pharmacopoeia deems both TEC and TBC appropriate to be used in pharmaceutical dosage forms (103). They are used in gelatin capsules, enteric coatings on pills, and transdermal drug delivery patches (154-156). They are also used in poly(vinyl chloride) and poly(vinyl acetate) components of medical devices, including tubing and films (157). Toxicology studies show that take orally, TEC can be toxic to rats at excessively high doses, corresponding to over half a liter in a 70 kg man. TBC is non-toxic in rats even at extremely high doses (158). For a wound that is 10 by 10 centimeters, a layered, drug loaded film would contain approximately 5 mL of plasticizer (0.07 mL/kg), which is well within the toxicity limits for a 70 mg man.

Triethyl citrate and tributyl citrate have molecular weights of 276.28 g/mol and 360.45 g/mol, respectively. This means that, for the same weight percent, more TEC



molecules are present in the films than TBC molecules (TEC: 0.74 mol per film for 10 wt%, TBC 0.58 mol per film for 10 wt%). The same molar concentration was not compared between TBC and TEC since plasticizers are most commonly added as a weight percent of the whole polymer. However, the 20 wt% films had 1.57x more plasticizing molecules than the 10 wt% TEC and they had very similar effects on the % elongation, UTS, and E, which shows that even with fewer molecules present, TEC plasticizes to a greater degree than TBC. Plasticizers with a lower molecular weight cause more flexibility in the material they are incorporated into because they have a higher mobility and allow polymer chains to more easily slide across one another (156). With more lubricating plasticizer added to the films, a greater number of molecules were present between the polymer chains, which thereby increased the molecular separation and decreased the packing order of CAP and Pluronic F-127 (103). Because of this, for the same weight percent of plasticizer added, the TEC had more of an impact on the mechanical properties of the CAP-Pluronic F-127 films.

The mechanical properties changed rapidly after films were incubated in PBS, because much of the plasticizer leached out in the first two hours of degradation (159). Mass spectroscopy confirmed the plasticizer leach out by the presence of plasticizer in the supernatants of plasticized samples (results not shown). The TEC may leach out more quickly than the TBC because it is more hydrophilic than the TBC, and having smaller molecules also allowed it to travel down its chemical gradient faster. Triethyl citrate is a water soluble plasticizer up to 65 g/L, while TBC is a water-insoluble

plasticizer (160, 161). Differences in the solubility of TBC and TEC explain the differences in the supernatant's appearance during degradation. The milky appearance was likely due to the TBC separating out from the PBS solution as the molecules leached out since it is insoluble in water, while the supernatant from the TEC films remained clear since it had not reached its solubility limit. Plasticizer leach out will not be an issue since the polymer will be in the shape of the wound and the film will only become stronger. After the film has been laid in place, there will no longer be a need for flexibility and the increased strength of the film will cause it to be a protective barrier during healing.

Pluronic F-127 may be eroding at a faster rate than CAP causing the porosity seen in the 0 wt% films. CAP is commonly used in enteric coatings because of its low water solubility. It dissolves at higher pH and therefore more slowly than Pluronic F-127 (162). This, in addition to the plasticizer leaching out, created the nanometer- and micron-sized voids seen in the SEM and microCT images. The pores increased the surface area and allowed the films to degrade at a faster rate. The films containing more plasticizer may allow the Pluronic degradation to occur more quickly. As voids are created in the film, PBS can penetrate the films more deeply. Water causes disassociation of the hydrogen bonds linking the ether oxygens from the Pluronic F-127 to the carboxylic acid groups on CAP, leaving behind a material that contains increasing amounts of CAP relative to all of the other materials. Because CAP is a stronger polymer than Pluronic and the association polymer they form together, erosion actually

increased the strength of the material (163, 164). The ultimate tensile strength and elastic modulus increased since the polymer chains could not stretch and begin to slide past each other as easily as before incubation. But interestingly, the elongation also increased. This is likely due to the small holes that were created in the polymer which allowed it to behave and stretch more like a sponge. As tension was applied to the wet material, the holes collapsed and caused the remaining chains to elongate. CAP is a stiffer, slower eroding material than Pluronic F-127, so even the 0 wt% samples had an increase in the elastic modulus and ultimate tensile strength as CAP became the predominant material in the films.

Before plasticization, the CAP-Pluronic system is less rigid than other drug delivery polymers such as Eudragit, which has a modulus of 500 MPa or chitosan, which has a modulus of over 1000 MPa without plasticizer (146, 165). CAP-Pluronic F-127 is a competitive system for drug delivery applications because it is surface eroding so drug is released as the device erodes, and since it erodes, no material is left behind to cause inflammation. Another beneficial property is its lower elastic modulus allowing it to be more flexible and contour and set to the shape of varying wounds when it is plasticized.

### **3.5 Conclusion**

The degradation behavior and mechanical properties of CAP-Pluronic films can be varied by the type and amount of plasticizer incorporated into the system. The material properties will change shortly after the CAP-Pluronic drug delivery films are exposed to fluid. These changes do not affect the integrity of the system, since the

material only gets stronger and will maintain the shape formed in the tissue. The CAP-Pluronic system is attractive for a variety of soft tissue drug delivery applications because it could be tailored to have different properties.

## Chapter 4

### The Combined Effects of Drugs and Plasticizers on the Properties of Drug Delivery Films

This chapter will be submitted for publication, "Rabek C. L., Dziubla T.D., and Puleo D.A., The Combined Effects of Drugs and Plasticizers on the Properties of Drug Delivery Films."

#### 4.1 Introduction

Large soft tissue defects are common in motor vehicle accidents as well as in military injuries. Open wounds accounted for 10.3% of the 5.3 million non-fatal injuries from traffic collisions in the U.S. in 2000, and about 50% of all military injuries involve musculoskeletal wounds to the extremities (1, 2). Aberrant wound healing results in extended inflammatory phases leading to the formation of fibrotic tissue (7, 12, 166). The greater the defect size, the longer the healing process will be (167), and infection and ischemia further prolong inflammation (60, 168). Wound location and the patient's health and age also affect duration of the inflammatory phase (169). Secondary union wounds, where exposed soft tissue requires re-epithelialization, can result in scar contractures with negative esthetic and functional consequences (28, 58, 170). As such, there is a need for treatments that can simultaneously enhance wound healing while reducing fibrotic scar tissue formation.

Scar tissue formation could potentially be reduced or prevented if wounds were treated with individual or a combination of molecules targeted to the specific pathways of the healing process. The two drugs used in this study were quercetin and pirfenidone. Quercetin is a naturally occurring molecule that increases cell proliferation, decreases superoxide activity, and reduces wound contraction (113, 116, 145, 171). Reactive oxygen species are predominately released by infiltrating macrophages during the wound healing process and act as pro-inflammatory mediators (3). Thus, quercetin can inhibit oxidative stress to decrease inflammation. Pirfenidone is a pharmaceutical that has been shown to reduce fibrosis and scarring by down-regulating adhesion molecules and certain cytokines and growth factors, including interleukin  $1\beta$  and transforming growth factor- $\beta_1$  (119-123).

The wound healing device examined in this study was an erodible drug delivery film made of cellulose acetate phthalate (CAP) and Pluronic F-127 (Pluronic) (95). As the polymer erodes, drugs can be released from the system in a zero-order manner (96, 99, 151). CAP-Pluronic films are rigid, glassy polymers, but the addition of plasticizer increases flexibility, potentially allowing the devices to contour to the shape of varying wounds (101). The effects of plasticizers, in combination with different drugs, loaded in CAP-Pluronic films have not been previously studied. Films containing quercetin or pirfenidone with either triethyl citrate (TEC) or tributyl citrate (TBC) were investigated to determine the combined effects of drug and plasticizer on erosion, release, and mechanical properties.

## 4.2 Materials and Methods

### 4.2.1 Film Fabrication

Cellulose acetate phthalate (Sigma-Aldrich, St. Louis, MO) and Pluronic F-127 (Sigma-Aldrich) were combined in a 70:30 weight ratio, respectively, for a total mass of 2 g per film. Either tributyl citrate (Sigma-Aldrich) or triethyl citrate (Sigma-Aldrich) was combined with the CAP and Pluronic at 0, 10, or 20 wt%. Quercetin (10 or 100 mg; Sigma-Aldrich) or pirfenidone (6.1 or 61 mg; Tokyo Chemical Industries, Portland, OR) was added to the mixture (Figure 1). The low and high loadings of the two drugs are molar equivalents at 0.033 and 0.33 mol. A 25% (w/v) polymer solution was made by adding acetone to the CAP, Pluronic F-127, plasticizer, and drug. Mixtures were vortexed to ensure uniform dissolution of the components, cast into Teflon dishes, and the acetone allowed to evaporate at 10°C overnight. Films were desiccated overnight before analysis. Each sample is subsequently referenced by the drug loading within individual samples (approximately 64 µg, 640 µg, 39 µg, or 390 µg).

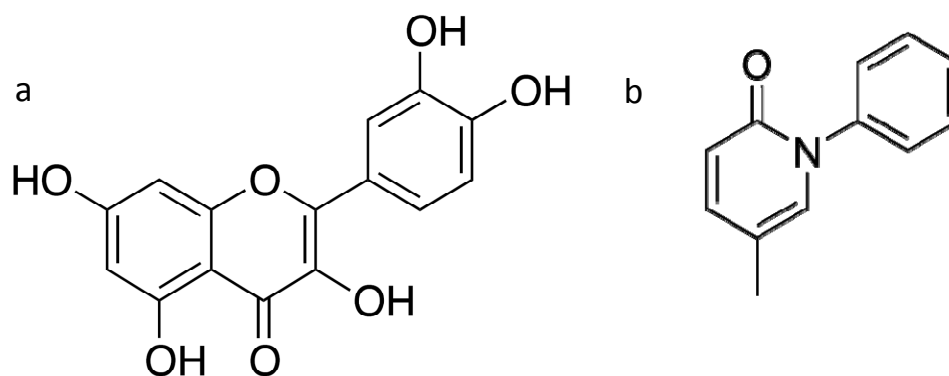


**Figure 4.1:** Chemical structures of quercetin (a) and pirfenidone (b).

#### 4.2.2 Erosion and Drug Release Studies

Five millimeter diameter discs were punched from the films. Samples were weighed to determine their initial mass and placed individually in 24-well plates. After adding phosphate-buffered saline (PBS), pH 7.4, to each well, the plates were gently agitated on an orbital shaker at 37°C. Three discs were collected and dried every hour, and their supernatants were saved for analysis of drug release. PBS in the remaining wells was replaced with fresh solution every hour. Dried samples were weighed to determine the final mass for calculating percentage mass loss.

High performance liquid chromatography (HPLC) analysis was performed using a Shimadzu Prominence system equipped with a Luna C-18 column (4.6 x 250 mm, 5 µm). For detection of quercetin, the mobile phase consisted of water containing 0.1% trifluoroacetic acid and methanol (30:70), with absorbance measurement at 254 nm. For detection of pirfenidone, the mobile phase consisted of water containing 0.2% acetic acid and acetonitrile (50:50), with detection at 310 nm. Injection volumes were 50 µl for all samples with a flow rate of 1 ml/min.

#### 4.2.3 Mechanical Properties

Microtensile test samples were punched from the films using a dog bone die (ASTM D1708) and the width and thickness of each sample measured using digital calipers. Tensile tests were performed in displacement control mode at a rate of 0.5 mm/sec using a BOSE ELF 3300 system. From the force and displacement data, along



with the dimensions of each sample, the elastic modulus (E), percent elongation normalized by the cross-sectional area, and ultimate tensile strength (UTS) were calculated.

#### **4.2.4 Statistics**

Samples of the same drug molar content, drug type, same plasticizer concentration, and plasticizer type, were compared against each other. Results were analyzed using two-way ANOVA, and a p-value < 0.05 was considered statistically significant. Regression comparisons to a 45° line representing surface erosion were performed on slopes and intercepts of the release vs. erosion plots. A linear regression p-value < 0.05 was considered statistically significant.

### **4.3 Results**

#### **4.3.1 Erosion and Release Studies**

The mass loss and drug release profiles for 0 and 10 wt% TEC and 0, 10, and 20 wt% TBC films loaded with 64 µg quercetin were linear (Figures 4.2a and 4.3a), with drug release rates from 9.3 to 13.0%/hr and erosion rates from 7.1 to 9.3%/hr. When mass loss and release were plotted against each other, quercetin-loaded TEC and TBC films followed along or below the 45° line that represents drug release based on only surface erosion (Figures 4.2b and 4.3b). The mass loss and drug release profiles for 20 wt% TEC films loaded with 64 µg quercetin both appeared more curved than the others but followed the 45° surface erosion line when plotted against each other. When the

same molar amount, 0.033 mol per film (39 µg per sample), of pirfenidone was added to the films, the cumulative drug release profile did not have the same linear behavior (Figures 4.2c and 4.3c). Over 9% more pirfenidone was released in the first six hours compared to the quercetin-loaded films ( $p < 0.001$ ). None of the TBC-plasticized, quercetin-loaded films reached 80% cumulative release at six hours, but all of the TBC-plasticized pirfenidone-loaded samples had released over 93% of their total loading (Figures 4.3a, 4.3c, 4.3e, and 4.3g). Similarly, with the TEC-plasticized films, the cumulative release at six hours was under 83% for all of the quercetin-loaded samples and was over 92% for all pirfenidone-loaded samples (Figures 4.2a, 4.2c, 4.2e, and 4.2g). Pirfenidone release slowed significantly after six hours (Figures 4.2c and 4.3c). The TEC-plasticized films loaded with 39 µg pirfenidone released 98% or more of the drug at six hours, while the 64 µg quercetin-loaded films had a maximum cumulative release of 91% at that time ( $p < 0.001$ ). When release from the TEC-plasticized films loaded with 39 µg pirfenidone was plotted against erosion, the first three data points were not significantly different from the 45° line for 10 and 20% TEC. For the last five data points, however, drug release was faster than the rate of mass loss (Figures 4.2d). The erosion versus release slope in this later region was significantly different from the 45° line ( $p < 0.01$ ) for both 10 and 20% TEC. The plot of release versus erosion for the TBC-plasticized, 39 µg pirfenidone-loaded films was initially above the 45° line, and even after the first half of the mass loss, release still increased faster than the films eroded (Figure 4.3d). When the quercetin loading was increased to 640 µg, TBC films released

drug over 1.5 times faster than mass was lost and did not fit the erosion-based model (Figures 4.3e and 4.3f). TEC films loaded with quercetin released the drug at a significantly slower rate than did the TBC films: 52-56% of the quercetin had been released by three hours for TEC-plasticized films, while 74-80% had been released by TBC-plasticized films ( $p < 0.001$ ). Quercetin release from TEC-plasticized films better followed the 45° erosion-based drug release line (Figures 4.2e and 4.2f). TEC and TBC films loaded with 39 and 390  $\mu\text{g}$  pirfenidone released drug at a faster rate than erosion occurred (Figures 4.2f, 4.2h, 4.3f, and 4.3h).

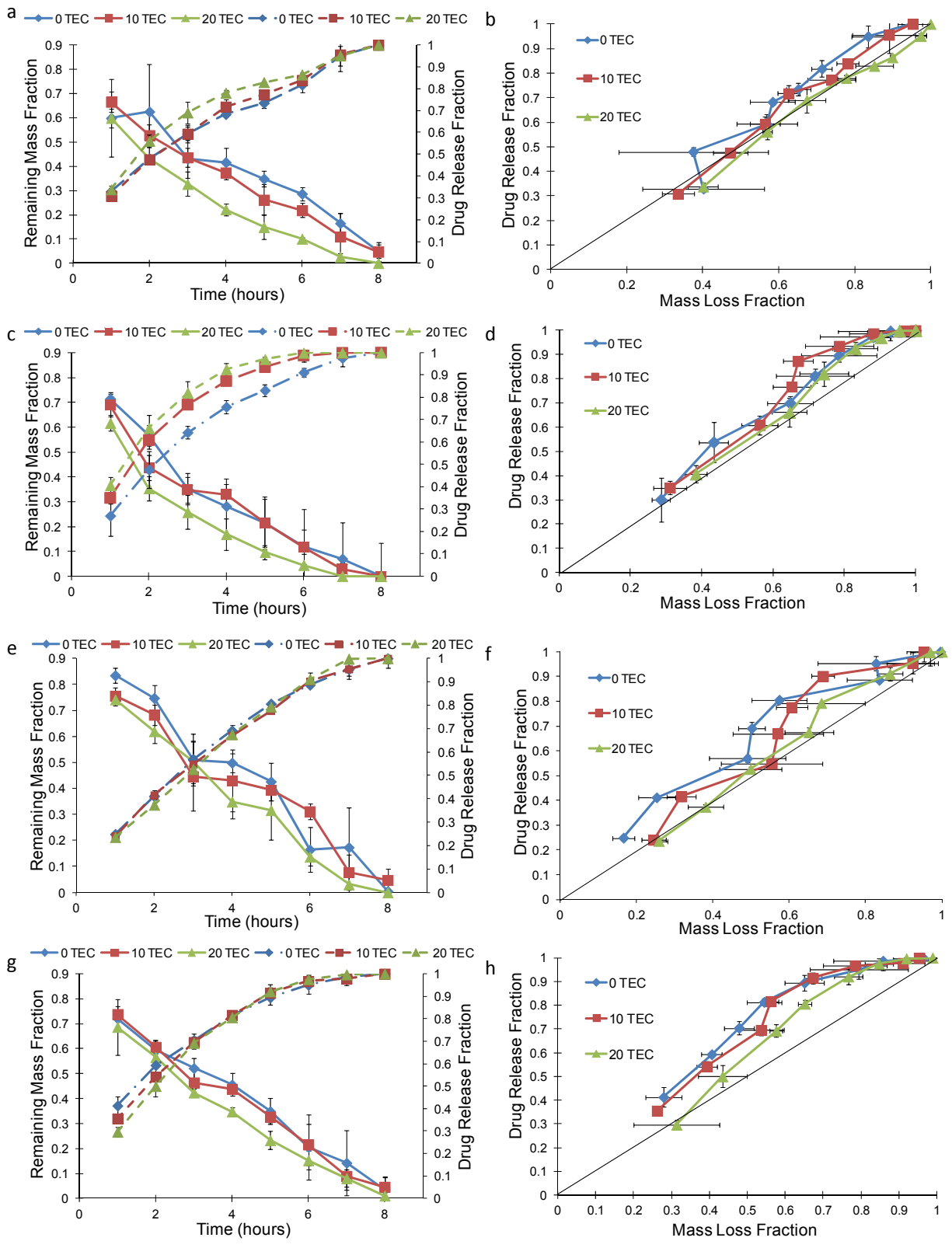


**Figure 4.2:** Release and erosion of TEC films loaded with 10 mg quercetin (a), 6.1 mg pirfenidone (c), 100 mg quercetin (e), and 61 mg pirfenidone (g). Release versus erosion of TEC films loaded with 10 mg quercetin (b), 6.1 mg pirfenidone (d), 100 mg quercetin (f), 61 mg pirfenidone (h). Data are mean  $\pm$  standard deviation (n=3).

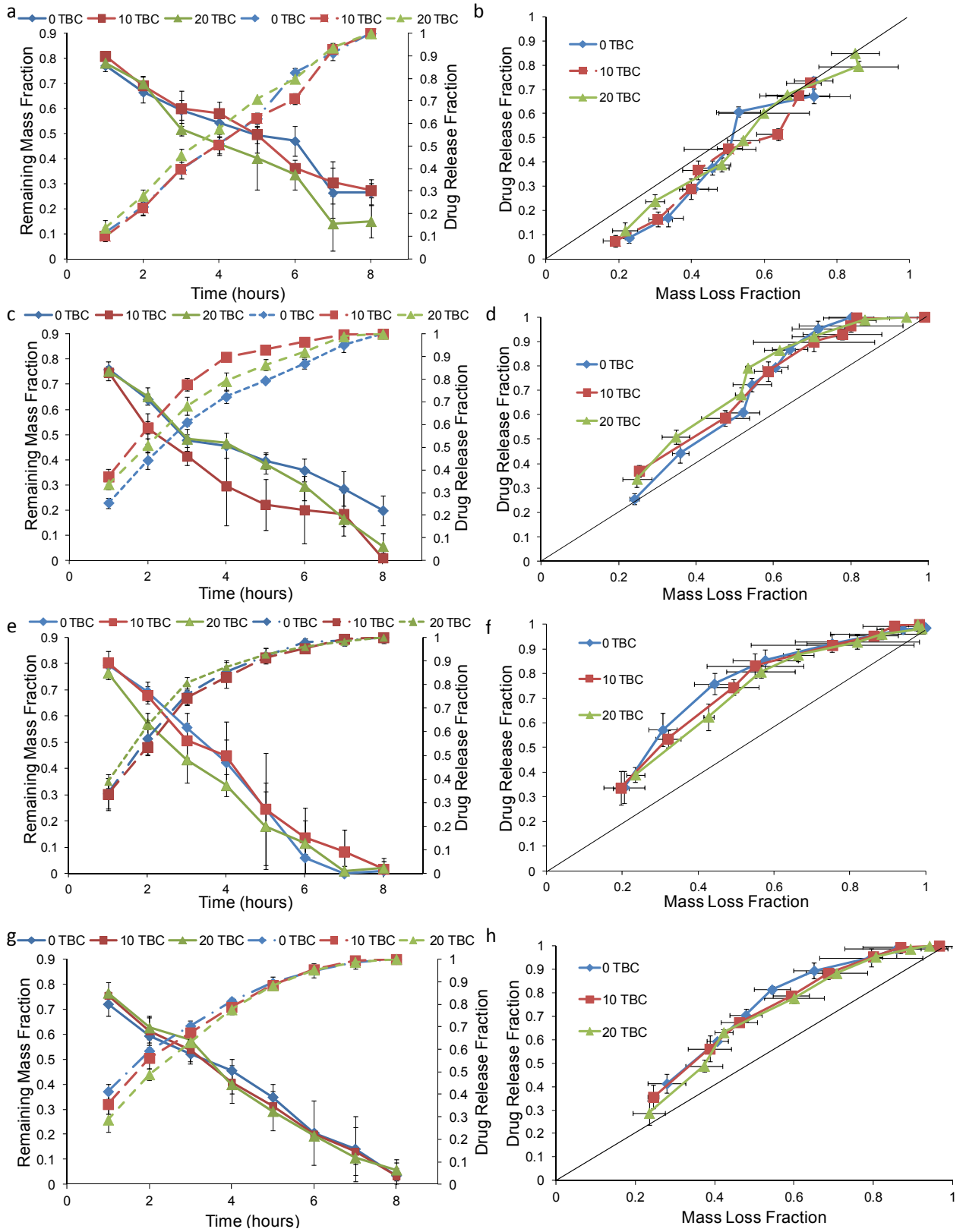


**Figure 4.3:** Release and erosion of TBC films loaded with 10 mg quercetin (a), 6.1 mg pirfenidone (c), 100 mg quercetin (e), and 61 mg pirfenidone (g). Release versus erosion of TBC films loaded with 10 mg quercetin (b), 6.1 mg pirfenidone (d), 100 mg quercetin (f), 61 mg pirfenidone (h). Data are mean  $\pm$  standard deviation (n=3).

#### 4.3.2 Mechanical Properties

Higher plasticizer contents of both TEC and TBC increased the elongation and decreased the elastic modulus of CAP-Pluronic films (Figure 4.4). Increased pirfenidone loading, from 0 to 390  $\mu\text{g}$ , in both TEC and TBC films caused a significant increase in E ( $p < 0.001$ ) (Figure 4.4a and Table 4.1). TEC films with 20 wt% plasticizer showed a significant decrease in E when quercetin loading increased from 0 to 640  $\mu\text{g}$  ( $p < 0.01$ ) (Figure 4.4b). The modulus of films plasticized with TBC and loaded with quercetin increased with drug content from 0 to 64  $\mu\text{g}$  and then decreased from 64 to 640  $\mu\text{g}$  ( $p < 0.001$  for 0 wt%;  $p < 0.01$  for 10 and 20 wt%) (Figure 4.4b). Increasing pirfenidone loading from 0 to 39  $\mu\text{g}$  significantly decreased elongation for all film types ( $p < 0.001$ ) (Figure 4.4c). Quercetin-loaded samples had significantly greater elongation with increasing drug content ( $p < 0.001$ ) (Figure 4.4d), and they elongated more than did pirfenidone-loaded films. For the same molar drug loading in 20 wt% TEC films, quercetin samples elongated 17 times more than did those containing pirfenidone ( $p < 0.001$ ). For 20 wt% TBC, quercetin films elongated 26 times more than pirfenidone-loaded samples ( $p < .001$ ).

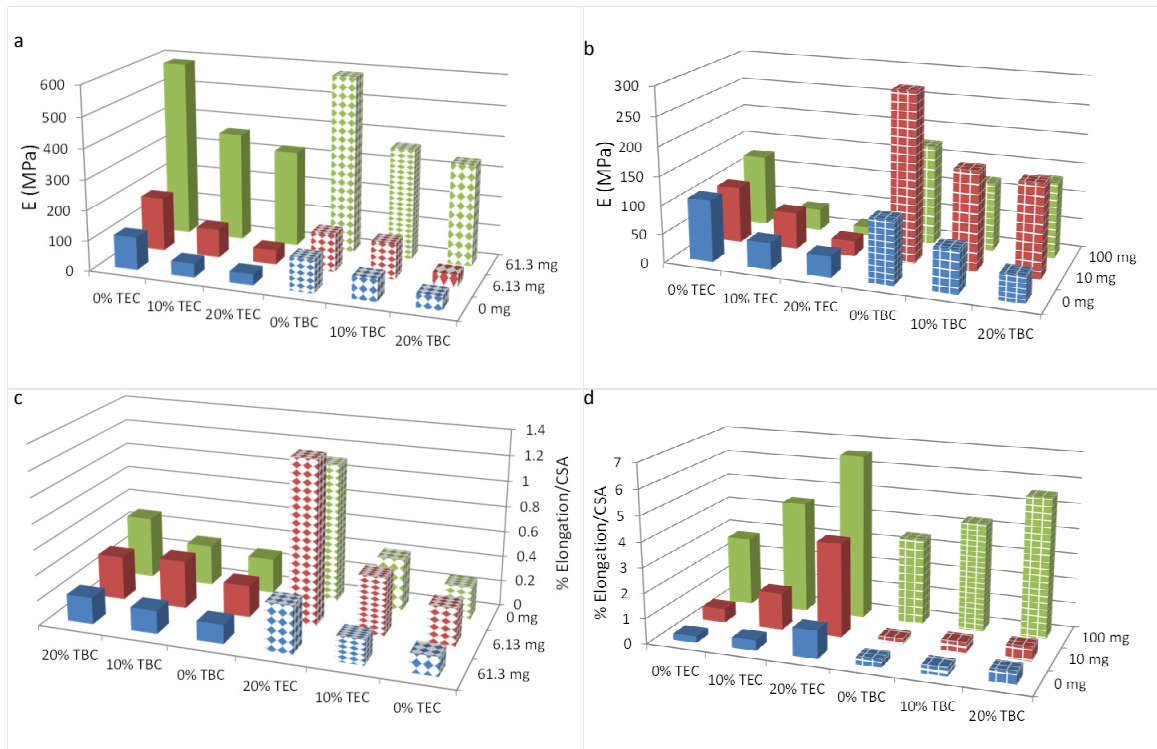


**Figure 4.4:** Elastic modulus of pirfenidone-loaded films (a) and quercetin-loaded films (b). Percent elongation normalized by the cross-sectional area of pirfenidone loaded films (c) and quercetin loaded films (d). Data are mean (n=3).



**Table 4.1:** Standard deviations of (a) elastic modulus and (b) elongation for pirfenidone or quercetin loaded films.

a

Plasticizer	TEC with pirfenidone			TBC with pirfenidone			TEC with quercetin			TBC with quercetin		
	0µg	39µg	390µg	0µg	39µg	390µg	0µg	64µg	640µg	0µg	64µg	640µg
0%	6.21	1.78	69.15	13.00	20.08	69.15	6.21	13.85	6.80	13.00	53.92	20.03
10%	0.43	27.90	44.84	9.84	7.35	56.19	0.43	3.97	3.25	9.84	65.17	7.74
20%	2.89	2.83	9.42	2.44	14.71	33.30	2.89	1.69	0.75	2.44	43.92	7.98

b

Plasticizer	TEC with pirfenidone			TBC with pirfenidone			TEC with quercetin			TBC with quercetin		
	0µg	39µg	390µg	0µg	39µg	390µg	0µg	64µg	640µg	0µg	64µg	640µg
0%	0.00	0.02	0.01	0.01	0.07	0.01	0.00	0.07	0.017	0.01	0.00	0.16
10%	0.01	0.00	0.02	0.01	0.05	0.01	0.01	0.11	0.28	0.01	0.03	0.30
20%	0.12	0.11	0.03	0.02	0.02	0.01	0.12	0.06	0.38	0.02	0.10	0.50

#### 4.4 Discussion

Two mechanisms govern drug release from CAP-Pluronic films: erosion and diffusion (172, 173). Erosion control release occurs when the loaded drug is released at the same rate at which the polymer vehicle erodes, which in the case of the CAP-Pluronic films is a zero-order process. In diffusion controlled release, water penetrates

the material to dissolve the drug or disassociate it from the polymer, thus enabling drug to diffuse from the matrix. Erosion and diffusion control represent two ends of the spectrum; release from most degradable or erodible polymer systems fall somewhere between the two. The mechanism of drug release from unplasticized 70:30 CAP-Pluronic films has been shown to be surface erosion (95, 98, 99). Other drug delivery systems, such as poly( $\epsilon$ -caprolactone), poly(DL-lactide-co-glycolide), ethylene vinyl acetate, and starch, are diffusion-controlled and would leave behind polymer once release is complete (81, 85, 174-176). In contrast, CAP-Pluronic films release drug as they erode, so material will not remain in the healing wound to cause an inflammatory reaction after the therapeutic dose is released (10, 97). Polyanhydrides can also be surface-eroding systems but require stabilizing co-monomers increase hydrophobicity to slow hydrolysis and thereby drug release (177, 178).

The effects of plasticizers on release of drugs from the CAP-Pluronic system had not been previously studied. In other polymers, plasticizers can increase or decrease the rate of release by either increasing the surface area after plasticizer leaches out or by creating a better barrier to the dissolution media (179, 180). The plasticizers, TEC and TBC, incorporated into the films are already commonly used in pharmaceuticals and in biomedical devices (103, 104, 181). Triethyl citrate is a hydrophilic plasticizer with an aqueous solubility of 12 mg/ml, but TBC exhibits limited solubility at 0.15 mg/ml (182-184). Tributyl citrate is a larger molecule than TEC, with molar masses of 276.28 g/mol and 360.45 g/mol, respectively.

The two drugs explored, pirfenidone and quercetin, have different solubility in water, 4.4 and 0.36 mg/ml at 25 °C, respectively (185, 186). The molar mass of quercetin is 302.24 g/mol, which is over 1.5 times that of pirfenidone at 185.22 g/mol. Quercetin also has 12 bonding sites (5 donor and 7 acceptor) that can interact and/or interfere with the association polymer system. For example, the phenol and enol groups of the drug can form hydrogen bonds with the ether oxygens in Pluronic F-127 (186, 187). Additionally, the ketones in quercetin may interact with the carboxylic acid of CAP. These associations could affect polymer erosion as well as the release of quercetin from the system. In contrast, pirfenidone has only two acceptor sites on the amide that could bond with the CAP-Pluronic system (185). Fewer acceptor sites, a smaller size, and increased hydrophilicity resulted in pirfenidone being released more easily from the micron-sized pores created as the system eroded(101).

Samples containing pirfenidone exhibited a dual mechanism of release. Surface erosion controlled the first half of the 39 µg pirfenidone release from TEC-plasticized films. The first half of release from 39 µg loaded pirfenidone TBC-plasticized films also predominantly occurred via surface erosion, but after the fourth hour, release occurred at a faster rate than polymer mass loss, signifying a transition to diffusion controlled release. The shift in the main mechanism of release did not occur for the other drug and plasticizer combinations. The 64 µg quercetin-loaded films all fit the 45° line closely, indicating that the mechanism of release was surface erosion. If some diffusion occurred, the effect was insignificant. Previous work found that film porosity, even in

unplasticized films, increased significantly after a two hour incubation in PBS (101). Development of pores increased the surface area by which drug was released from the surface-eroding system. As more drug was added to the system, the leading mechanism of release shifted from erosion to diffusion and increased the release rate. This shift has been seen in other drug release systems, including atenolol loaded ethylene-vinyl acetate films (81). With increased drug loading, the concentration gradient is steeper and less CAP-Pluronic is present to control the release. The voids left behind by the released drug allow molecules deeper in the device to also diffuse out. This was seen for higher loadings of both quercetin and pirfenidone.

As observed in previous studies, increasing the plasticizer content of both TEC and TBC led to decreased elastic modulus and increased elongation, resulting in a CAP-Pluronic film that will conform better to the complex shapes of wounds (101, 188, 189). Triethyl citrate plasticized the films to a greater degree than did TBC because it is a smaller molecule, and for the same mass, there were over 1.25 times as many TEC as TBC molecules present in the films. Although pirfenidone is a smaller molecule than either of the two plasticizers, it still may have physically interfered with the ability of TEC or TBC to plasticize the films by separating the polymer chains and interacting with the carboxylic acid of CAP. In the unplasticized films, this pirfenidone interaction reduced what little flexibility the CAP-Pluronic films alone had, which resulted in an increased modulus and decreased elongation as pirfenidone content increased. It is not uncommon to see an “antiplasticizer” effect when small amounts of drug or plasticizer

are added to polymer (174, 188, 190). The chemical structures of pirfenidone and quercetin fit Jackson and Caldwell's "antiplasticizer criteria" because they contain polar atoms, have at least two nonbridged rings, and have one dimension less than about 5.5 Å (190). The side groups of quercetin likely interacted with both polymers in the CAP-Pluronic system to result in synergistic effects on elongation and an increased modulus (191-193). The changes in the mechanical properties caused by the plasticizers and drugs did not correlate with differences in the release profiles. Mechanical testing occurred when the films were dry, and release occurred when the samples were wet, however. Previous work found that devices incubated in saline for two hours leached plasticizer resulting in increased strength (101). This phenomenon has been seen in other systems before, including sodium alginate-magnesium aluminum silicate films plasticized with polyethylene glycol 400 or glycerin (194). The chemical and mechanical changes that occur once the films are wet reduced any observable difference in the release.

#### **4.5 Conclusion**

Release from drug delivery films, particularly CAP-Pluronic films, can be controlled by the amount loaded and the drug properties, including size, hydrophobicity, and interactive side groups. The mechanical properties are also controlled by loading and the drug properties. Plasticizer can be introduced to further modulate films to achieve the desired mechanical properties. The combined effects of

drug and plasticizer on the properties of drug delivery films can range from antagonistic to synergistic. Different drugs and plasticizers can be added to CAP-Pluronic films to tailor the erosion, release, and mechanical properties needed for varying applications.

## Chapter 5

### Sequential Release of Multiple Drugs from Flexible Drug Delivery Films

This chapter will be submitted for publication, "Rabek C. L., Dziubla T.D., and Puleo D.A., Sequential Release of Multiple Drugs from Flexible Drug Delivery Films."

#### 5.1 Introduction

Sequential drug release is necessary for targeting the healing phases of soft tissue defects. After hemostasis, wounds undergo inflammation that, if not controlled, can result in excessive scar tissue formation during the proliferation stage (28, 195). Current research in drug delivery devices has fallen short in providing surface eroding systems capable of delivery multiple drugs in a sequential order and lasting for more than a couple days (196-199). In most systems, drug diffuses out leaving behind the polymer vehicle that could further inflame wounds.

The polymer films explored in this study were composed of cellulose acetate phthalate (CAP) and Pluronic F-127 (Pluronic). Together they form an association polymer that releases drug as the system erodes. Alone, CAP and Pluronic make a rigid polymer. To add flexibility to the system and allow it to contour to the shape of varying wound geometries, plasticizers were added. The two plasticized explored are citrates, triethyl citrate and tributyl citrate (Figure 5.2).

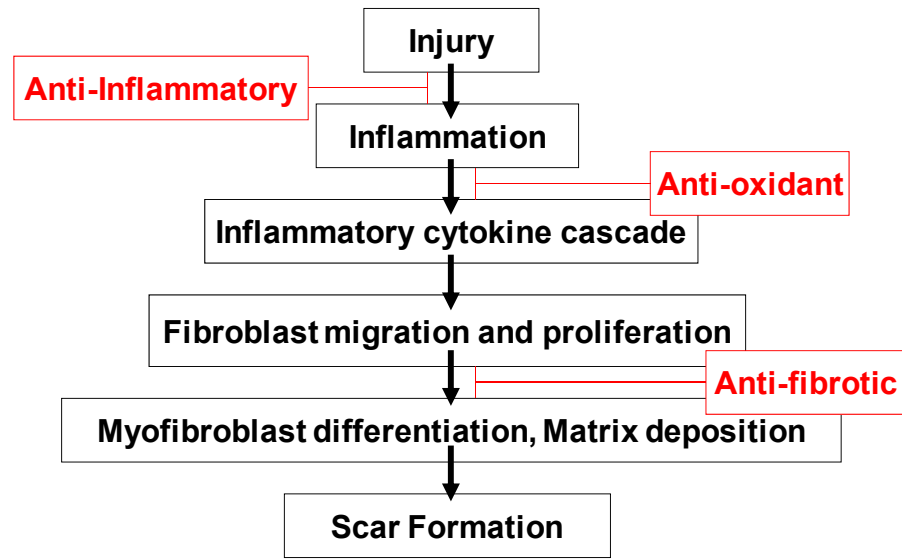


**Figure 5.1:** Wound healing stages and the planned drug targets.

The drugs examined during these experiments were chosen to combat the scar tissue formation outlined in Figure 5.1. The anti-inflammatory, anti-oxidant, and anti-fibrotic drugs chosen were ketoprofen, quercetin, and pirfenidone, respectively (Figure 5.2). Ketoprofen is an anti-inflammatory drug that reduces inflammation by non-selectively inhibiting cyclooxygenase (COX) (63, 108). Quercetin was the anti-oxidant drug chosen because it decreases superoxide activity and reduces wound contraction (114-116). Pirfenidone, an anti-fibrotic drug, was chosen because it reduced scar formation by decreasing cell adhesion molecules and reducing cytokines and growth factors, including interleukin 1 $\beta$  and transforming growth factor- $\beta$ 1 (119, 121, 123).



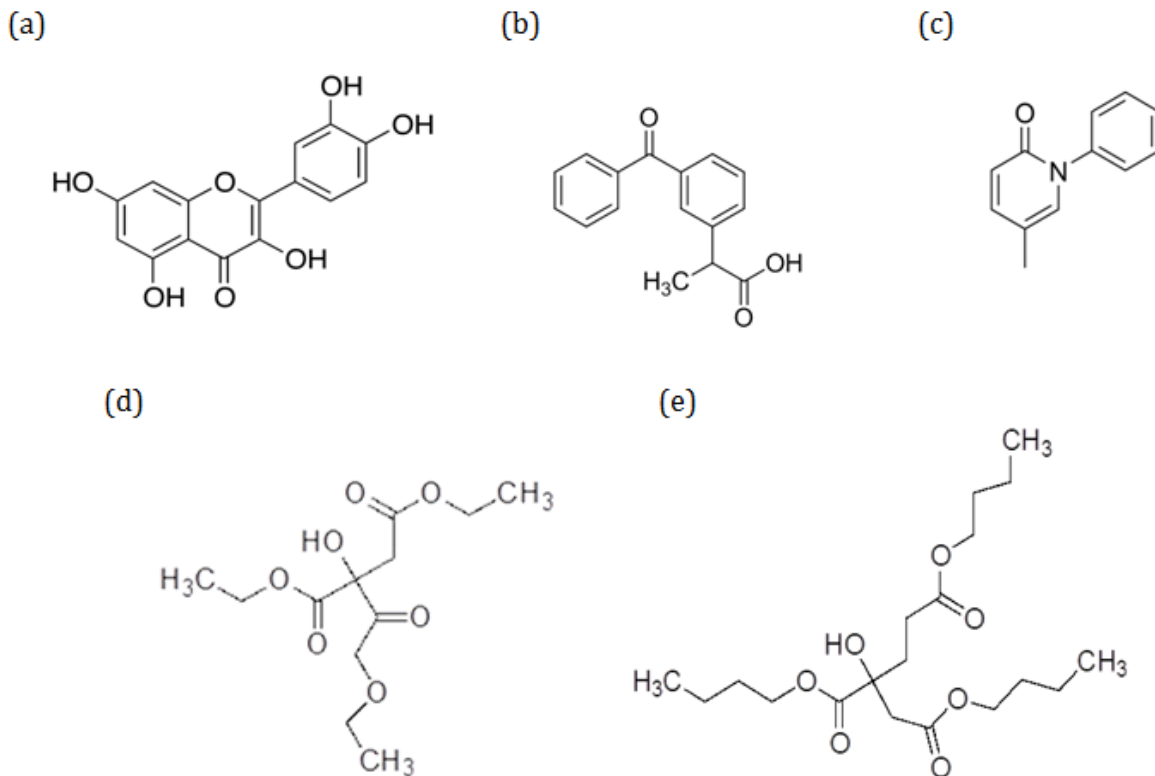


**Figure 5.2:** Chemical structures of drugs (a) quercetin, (b) ketoprofen, and (c) pirfenidone, and plasticizers, (d) triethyl citrate and (e) tributyl citrate.

## 5.2 Materials and Methods

### 5.2.1 Cytotoxicity Studies

Mouse myoblast cells (C2C12; ATCC CRL-1772) were seeded into 24-well plates at density of 15,000 cells/cm<sup>2</sup> and cultured in DMEM supplemented with 10% fetal bovine serum at 37°C in a humidified, 5% CO<sub>2</sub> incubator. After 24 hours, the medium was changed, and cells were exposed to different concentrations of TEC or TBC plasticizer diluted into the DMEM media for 24 hours. To determine the remaining viability of the cells after plasticizer exposure, an MTT (3-(4, 5-dimethylthiazolyl-2)-2,5-

diphenyl tetrazolium bromide) assay was performed. Three hundred  $\mu\text{L}$  of MTT, 5 mg/mL, were added to each well and incubated for 2 hours. After replacing the medium with 500  $\mu\text{L}$  of the extraction buffer, 20% sodium dodecyl sulfate in 50% N,N-dimethyl formamide, the plates were incubated at 37°C on an orbital shaker for 24 hr before reading absorbance at 570 nm.

### 5.2.2. Film and Device Fabrication

Polymer films were made by combining Pluronic F-127 (Sigma-Aldrich) and cellulose acetate phthalate (CAP; Sigma-Aldrich, St. Louis, MO) in a 30:70 weight ratio, respectively. Triethyl citrate (Sigma-Aldrich) or tributyl citrate (Sigma-Aldrich) were added to the CAP and Pluronic at 0, 10, or 20 wt% to create a 2 g film. Ketoprofen (100 mg; Sigma-Aldrich), quercetin (10 mg; Sigma-Aldrich) or pirfenidone (6.13 mg; Tokyo Chemical Industries, Portland, OR) were combined with the polymers and plasticizer. Acetone was added to make a 25% (w/v) mixture. To ensure homogeneity, the mixtures were vortexed. Then they were poured into Teflon dishes and kept in a 10°C refrigerator overnight to let the acetone evaporate slowly.

Two different device types were made, 4-layered devices and 9-layered devices. For the 4 layered devices, films were laminated using acetone and then punched into cylinders (6 mm). Ketoprofen and pirfenidone loaded films were separated by two blank films. The cylinders were inserted into polystyrene wells to ensure unidirectional erosion and release. Two device orientations were made, “forward” where the

ketoprofen layer was exposed first and “reverse” where the pirfenidone layer was exposed first (Figure 5.3).

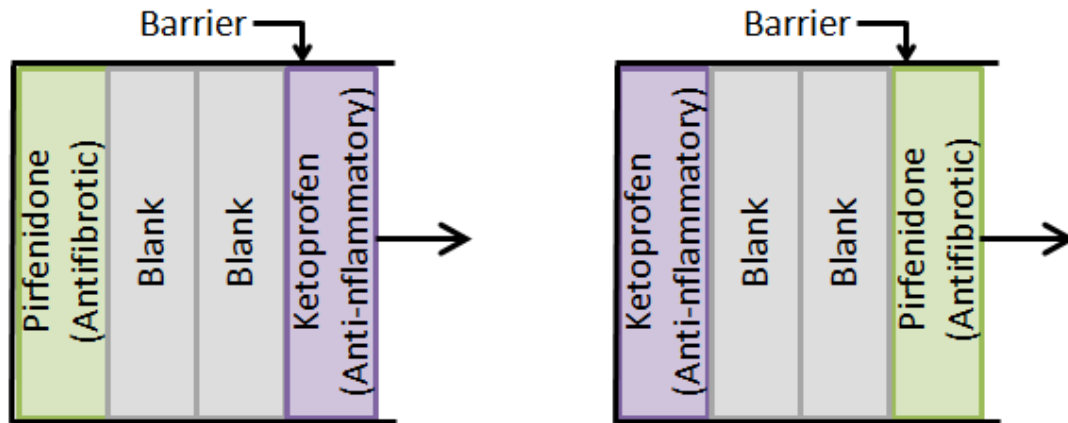


**Figure 5.3:** “Forward” (left) and “reverse” (right) device types.

For the 9 layered devices, the films were cut with cylindrical punches of increasing in diameter (Figure 5.4). The smallest layer (3.8 mm diameter), loaded with pirfenidone, was covered on either side by a blank layer of a larger diameter (5.5 mm diameter). The layers were laminated by painting acetone between the films. Larger diameter quercetin loaded layers (8 mm diameter) encased the blank layers. Another two blank layers (13.0 mm diameter) covered the quercetin-loaded layers. Ketoprofen-loaded films made up the outermost layers (18.2 mm diameter). All of the devices were desiccated overnight to remove all remnant acetone. Devices were then desiccated for 24 hours before analysis.

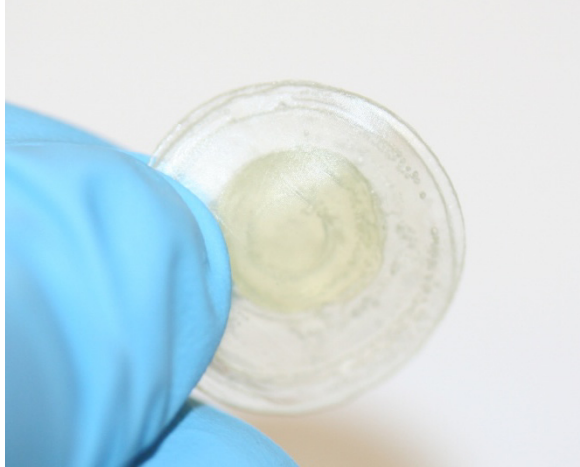


**Figure 5.4:** Nine layered device.

### 5.2.3 Drug Release Studies

Four-layered devices were placed individually into glass vials with 4 ml of phosphate-buffered saline (PBS). Samples were incubated at 37°C on an orbital shaker. Every 4 hours, supernatants were collected and replaced with fresh PBS. The nine-layered devices were placed into 50 mL test tubes with 30 mL of PBS. Every 12 hours, supernatants were collected (n=3) and replaced with fresh PBS. Supernatants were analyzed using high performance liquid chromatography (HPLC) to determine drug release at each time point. HPLC analysis was performed with a Hitachi Primaide system equipped with a Kinetix C-18 column (4.6 x 150 mm, 5 µm; Phenomenex). For detection of ketoprofen, the mobile phase consisted of water containing 0.1% TFA and acetonitrile (40:60), and UV absorbance was measured at 258 nm. For detection of pirfenidone, the mobile phase was water containing 0.2% acetic acid and acetonitrile (50:50) and

measurement occurred at 310 nm. Flow rates were 1 ml/min with injection volumes of 50  $\mu$ l for all samples.

#### **5.2.4 Erosion Studies**

Initial masses were determined for the 9-layered devices. Every 8 hours devices were removed from the supernatant, lightly patted dry, and weighed.

#### **5.2.5 Mechanical Properties**

A dog bone-shaped die (ASTM D1708) was used to punch the four-layered microtensile test samples. Samples were desiccated overnight before calipers were used to measure the width and thickness of the laminated samples. Tensile testing was performed on a BOSE ELF 3300 system in ramp mode with a displacement rate of 0.5 mm/sec. The elastic modulus (E), percent elongation normalized by the cross-sectional area, and ultimate tensile strength (UTS) were calculated using the sample dimensions and force and displacement data.

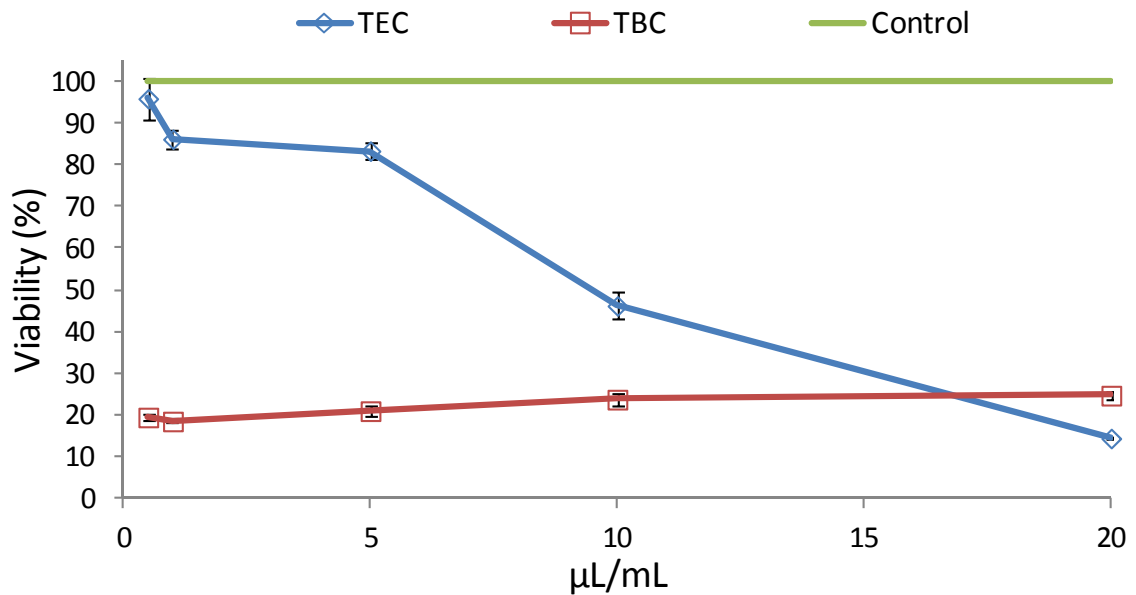
#### **5.2.6 Statistics**

All of the samples of the same plasticizer concentration or plasticizer type were compared against each other. Results were analyzed using two-way ANOVA, and a p-value < 0.05 was considered statistically significant.

## 5.3 Results

### 5.3.1 Cytotoxicity Studies

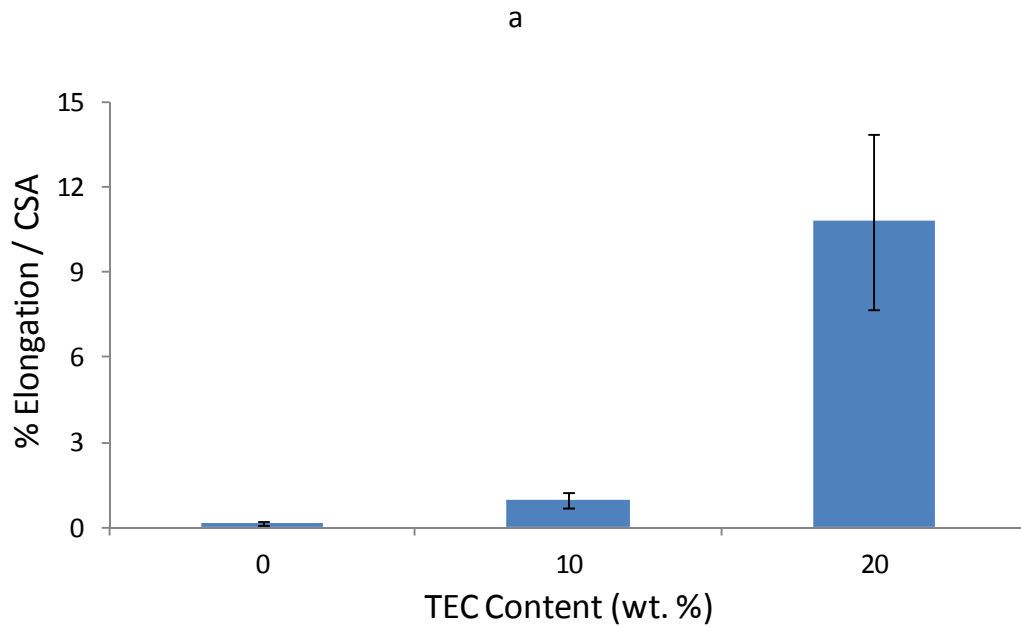
Triethyl citrate was significantly less toxic to C2C12 cells than was tributyl citrate at 0.5, 1, 5, and 10  $\mu\text{L}/\text{mL}$  ( $p < 0.001$ ). Even at low concentrations, 0.5  $\mu\text{L}/\text{mL}$ , TBC was found to be toxic to the cells (Figure 5.5). In contrast, TEC had no significant impact on cell viability at this concentration. At 10  $\mu\text{L}/\text{mL}$  of TEC, only about half of the exposed cells were still viable. As the concentration of TEC increased, cell viability decreased. Because of these results, all further studies were performed using only TEC-plasticized films.



**Figure 5.5:** Cell viability after plasticizer exposure. Data are mean  $\pm$  standard deviation ( $n=3$ ).

### 5.3.2 Mechanical Properties

Increasing plasticizer concentration increased the elongation and decreased the ultimate tensile strength and modulus (Figure 5.6). Layered films that were not plasticized (0 wt % TEC) had a significantly higher elastic modulus and ultimate tensile strength than films that were plasticized ( $p < 0.01$  and  $p < 0.0001$ , respectively). For elongation, every increase in plasticizer concentration was significantly different ( $p < 0.05$ ).



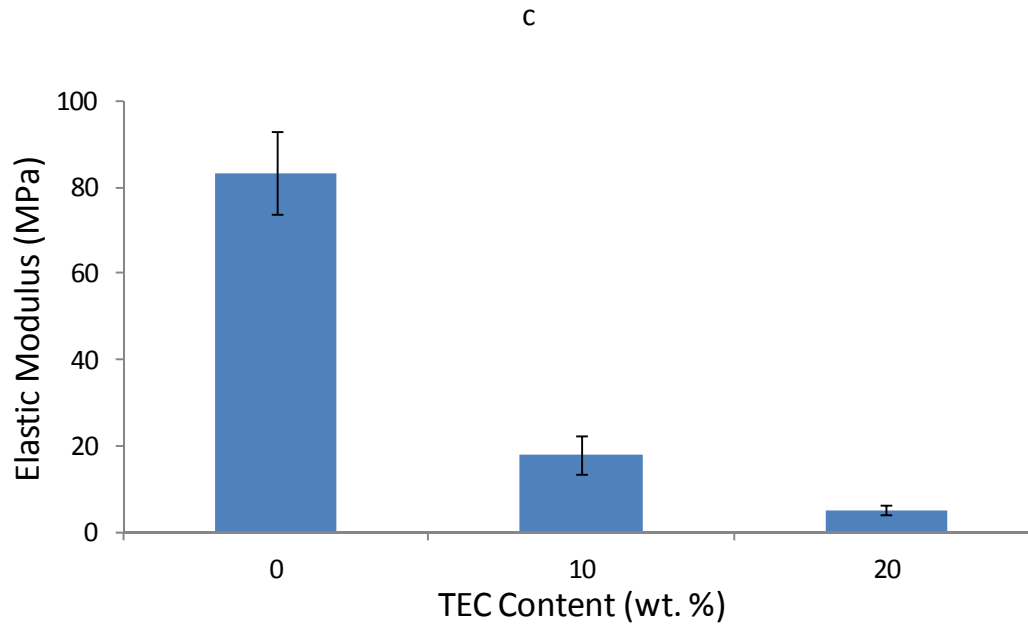
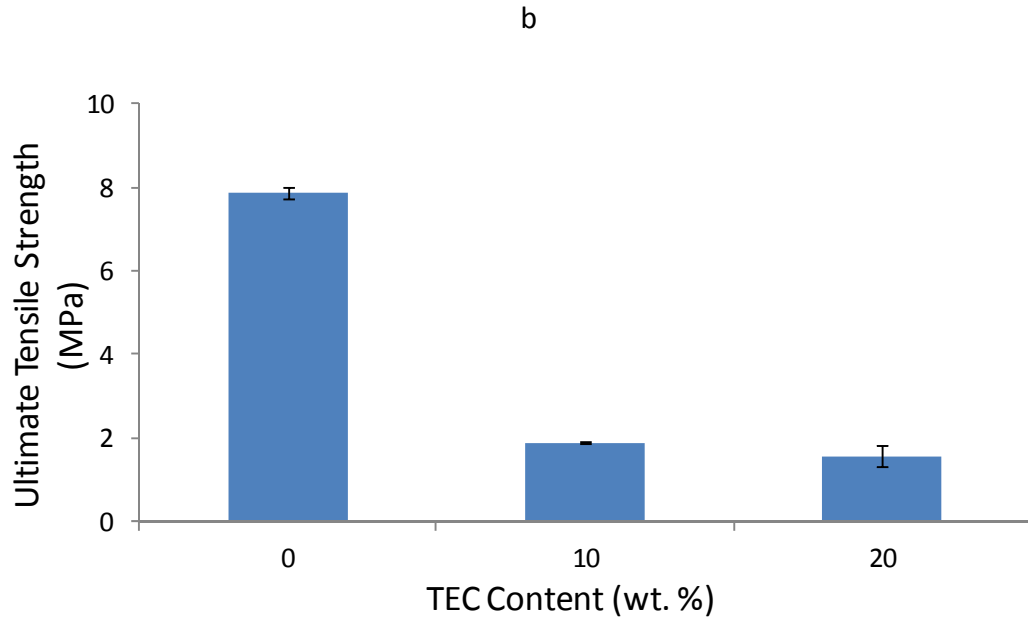
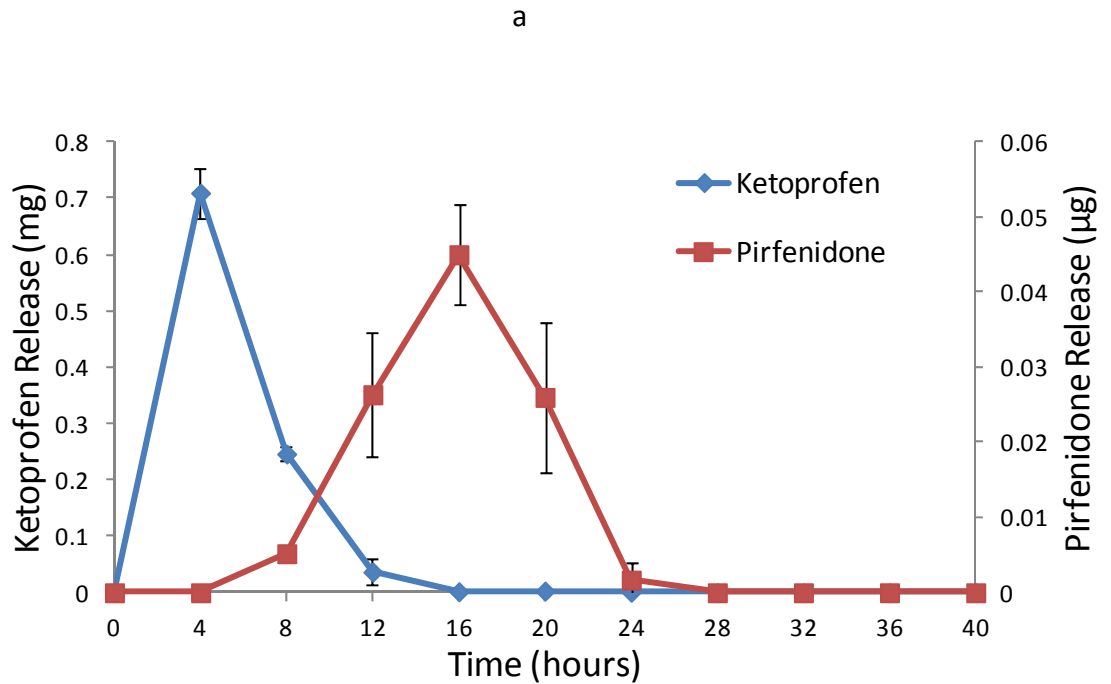


**Figure 5.6:** Mechanical properties of 4-layered devices: (a) % elongation, (b) ultimate tensile strength, and (c) elastic modulus. Data are mean  $\pm$  standard error (n=3).



### 5.3.3 Four-Layered Device Release Studies

For the 4-layered “forward” devices, peaks of ketoprofen and pirfenidone release occurred at 4 and 16 hours, respectively, regardless of plasticizer concentration (Figure 5.7). The overlap of the ketoprofen and pirfenidone peaks was 12 hours for all three plasticizer concentrations. The area under the two release curves corresponds to overlap release of both ketoprofen and pirfenidone. This “area under the curves” was also not significantly affected by the plasticizer concentration (Figure 5.8).



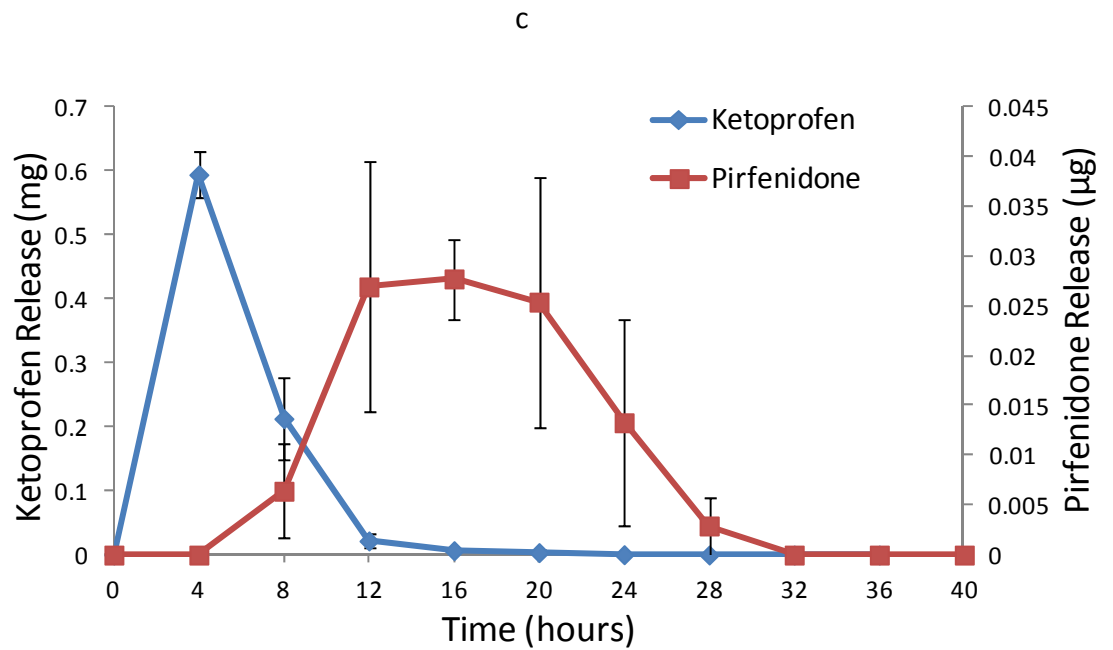
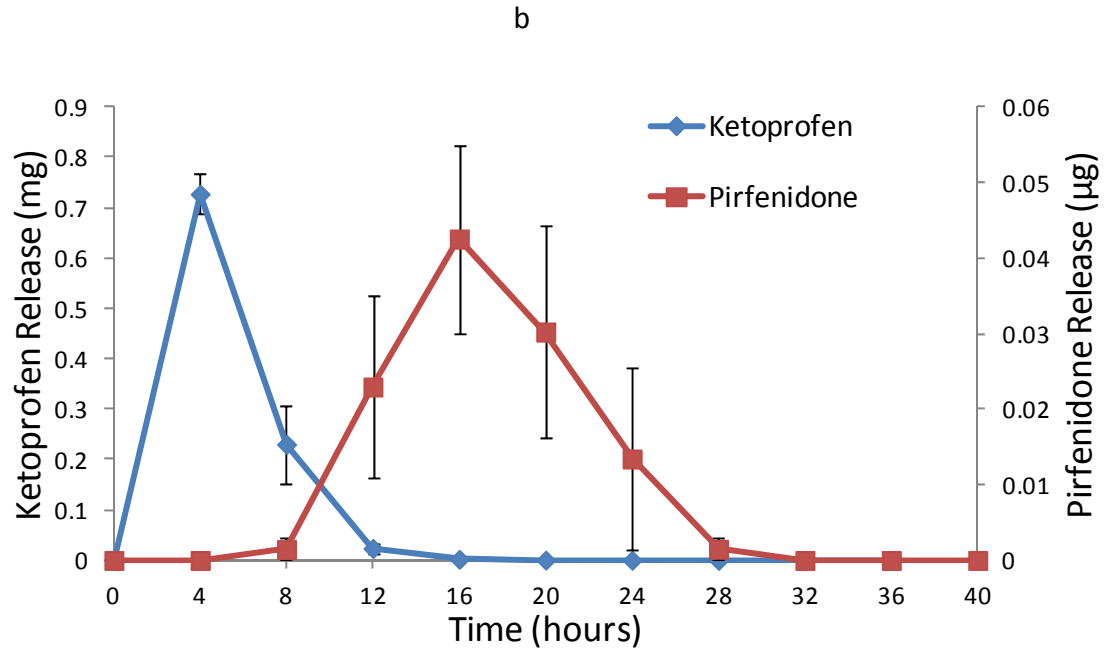


**Figure 5.7:** Release from “forward” 4-layered devices plasticized with (a) 0 TEC,

(b) 10 TEC, and (c) 20 TEC. Data are mean  $\pm$  standard error (n=3).

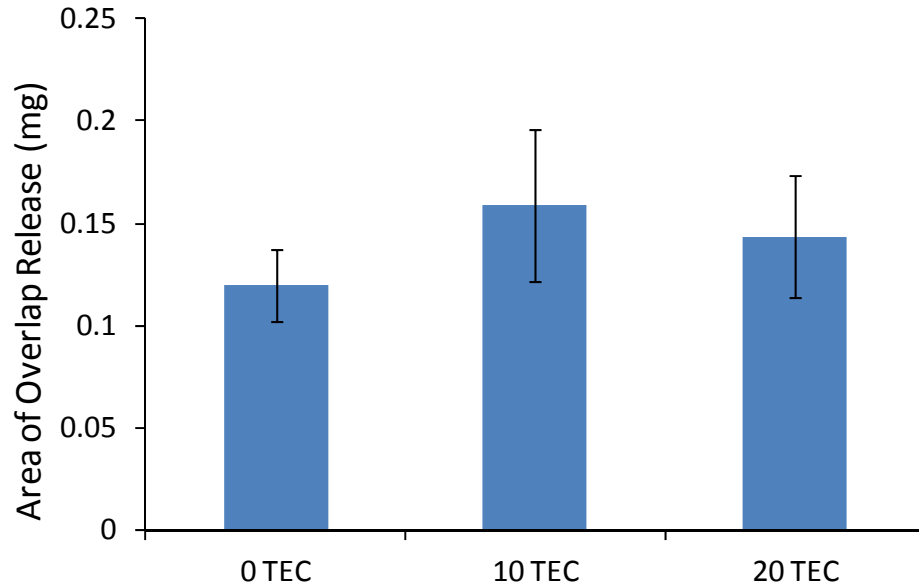
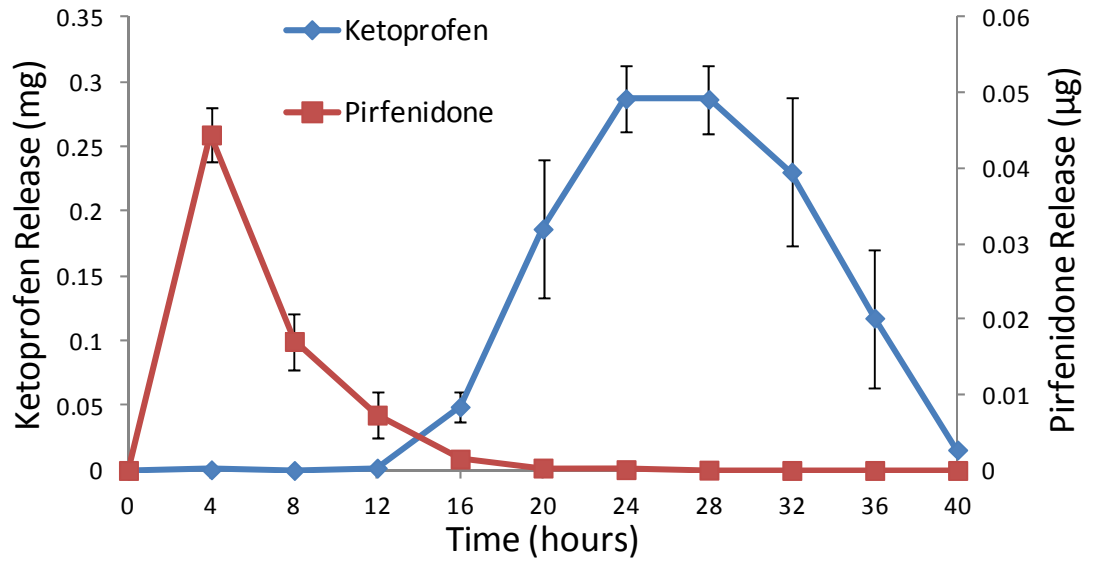


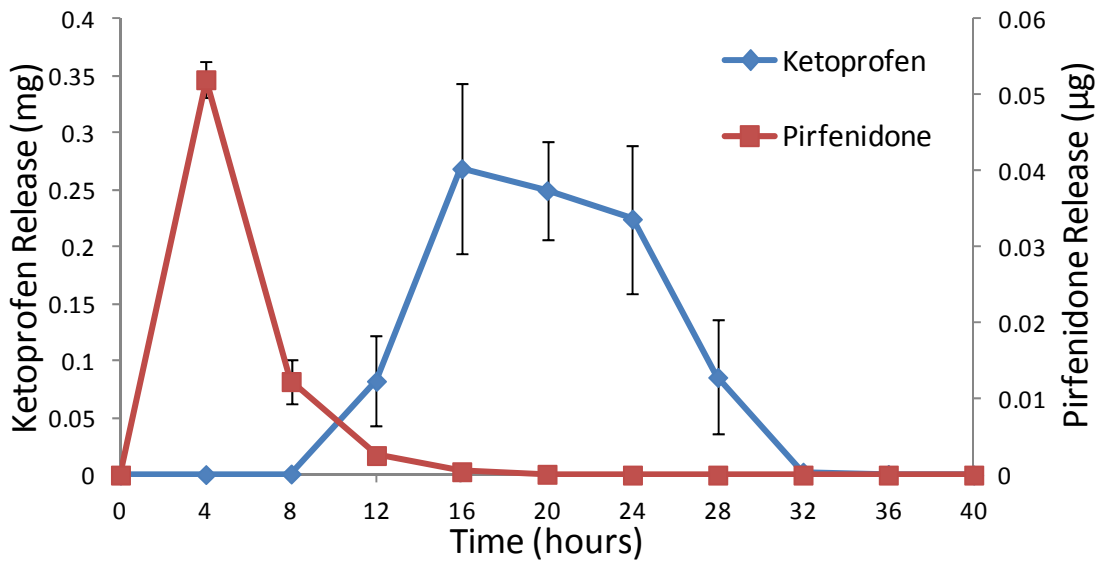
**Figure 5.8:** Area under the curves during ketoprofen and pirfenidone overlap release from 4-layered “forward” devices. Data are mean  $\pm$  standard error (n=3).

For the “reverse” devices, the peak of the first drug, pirfenidone, still occurred at 4 hours (Figure 5.9). The peak of the second drug, ketoprofen, occurred at 24 hours for 0 wt% TEC devices, and at 16 hours for the plasticized devices. The overlap of the release of both drugs was 12 hours long for the 0 and 10 wt% TEC devices and 16 hours for the 20 wt% TEC devices. The area under the curve of the dual release was significantly different between the 20 wt% TEC devices and the 0 wt% and 10 wt% TEC devices ( $p < 0.05$ ) (Figure 5.10).

a



b



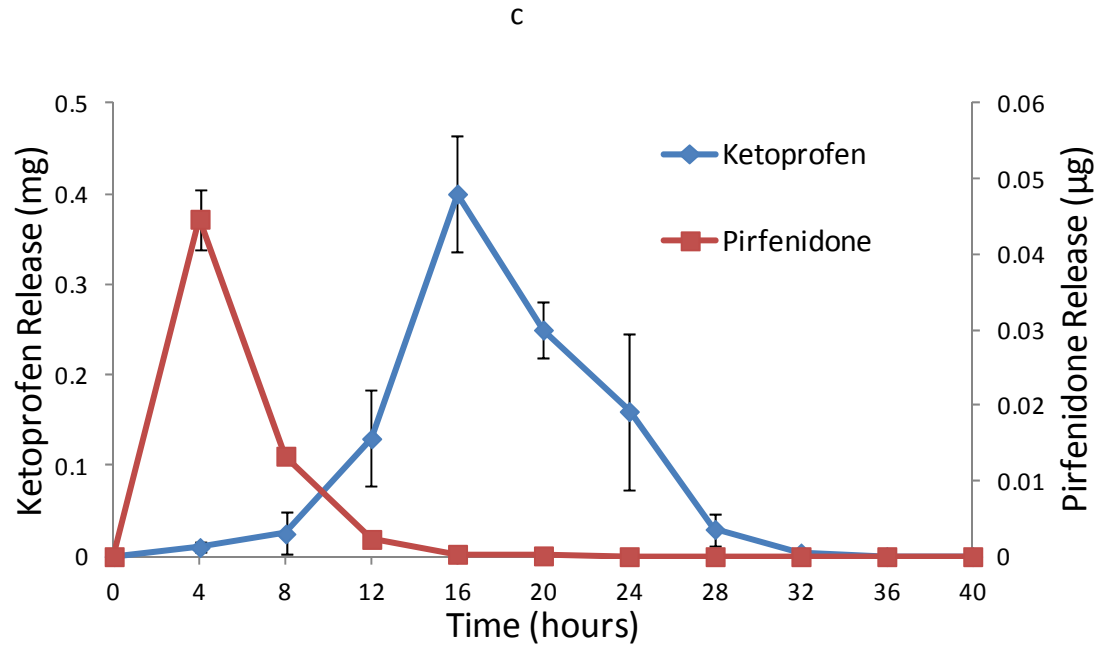


**Figure 5.9:** Release from “reverse” 4-layered devices plasticized with (a) 0 TEC, (b) 10 TEC, and (c) 20 TEC. Data are mean  $\pm$  standard error (n=3).

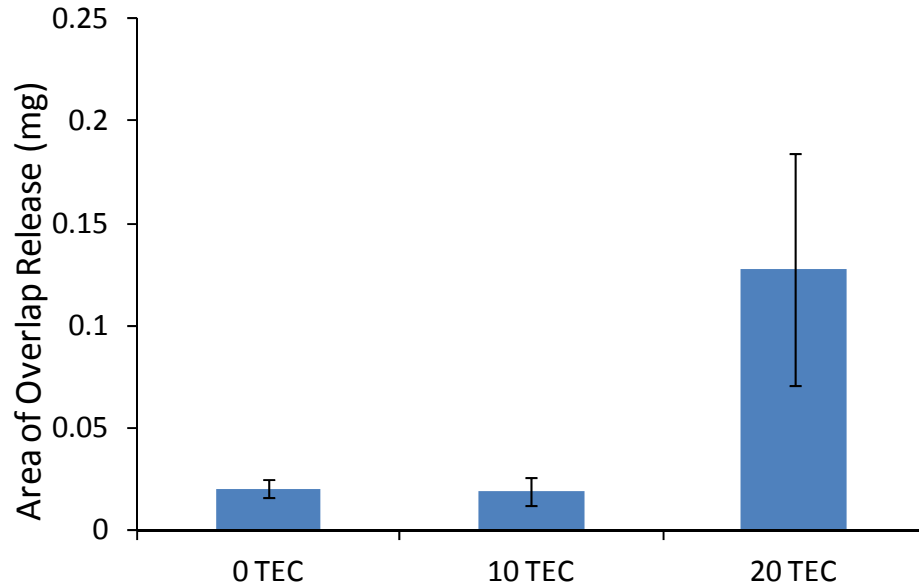
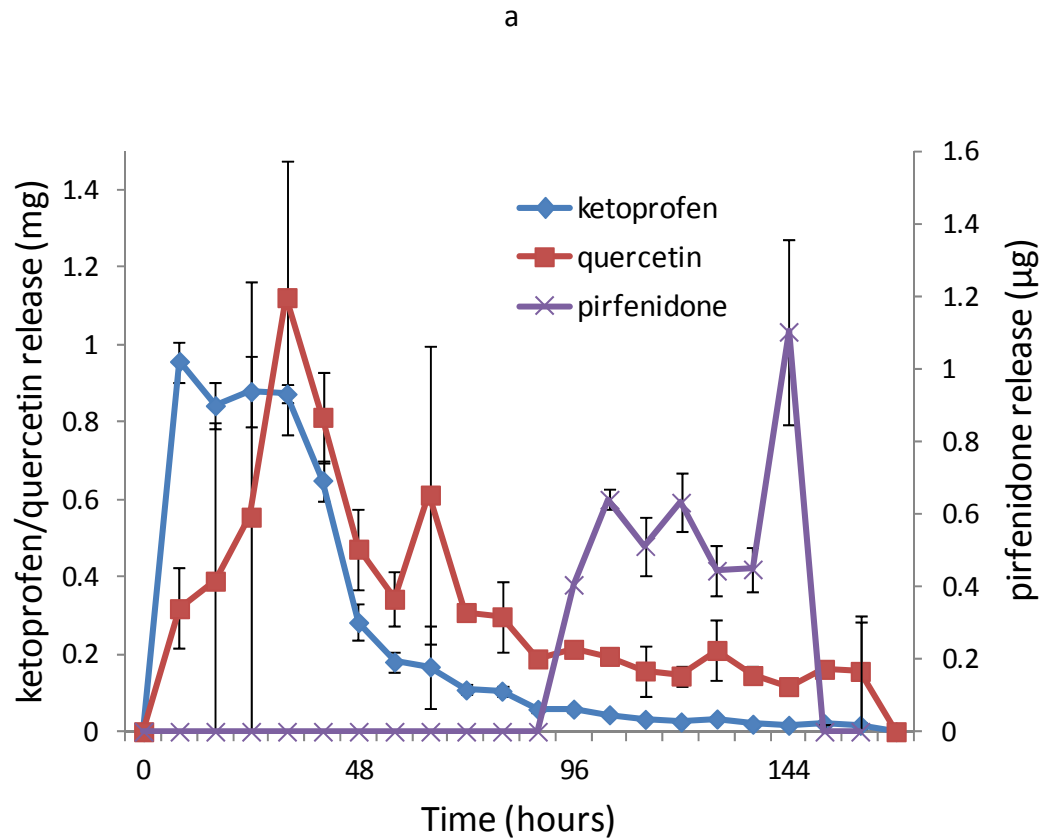


**Figure 5.10:** Area under the curves during ketoprofen and pirfenidone overlap release from 4-layered “reverse” devices. Data are mean  $\pm$  standard error (n=3).

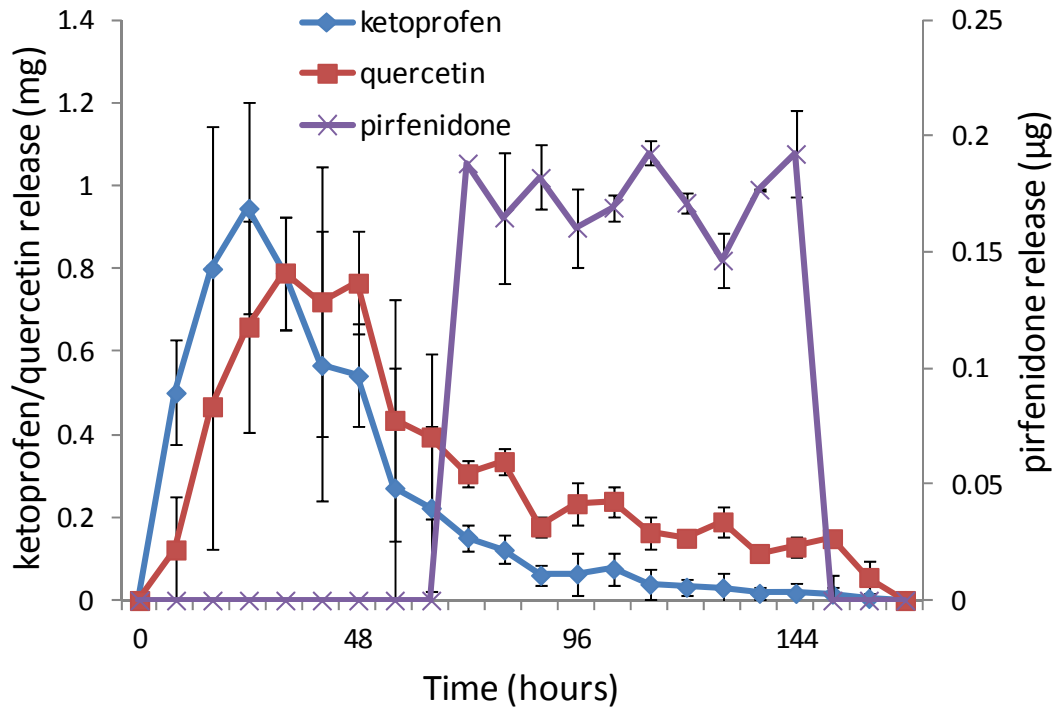
#### 5.3.4 Nine-Layered Device Release Studies

For the 9-layered devices, overlapping drug release was observed from the first time point with ketoprofen and quercetin (Figure 5.11). The ketoprofen peak is delayed with increasing plasticizer; peaks occurred at 8, 24, and 32 hours for 0, 10, and 20 wt% TEC, respectively. For all three device types, the peak quercetin release occurred at 32 hours. With increasing plasticizer concentration, the pirfenidone peak is release occurred earlier. The 0 wt% TEC devices had a pirfenidone peak at 144 hours, the 10 wt% TEC pirfenidone peak occurred at 84 hours, and the 20 wt% TEC devices at 64 hours. Pirfenidone is also more quickly released with increasing plasticizer. Pirfenidone

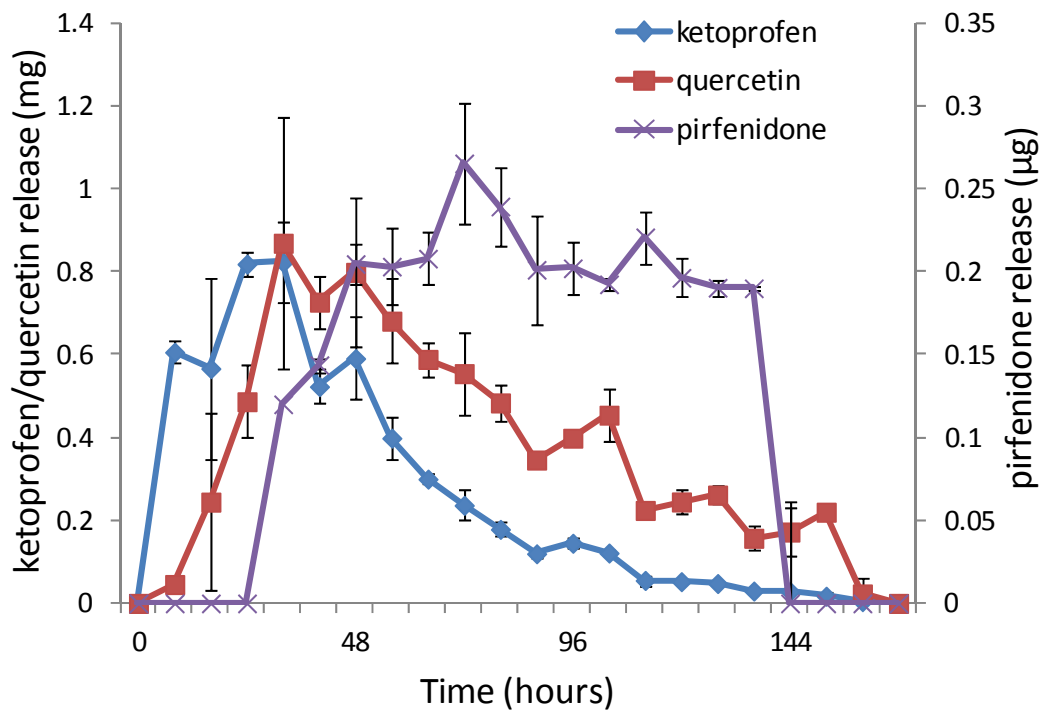
is first detected at 96, 64, and 32 hours for 0, 10, and 20 wt% TEC devices, respectively. Peak pirfenidone release for 0 wt% TEC samples was significantly different from the peak pirfenidone release from 10 and 20 wt% samples ( $p < 0.05$  and  $p < 0.001$ , respectively).



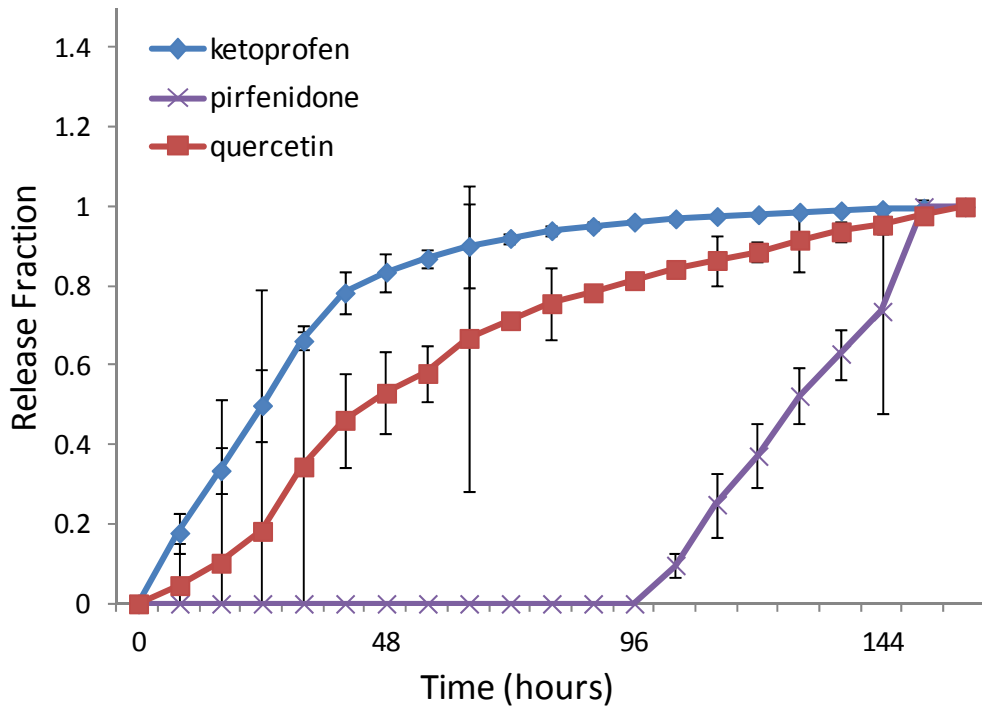
b



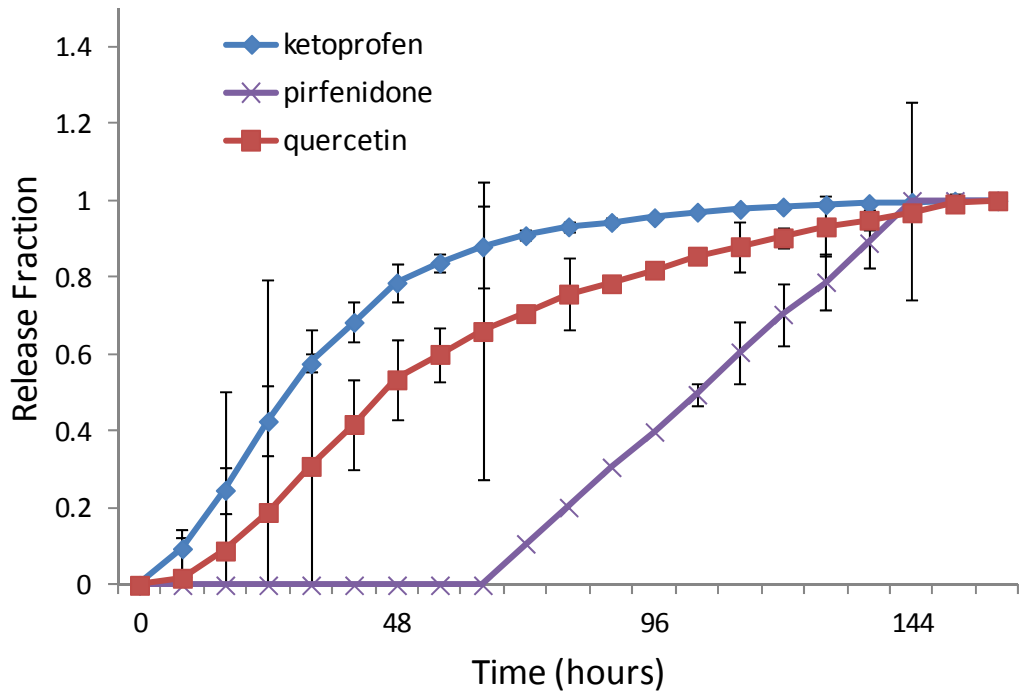
c







e



81

f

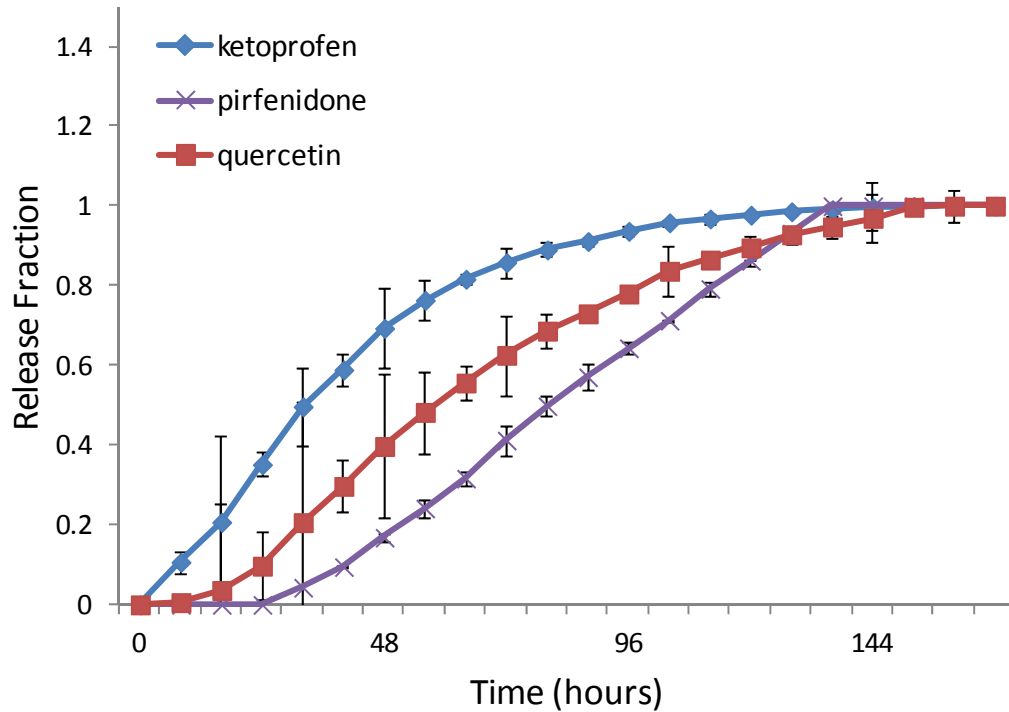


**Figure 5.11:** Instantaneous release from 9-layered devices plasticized with (a) 0 TEC, (b) 10 TEC, and (c) 20 TEC. Cumulative release from 9-layered devices plasticized with (d) 0 TEC, (e) 10 TEC, and (f) 20 TEC. Data are mean  $\pm$  standard error (n=3).

With increasing plasticizer content, increased mass gain occurred (Figure 5.12). Eight hours after the study began, the 20 wt% TEC devices gained 1.5 times their initial mass, the 10 wt% TEC increased in mass by 38%, and the 0 wt% TEC devices gained the least, with an additional 30% mass. The mass gain of the 20 wt% samples was significantly different from the 0 wt% samples ( $p < 0.01$ ). The slopes of the mass loss

were 18.8, 21.2, and 25.0 for 0, 10, and 20 wt% TEC devices, respectively. The mass loss of the 20 wt% samples were significantly different from the 0 and 10 wt% samples ( $p < 0.001$  and  $p < 0.05$ , respectively).

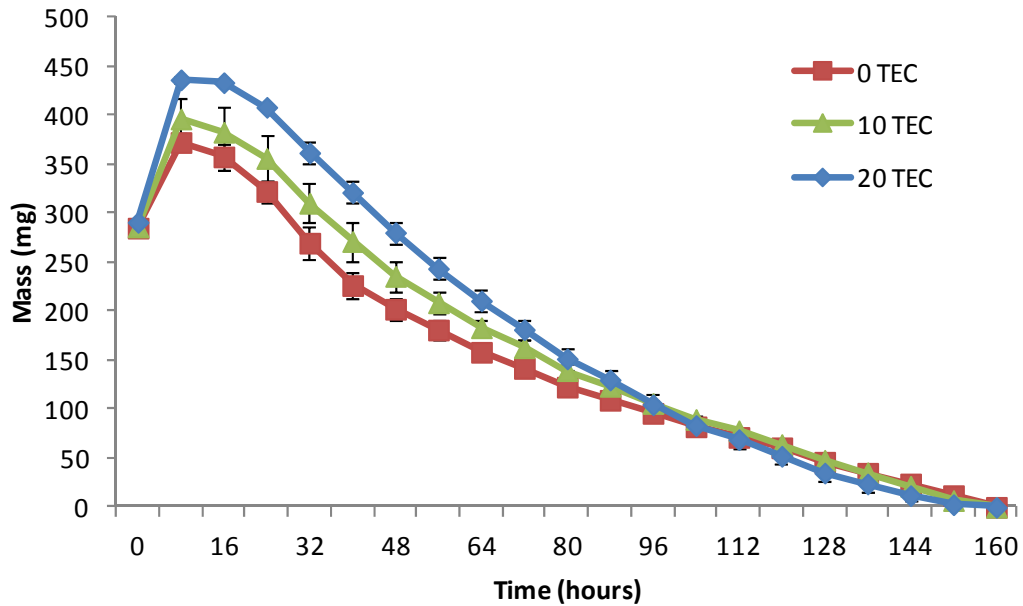


**Figure 5.12:** Mass loss of 9-layered devices. Data are mean  $\pm$  standard error (n=3).

#### 5.4 Discussion

Mouse myoblast cells were analyzed in the cytotoxicity study since they differentiate into muscle cells; muscle cells are what would be exposed to this polymeric drug delivery system. Tributyl citrate can be toxic to different organ systems, including the cardiovascular, respiratory, and central nervous systems (200-202). However, when taken orally, it is non-toxic even in high doses, equating 2 liters in a 70 kg man (158). Molecules delivered orally must travel from the intestines, through the hepatic portal

vein, and filter through the liver before circulating through the rest of the bloodstream. Many TBC molecules are excreted through the process and will never circulate through the body. The mouse myoblast cells examined did not have a lymphatic system or blood vessels to remove the TBC so they were unable to survive the toxic effects.

Compared to mechanical properties of single films plasticized with TEC or TBC (101), the four-layered films elongated more and had a lower UTS and modulus. Two of the four layers were drug loaded. The drug likely acted as plasticizer further affecting the mechanical properties of the films (191). Because of the additional thickness of the four-layered films, it is also possible that the acetone used to laminate the layers was not able to completely diffuse out of the polymer within 24 hours. Any remnant acetone would further plasticize the films (203).

Both the “forward” and “reverse” four-layered devices sequentially released pirfenidone and ketoprofen. The first drug released always had a sharp peak that occurred at 4 hours, whereas the second peak was much wider than the first, regardless of drug order. It was observed during the study that the center of the devices eroded faster than the outer edges, resulting in donut-shaped devices in the last few hours of release. A couple factors likely affected the second peak and the mechanism of erosion; the geometry and material of the wells. The geometry of the wells allowed for more turbulence towards the center of the wells; the walls of the wells protected the outer edges of the films. In addition to the geometry of the wells, the material they were composed of may also play a role in the inconsistent erosion. Polystyrene is a very

hydrophobic polymer, it may form nanobubbles on the surface preventing complete wetting of the material closest to the walls (204). This allowed the last drug-loaded layer to erode before the two blank layers separating them had completely eroded. Lastly, CAP-Pluronic films develop pores as they erode, and these pores could allow for diffusion of the second drug to extend its release peak (101).

The second drug release profiles in the 0 wt% TEC “forward” and “reverse” devices were quite different. The “forward” device had a steep slope before and after the peak release at 16 hours, while, the “reverse” device had a much gentler slope before and after the peak release. Differences in the drugs account for the release profiles. Pirfenidone and ketoprofen have different solubilities in water, 4.4 mg/mL and 51 µg/mL, respectively (185, 205). Ketoprofen is also 1.37 times larger than pirfenidone. Pirfenidone as the second drug was released more easily than ketoprofen. Ketoprofen, being larger and less water soluble than pirfenidone, cannot as easily diffuse out of the film as easily as pirfenidone. This is also supported by the differences between the “forward” and “reverse” overlap release. The “forward” 0 and 10 wt% TEC devices had larger overlaps of the two drugs than the “reverse” devices. Plasticizer did not affect release of pirfenidone as the second drug, but it did significantly increase the release of ketoprofen from 20 wt% TEC “reverse” devices compared to the 0 and 10 wt% TEC devices.

In the 9-layered devices, the concentration of TEC affected the release profiles of the three drugs. Increasing plasticizer increased mobility of the 3 drugs. TEC is 1.5x and

1.1x larger than pirfenidone and ketoprofen, respectively, and comparable in size to quercetin. As TEC leaches out of the films, it leaves behind pores large enough for the drugs to diffuse out (101, 206, 207). This increased porosity also accounts for the mass gain seen by the 10 and 20 wt% TEC films (208).

## 5.5 Conclusion

CAP-Pluronic films are surface eroding systems capable of sequentially releasing multiple drugs over several days. The release profiles can be tailored by the concentration of the plasticizer and by the type of drug loaded into the films. This makes them to be an appealing system for flexible drug delivery films, particularly for the prevention of scar tissue formation in soft tissue defects.

## Chapter 6

### Comparison of *In vitro* and *In vivo* Erosion and Release from Drug Delivery Films

#### 6.1 Introduction

Chronic wound healing occurs when an injury undergoes excessive inflammation and often results in fibrotic scar tissue that can have both aesthetic and functional consequences (12, 209). In secondary union wounds, mass amounts of epithelial cells have been destroyed and the wound cannot be neatly sewn together with sutures. The healing process is longer and the wound experiences more inflammation than primary union wounds. Chronic inflammation causes the differentiation of superfluous myofibroblasts resulting in the development of fibrotic tissue (210).

Most common treatment for secondary union wounds begins with debridement, the process of removing foreign debris and dead tissue (6). Macrophages and foreign body giant cells will work hard to phagocytose debris and necrotic tissue. Once the wound has been cleaned, bandages will be applied and the wound will be redressed every couple days (37). During treatment, patients will also be administered oral anti-inflammatory drugs to help reduce pain and swelling. Depending on the severity of the wound, patients may take either non-steroidal anti-inflammatory drugs (NSAIDs) or corticosteroids. Current treatments do not target the pharmacotherapy for the different healing stages that occur. Also, with oral medications, much of the dose is lost

through the first-pass effect and what makes it to the bloodstream circulates through the whole body of the patient so most of the remaining molecules are provided to areas that do not need treatment. Hence, there is a need for localized treatments for soft tissue defects tailored to the healing process that can prevent or reduce fibrotic scar tissue formation and encourage proper wound healing.

Films composed of cellulose acetate phthalate (CAP) and Pluronic F-127 (Pluronic) and plasticized with triethyl citrate (TEC) have been proven to be surface eroding drug delivery systems capable of sequential release *in vitro* (95, 97, 99, 211). In this study, devices made from CAP-Pluronic films were loaded with anti-inflammatory, anti-oxidant, and anti-fibrotic drugs to determine the *in vivo* release profiles. The four drugs used were meloxicam or ketoprofen, quercetin, and pirfenidone (Figure A.1). Ketoprofen and meloxicam are common anti-inflammatory drugs that reduce inflammation by inhibiting cyclooxygenase (COX); ketoprofen is nonselective while meloxicam preferentially binds to COX-2 (63, 108). Quercetin is an anti-oxidant biomolecule that has been shown to increase cell proliferation, decrease superoxide activity, and reduce wound contraction when incorporated into a collagen matrix (114-116). Pirfenidone is an anti-fibrotic drug that has been shown to reduce scar formation by decreasing cell adhesion molecules and reducing cytokines and growth factors, including interleukin 1 $\beta$  and transforming growth factor- $\beta_1$  (119, 121, 123).



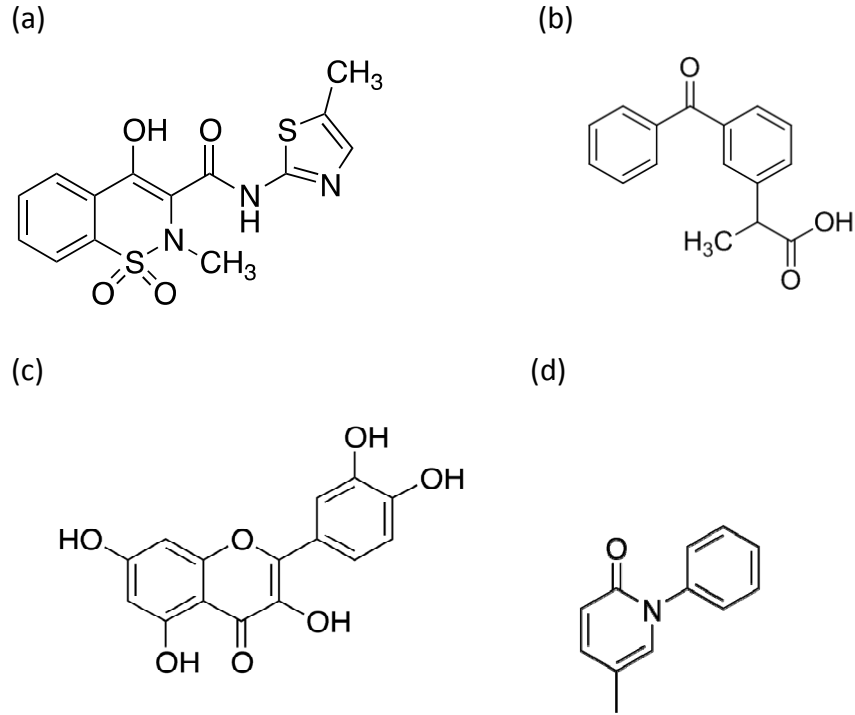


**Figure 6.1:** Chemical structures of (a) meloxicam, (b) ketoprofen, (c) quercetin, and (d) pirfenidone.

## 6.2. Materials and Methods

### 6.2.1 CAP-Pluronic Film Fabrication

Cellulose acetate phthalate (Sigma-Aldrich, St. Louis, MO) and Pluronic F-127 (Sigma-Aldrich) were added in a 70:30 weight ratio to a test tube. Twenty weight percent triethyl citrate (Sigma-Aldrich) was combined to the mixture for plasticized devices. For drug loaded films, pirfenidone, quercetin, ketoprofen, or meloxicam were added to the 2 g mix of polymers at 6.1 mg, 10 mg, 100 mg, and 45 mg, respectively. Acetone was added to create a 25% (w/v) solution. To ensure homogeneity, the test

tubes were vortexed, then poured into Teflon dishes, and stored at 10°C overnight. Acetone evaporation yielded casted films. Before device fabrication, films were desiccated overnight.

### **6.2.2 EVA Film Fabrication**

Poly(ethylene-co-vinyl acetate) (poly(EVA)) 18 wt% vinyl acetate (Sigma-Aldrich, St. Louis, MO) was dissolved in 100 °C toluene to make a 10% w/v solution. Once homogeneous, the solution was poured into a Teflon dish. Toluene evaporation left behind a cast film.

### **6.2.3 Device Fabrication**

Cylindrical punches were used to make CAP-P layers increasing in diameter. The smallest layer, pirofenidone, was covered by the next smallest and so on until reaching the outermost drug loaded layer, ketoprofen or meloxicam (Table A.1). Layers were laminated with acetone. For the devices with backing layers, a poly(EVA) film was used to ensure unidirectional release. For devices with a mesh encasing, layers were covered in a polypropylene mesh that was stitched closed with nylon suture (Figure A.2). The devices were desiccated overnight to remove all remnant acetone. Devices were weighed and measured to determine their initial mass and dimensions.

**Table 6.1:** Device fabrication information for animal trials

Study	Number of Devices/Rats	Layers	Backing Layer	Mesh Encasing	Drug Loaded Devices	Blank Devices	Plasticizer Types	Time Points
1	12	9 CAP-Pluronic Layers	No	No	Ketoprofen, Quercetin, Pirfenidone (6)	Yes (6)	0% and 20% TEC	48 and 72 hours
2	8	5 CAP-Pluronic Layers	Yes	No	Ketoprofen, Quercetin, Pirfenidone (4)	Yes (4)	20% TEC	24 and 48 hours
3	4	5 CAP-Pluronic Layers	Yes	Yes	Ketoprofen, Quercetin, Pirfenidone (4)	No (4)	20% TEC	24 and 48 hours

**Table 6.2:** Fabrication of devices used for the third trial

Layer	Diameter (mm)
Polypropylene Mesh	19
Poly(EVA)	16.9
Pirfenidone	3.8
Blank	5.5
Quercetin	11
Blank	13
Meloxicam	16.9
Polypropylene Mesh	19



**Figure 6.2:** Eight layered devices for animal study.

#### 6.2.4 Animal Methodology and Procedure

The animal study was conducted at the University of Kentucky in accordance with a protocol approved by the Institutional Animal Care and Use Committee (IACUC). The study consisted of three separate experiments,: (1) devices without a backing layer or mesh encasement, (2) devices with a backing layer and no mesh encasement, (3) devices with both a backing layer and mesh encasement (Table A.2). Twelve week old, male Sprague-Dawley rats weighing between 350 and 400 g were used. The surgical area was prepared by shaving and disinfection with a povidone iodine solution. A roughly 3 cm incision was made on the left thigh over the quadriceps. Skin was separated from the muscle to create a pocket for the device. The device was placed into the pocket with the CAP-Pluronic side down (Figure 3). The incision was closed using wound clips. Rats were euthanized after 24, 48, or 72 h, and devices were retrieved. Final mass and dimensions of the devices were determined.

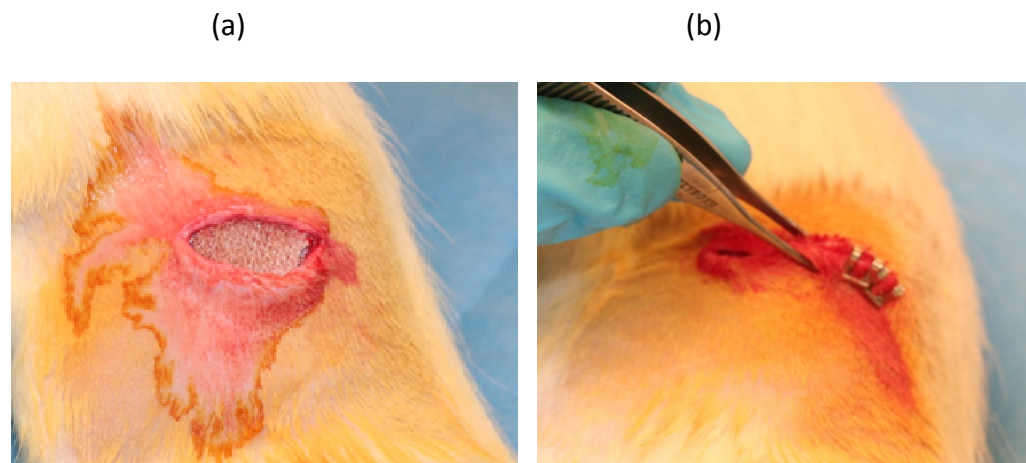


**Figure 6.3:** Images of animal procedure: (a) implant in surgical site and  
(b) wound closure.

### 6.3 Results

All devices from the first animal study had completely eroded by the retrieval time points, 48 and 72 hours. Also, the animal study resulted in unexpected death for several of the rats implanted with drug loaded devices. The rats had an adverse reaction to the ketoprofen even though it is an approved and commonly used anti-inflammatory drug for rats. Rats that underwent planned euthanasia still had negative reactions to the ketoprofen, including porphyrin staining and diarrhea, and remained lethargic 48 hours after implantation.

For the second study, several parameters were modified. First the anti-inflammatory drug choice was changed to meloxicam, another approved anti-inflammatory drug for rats. To extend the device length *in vivo*, polypropylene mesh backing layers were bonded to the CAP-Pluronic layers to promote unidirectional release and erosion. Also, only 20% TEC plasticized devices were used, to reduce the number of rats needed and evaluate the worst-case-scenario *in vivo* duration devices (20% TEC devices were the fastest eroding devices). All of the rats lived until euthanized. When devices were retrieved at 24 hours after implantation, two of the four devices had completely eroded leaving behind only a backing layer. By 48 hours, all four devices had completely eroded.

Further modifications were made to extend the device life *in vivo* for the third study. A polypropylene mesh encased the CAP-P device and backing layer. For this study, four 20% TEC plasticized, drug loaded devices were used. Table A.3 shows that

devices used for the 48 hour time points were slightly larger, averaging an additional 0.024 g, or 7.5% more mass, than the devices used for the 24 hour time points. No blank devices were evaluated in this study. After 24 hours, the two devices lost 91.7% of their CAP-Pluronic mass (Figure 4). After 48 hours, the two other devices dropped in CAP-Pluronic mass by an additional 2.0%, with a total of 93.7% mass loss.

**Table 6.3:** Initial and final weights of *in vivo* device components for third study.

Timepoint (hours)	Initial Weight (g)	Initial Weight of CAP-Pluronic Layers (g)	Weight of Mesh (g)	Weight of Backing Layer (g)	Final Weight of CAP-Pluronic Layers (g)	Percentage of CAP-Pluronic Remaining
24	0.3165	0.2340	0.0700	0.0125	0.0188	8.0342
24	0.3178	0.2446	0.0643	0.0089	0.0208	8.5037
48	0.3259	0.2616	0.0717	0.0126	0.0092	3.8079
48	0.3558	0.2604	0.0737	0.0217	0.0228	8.7558

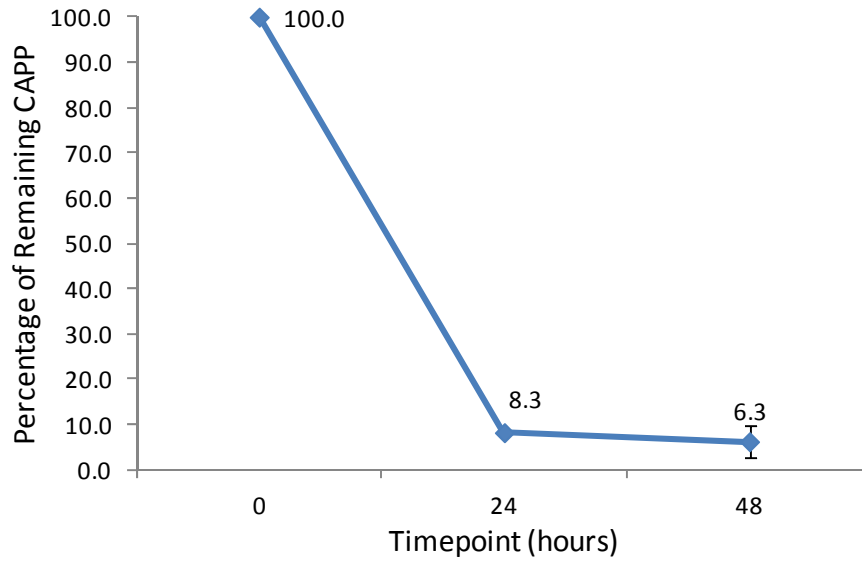


**Figure 6.4:** Study 3 *in vivo* CAP-Pluronic mass loss over time.

#### 6.4 Discussion

Although ketoprofen has been considered a safe anti-inflammatory drug for use on rats, this study is not the first to observe adverse reactions. Shientag et al. found ketoprofen at 5 mg/kg doses to cause gastrointestinal bleeding and ulcers in rats after 24 hours (212). Combining anesthesia with the ketoprofen dose heightened the effects. Lamon et al. found the toxicity of ketoprofen on Sprague-Dawley rats to be effected by their genetic strains and certain genotypes exhibited more exaggerated reactions (213). Ketoprofen is a nonselective cyclooxygenase (COX) inhibitor that interferes with prostaglandin production and inflammation reducing pain (108). Ketoprofen is known to irritate the intestine and kidneys resulting in ulcers. Thrombosis, by inhibition of



thromboxane B<sub>2</sub>, will allow bleeding to continue from any consequential ulcers (108). Meloxicam is also an NSAID that is a cyclooxygenase inhibitor, preferentially binding to COX-2 (108). There is no literature supporting toxic interactions for meloxicam like are found with ketoprofen; COX-2 inhibitors are less likely to cause the gastrointestinal and renal damage that COX-1 inhibitors do, but they are also less effective as reducing inflammation (214).

The insignificant difference in erosion after 24 and 48 hours in the third animal study was caused by geometry changes over time, plasticizer leaching, and also possibly separation of the poly(EVA) from the CAP-Pluronic layers that was also seen in the second study. The ratio of the thickness to the diameter of the devices used in the third study was about 1:6. The device was thickest in the middle where all 8 layers were and got increasingly thinner towards the edges where fewer layers made up the thickness. CAP-Pluronic films are surface eroding systems (95). The surface area was its largest at t=0 resulting in the fastest erosion. As the outer edges eroded, the ratio of thickness to diameter increased and less relative mass was exposed on the surface, which slowed the erosion rate. The two devices used for the 48 hour time points weighed roughly 7.5% more but were no wider in diameter than the two 24 hour devices. This caused those two devices to have a lower relative mass exposure from t=0 which in turn resulted in slower erosion.

Most of the plasticizer leach out occurs in the first few hours of CAP-Pluronic erosion (101). Each CAP-Pluronic layer contained 20 wt% TEC. Because erosion

occurred so quickly, this leaching was captured in the mass loss of the 24 hour time points but not in the 48 hour time points. Plasticizer leaching has been shown to create porosity further increasing the surface area and increasing erosion. It is also possible that the poly(EVA) backing layer separated around the edges from the CAP-Pluronic layers allowing erosion to occur from both sides of the CAP-Pluronic films.

Compared to *in vitro* studies of layered devices, in Chapter 5, erosion occurred much faster *in vivo*. About 94% of the CAP-Pluronic in the *in vivo* devices was gone after 48 hours, whereas layered CAP-Pluronic devices without a backing layer and in sink conditions only lost 31% after 48 hours. This indicates that there are other factors increasing the erosion *in vivo*.

*In vitro* results cannot always predict what *in vivo* results will be (215). Chemical, enzymatic, and mechanical interactions can cause significant differences. Influx of inflammatory cells, including neutrophils and macrophages, to the wound may have sped up erosion through phagocytosis of the implant (9, 10, 216). Phagocytosis can occur for molecules on the micron scale; all of the components of this system, including the largest two, CAP and Pluronic, are that size or smaller (41, 42, 217). Enzymes *in vivo* may also have affected the erosion of the implant. The degree of substitution of cellulose acetate phthalate is 2.2 which prevents its cellulose backbone from being broken down into glucose units (218, 219). However, the ester bonds of the phthalic acid groups could be enzymatically broken. Since those functional groups are responsible for the association of the CAP and Pluronic, breaking its ester bond will

speed up erosion. In addition, mechanical erosion had a significant impact on the difference between the *in vitro* and *in vivo* results (220). CAP-Pluronic devices have been implanted on the calvaria of rats for other studies and significant mass loss after two days was not observed (97). The location of the implant had a significant effect on the erosion. The mechanical forces experienced by an implant are very difficult to model realistically *in vitro*. The rats in this study remained active and were not immobilized in any way. The rats activated their quadriceps anytime they needed to eat, drink, or play with their cage mate. The device was taut between the skin and muscle of the rat so as the muscle engaged, the devices were mechanically worn away. These mechanical forces could not be mimicked *in vitro*.

## 6.5 Conclusion

*In vivo* variances that cannot be replicated *in vitro* caused the CAP-Pluronic devices to erode faster than previously seen. Regardless, CAP-Pluronic devices still sequentially release drug and can be loaded with a multitude of molecules to locally treat an array of conditions. Furthermore, modifications could be made to prolong the duration of devices if needed, including adding slower degrading polymers between the layers, and allow for improved control over the drug delivery films.

## Chapter 7

### Conclusion

Improved treatments are needed for soft tissue defects to encourage proper wound healing and reduce scar tissue formation. In this research, a flexible, layered drug delivery film capable of sequential, localized release of anti-inflammatory, anti-oxidant, and anti-fibrotic molecules was developed and characterized to determine if it was feasible of meeting these needs. In the initial studies, mechanical analysis on plasticized films demonstrated that the properties and erosion of CAP-Pluronic films are varied by the type and amount of plasticizer incorporated into the system. The mechanical properties change shortly after exposure to fluid as plasticizer leaches out leaving behind a stronger film shaped by the surrounding tissue.

The following studies examined how characteristics of drugs, including size, hydrophobicity, and interactive side groups, influenced the release from CAP-Pluronic films. Mechanical properties of the films were also controlled by loading and the drug properties. Plasticizer can be introduced to further modulate films to achieve the desired mechanical properties. When drug and plasticizer were combined, the effect on the film's properties ranged from antagonistic to synergistic. These studies concluded that different drugs and plasticizers can tailor the erosion, release, and mechanical properties needed to target healing in the soft tissue defects.

Layered CAP-Pluronic devices proved to be surface eroding systems capable of sequentially releasing anti-inflammatory, anti-oxidant, and anti-fibrotic molecules over several days. The devices maintained sequential release regardless of drug order.

Lastly, *in vivo* variances caused the CAP-Pluronic devices to erode faster than previously seen *in vitro*. Future work would involve reducing the erosion or mechanical wear. Changing the ratios of CAP to Pluronic, incorporation of a slower eroding polymer into the films, or modification of the implant site or animal model could also be explored to extend the device duration *in vivo*.

Current treatments for soft tissue defects are inadequate because they are either invasive, require multiple doses, or are not controlled to the healing phases to obtain optimal healing. CAP-Pluronic are a promising solution for the prevention of scar tissue formation in soft tissue defects because they can provide sequential release of anti-inflammatory, anti-oxidant, and anti-fibrotic drugs locally to healing wounds, which was the objective of this research.

Copyright © Cheryl Lynn Rabek 2015

## References

1. World report on road traffic injury prevention. 2002 [1/18/2015]; Available from: [http://www.who.int/violence\\_injury\\_prevention/publications/road\\_traffic/world\\_report/en/](http://www.who.int/violence_injury_prevention/publications/road_traffic/world_report/en/).
2. Owens BD, Kragh JF, Wenke JC, Macaitis J, Wade CE, Holcomb JB. Combat wounds in operation Iraqi freedom and operation enduring freedom. *Journal of Trauma-Injury Infection and Critical Care*. 2008;64(2):295-9.
3. Cotran. Robbins Pathologic Basis of Disease: Edition 5. Company WBS, editor. Philadelphia, Pennsylvania1994.
4. Kessler HH. Accidental injuries: Their end-results and evaluation. *The American Journal of Surgery*. 1935;27(1):155-67.
5. Lin P, Hirko M, Von Fraunhofer J, Greisler H. Wound healing and inflammatory responses to biomaterials. *Wound Closure Biomaterials and Devices*. 1996:7-24.
6. Myers. Principles of Pathophysiology and Emergency Medical Care. Delmar, editor. Clifton Park, New York2002.
7. Braiman-Wiksman L, Solomonik I, Spira R, Tennenbaum T. Novel insights into wound healing sequence of events. *Toxicologic Pathology*. 2007;35(6):767-79.
8. Strecker-McGraw MK, Jones TR, Baer DG. Soft tissue wounds and principles of healing. *Emergency medicine clinics of North America*. 2007;25(1):1-22.
9. David Keast HO. The Basic Principles of Wound Healing. *Ostomy and Wound Management*. 1998;44(8).
10. Anderson JM. Biological responses to materials. *Annual Review of Materials Research*. 2001;31:81-110.
11. Colman RW, Hirsh J, Marder VJ, Colman, Hirsh, Marder, et al. Hemostasis and thrombosis: basic principles and clinical practice. 2006.
12. Schreml S, Szeimies RM, Prantl L, Landthaler M, Babilas P. Wound healing in the 21st century. *Journal of the American Academy of Dermatology*. 2010;63(5):866-81.
13. Kupietzky A, Levi-Schaffer F. The role of mast cell-derived histamine in the closure of an in vitro wound. *Inflammation Research*. 1996;45(4):176-80.
14. Artuc M, Hermes B, Stckelings U, Grützkau A, Henz B. Mast cells and their mediators in cutaneous wound healing—active participants or innocent bystanders? *Experimental Dermatology*. 1999;8(1):1-16.
15. Kahlson G, Nilsson K, Rosengren E, Zederfeldt B. WOUND HEALING: AS DEPENDENT ON RATE OF HISTAMINE FORMATION. *The Lancet*. 1960;276(7144):230-4.
16. Lykke A, Cummings R. Inflammation in Healing: I. Time-Course and Mediation of Exudation in Wound Healing in the Rat. *British journal of experimental pathology*. 1969;50(3):309.

17. Kawai K, Larson BJ, Ishise H, Carre AL, Nishimoto S, Longaker M, et al. Calcium-based nanoparticles accelerate skin wound healing. *PloS one*. 2011;6(11):e27106. Epub 2011/11/11.
18. Kavalukas SL, Uzgare AR, Bivalacqua TJ, Barbul A. Arginase inhibition promotes wound healing in mice. *Surgery*. 2012;151(2):287-95. Epub 2011/10/07.
19. Serhan CN, Savill J. Resolution of inflammation: the beginning programs the end. *Nature immunology*. 2005;6(12):1191-7.
20. James M, Penglis P, Caughey G, Demasi M, Cleland L. Eicosanoid production by human monocytes: does COX-2 contribute to a self-limiting inflammatory response? *Inflammation Research*. 2001;50(5):249-53.
21. Tonnesen MG, Feng X, Clark RAF. Angiogenesis in Wound Healing. *J Investig Dermatol Symp Proc*. 2000;5(1):40-6.
22. Risau W. Mechanisms of angiogenesis. *Nature*. 1997;386(6626):671-4.
23. al. Ke. *Basic Pathology: Edition 5*. Philadelphia, Pennsylvania: W.B. Saunders Company; 1992.
24. Ruoslahti E. Structure and biology of proteoglycans. *Annual review of cell biology*. 1988;4(1):229-55.
25. Gabbiani G. The myofibroblast in wound healing and fibrocontractive diseases. *The Journal of pathology*. 2003;200(4):500-3.
26. Tomasek JJ, Gabbiani G, Hinz B, Chaponnier C, Brown RA. Myofibroblasts and mechano-regulation of connective tissue remodelling. *Nature Reviews Molecular Cell Biology*. 2002;3(5):349-63.
27. Behm B, Babilas P, Landthaler M, Schreml S. Cytokines, chemokines and growth factors in wound healing. *Journal of the European Academy of Dermatology and Venereology*. 2012;26(7):812-20.
28. Kwan P, Hori K, Ding J, Tredget EE. Scar and Contracture: Biological Principles. *Hand Clinics*. 2009;25(4):511-+.
29. Schultz GS, Mast BA. Molecular analysis of the environments of healing and chronic wounds: cytokines, proteases and growth factors. *Primary Intention*. 1999;7:7-15.
30. Jeon H, Kim E, Grigoropoulos CP. Measurement of contractile forces generated by individual fibroblasts on self-standing fiber scaffolds. *Biomedical microdevices*. 2011;13(1):107-15. Epub 2010/09/24.
31. Klinger M, Caviggioli F, Forcellini D, Villani F. Scars: A Review of Emerging and Currently Available Therapies. *Plastic and Reconstructive Surgery*. 2009;124(1):330-.
32. Barron L, Wynn TA. Fibrosis is regulated by Th2 and Th17 responses and by dynamic interactions between fibroblasts and macrophages. *American journal of physiology Gastrointestinal and liver physiology*. 2011;300(5):G723-8. Epub 2011/02/05.
33. Diegelmann RF, Evans MC. Wound healing: an overview of acute, fibrotic and delayed healing. *Front Biosci*. 2004;9(1):283-9.

34. Martin P, Leibovich SJ. Inflammatory cells during wound repair: the good, the bad and the ugly. *Trends in cell biology*. 2005;15(11):599-607.
35. Stramer BM, Mori R, Martin P. The inflammation–fibrosis link? A Jekyll and Hyde role for blood cells during wound repair. *Journal of Investigative Dermatology*. 2007;127(5):1009-17.
36. Brown TS, Hawksworth JS, Sheppard FR, Tadaki DK, Elster E. Inflammatory response is associated with critical colonization in combat wounds. *Surgical infections*. 2011;12(5):351-7. Epub 2011/09/23.
37. Brickner. Brickner et al, *American Journal of Surgery: Volume XXVII*. New York, New York: Surgery Publishing Company; 1914.
38. Wound Bed Preparation. [cited 2015]; Available from: <http://www.smith-nephew.com/professional/products/featured-products/wound-bed-preparation/background/debridement/>.
39. Enoch S. Wound Bed Preparation: The Science Behind the Removal of Barriers to Healing. 2003 [cited 2015]; Available from: [http://www.medscape.com/viewarticle/459733\\_6](http://www.medscape.com/viewarticle/459733_6).
40. Types of Wound Debridement. Wound Care Information Network2013 [cited 2015]; Available from: <http://www.medicaledu.com/debridhp.htm>.
41. Doshi N, Mitragotri S. Macrophages Recognize Size and Shape of Their Targets. *PloS one*. 2010;5(4):e10051.
42. Swanson GJCaJA. The Macrophage Capacity for Phagocytosis. *Journal of Cell Science*. 1992;101:907-13.
43. Polk HC, Jr, Trachtenberg L, Finn MP. Antibiotic activity in surgical incisions: The basis for prophylaxis in selected operations. *JAMA*. 1980;244(12):1353-4.
44. Papel. *Facial Plastic and Reconstructive Surgery: Edition 3*. New York, New York: Thieme Medical Publishers; 2009.
45. Green B. Taking a closer look at what we understand about negative pressure wound therapy : review2014; 7(1):[13-6 pp.]. Available from: [http://reference.sabinet.co.za/webx/access/electronic\\_journals/mp\\_whsa/mp\\_whsa\\_v7\\_n1\\_a4.pdf](http://reference.sabinet.co.za/webx/access/electronic_journals/mp_whsa/mp_whsa_v7_n1_a4.pdf).
46. Guo S, Dipietro LA. Factors affecting wound healing. *J Dent Res*. 2010;89(3):219-29. Epub 2010/02/09.
47. Cosmetic Procedures: Scars. [2015]; Available from: <http://www.webmd.com/beauty/skin/cosmetic-procedures-scars>.
48. Spina V, Raia R, Reginato L. Treatment of Keloid. *Plastic and Reconstructive Surgery*. 1954;14(5):390-1.
49. Alster TS. Laser treatment of hypertrophic scars, keloids, and striae. *Dermatologic clinics*. 1997;15(3):419-29.
50. Neshat AA. Treatment of keloid. *The Laryngoscope*. 1977;87(7):1095-9.
51. Coolen NA, Schouten KC, Boekema BK, Middelkoop E, Ulrich MM. Wound healing in a fetal, adult, and scar tissue model: a comparative study. *Wound repair and regeneration : official publication of the Wound Healing*



- Society [and] the European Tissue Repair Society. 2010;18(3):291-301. Epub 2010/04/24.
52. Satish L, Kathju S. Cellular and Molecular Characteristics of Scarless versus Fibrotic Wound Healing. *Dermatology Research and Practice*. 2010;2010.
  53. Lorenz HP, Whitby DJ, Longaker MT, Adzick NS. Fetal wound healing. The ontogeny of scar formation in the non-human primate. *Annals of surgery*. 1993;217(4):391.
  54. Mast BA, Diegelmann RF, Krummel T, Cohen I. Scarless wound healing in the mammalian fetus. *Surg Gynecol Obstet*. 1992;174(5):441-51.
  55. Coolen NA, Schouten K, Boekema B, Middelkoop E, Ulrich MMW. Wound healing in a fetal, adult, and scar tissue model: A comparative study. *Wound Repair and Regeneration*. 2010;18(3):291-301.
  56. Korla P. Delivery of growth factors for tissue regeneration and wound healing. *BioDrugs*. 2012;26(3):163-75.
  57. Steed DL. THE ROLE OF GROWTH FACTORS IN WOUND HEALING. *Surgical Clinics of North America*. 1997;77(3):575-86.
  58. Kim YS, Lew DH, Tark KC, Rah DK, Hong JP. Effect of Recombinant Human Epidermal Growth Factor Against Cutaneous Scar Formation in Murine Full-thickness Wound Healing. *Journal of Korean Medical Science*. 2010;25(4):589-96.
  59. Mizuno K, Yamamura K, Yano K, Osada T, Saeki S, Takimoto N, et al. Effect of chitosan film containing basic fibroblast growth factor on wound healing in genetically diabetic mice. *Journal of Biomedical Materials Research Part A*. 2003;64A(1):177-81.
  60. Gute DC, Ishida T, Yarimizu K, Korthuis RJ. Inflammatory responses to ischemia and reperfusion in skeletal muscle. *Molecular and cellular biochemistry*. 1998;179(1-2):169-87.
  61. Gradel C, Jain D, Batsford W, Wackers FT, Zaret B. Relationship of scar and ischemia to the results of programmed electrophysiological stimulation in patients with coronary artery disease. *J Nucl Cardiol*. 1997;4(5):379-86.
  62. Moriya J, Wu X, Zavala-Solorio J, Ross J, Liang XH, Ferrara N. Platelet-derived growth factor C promotes revascularization in ischemic limbs of diabetic mice. *Journal of vascular surgery*. 2014;59(5):1402-9. e4.
  63. Ricci M, Blasi P, Giovagnoli S, Rossi C, Macchiarulo G, Luca G, et al. Ketoprofen controlled release from composite microcapsules for cell encapsulation: Effect on post-transplant acute inflammation. *Journal of Controlled Release*. 2005;107(3):395-407.
  64. Arockianathan PM, Sekar S, Sankar S, Kumaran B, Sastry TP. Evaluation of biocomposite films containing alginate and sago starch impregnated with silver nano particles. *Carbohydrate Polymers*. 2012;90(1):717-24.

65. Pawar HV, Boateng JS, Ayensu I, Tetteh J. Multifunctional Medicated Lyophilised Wafer Dressing for Effective Chronic Wound Healing. *Journal of Pharmaceutical Sciences*. 2014;103(6):1720-33.
66. Wong TW, Ramli NA. Carboxymethylcellulose film for bacterial wound infection control and healing. *Carbohydrate Polymers*. 2014;112:367-75.
67. Ng SF, Jumaat N. Carboxymethyl cellulose wafers containing antimicrobials: A modern drug delivery system for wound infections. *European Journal of Pharmaceutical Sciences*. 2014;51:173-9.
68. Minagawa T, Okamura Y, Shigemasa Y, Minami S, Okamoto Y. Effects of molecular weight and deacetylation degree of chitin/chitosan on wound healing. *Carbohydrate Polymers*. 2007;67(4):640-4.
69. Pilakasiri K, Molee P, Sringernyuang D, Sangjun N, Channasanon S, Tanodekaew S. Efficacy of chitin-PAA-GTMAC gel in promoting wound healing: animal study. *Journal of materials science Materials in medicine*. 2011;22(11):2497-504. Epub 2011/08/20.
70. Mogosanu GD, Grumezescu AM. Natural and synthetic polymers for wounds and burns dressing. *International Journal of Pharmaceutics*. 2014;463(2):127-36.
71. Salcedo I, Aguzzi C, Sandri G, Bonferoni MC, Mori M, Cerezo P, et al. In vitro biocompatibility and mucoadhesion of montmorillonite chitosan nanocomposite: A new drug delivery. *Appl Clay Sci*. 2012;55:131-7.
72. Friess W. Collagen–biomaterial for drug delivery. *European Journal of Pharmaceutics and Biopharmaceutics*. 1998;45(2):113-36.
73. Khanbanha N, Atyabi F, Taheri A, Talaie F, Mahbod M, Dinarvand R. Healing Efficacy of an EGF Impregnated Triple Gel Based Wound Dressing: In Vitro and In Vivo Studies. *Biomed Res Int*. 2014.
74. Chang WH, Chang Y, Lai PH, Sung HW. A genipin-crosslinked gelatin membrane as wound-dressing material: in vitro and in vivo studies. *Journal of Biomaterials Science-Polymer Edition*. 2003;14(5):481-95.
75. Luo Y, Kirker KR, Prestwich GD. Cross-linked hyaluronic acid hydrogel films: new biomaterials for drug delivery. *Journal of controlled release : official journal of the Controlled Release Society*. 2000;69(1):169-84.
76. Roy N, Saha N, Kitano T, Lehocky M, Vitkova E, Saha P. Significant Characteristics of Medical-Grade Polymer Sheets and their Efficiency in Protecting Hydrogel Wound Dressings: A Soft Polymeric Biomaterial. *Int J Polym Mater*. 2012;61(1-4):72-88.
77. Chen X, Peng LH, Shan YH, Li N, Wei W, Yu L, et al. Astragaloside IV-loaded nanoparticle-enriched hydrogel induces wound healing and anti-scar activity through topical delivery. *International Journal of Pharmaceutics*. 2013;447(1-2):171-81.

78. Shukla A, Fang JC, Puranam S, Hammond PT. Release of vancomycin from multilayer coated absorbent gelatin sponges. *Journal of Controlled Release*. 2012;157(1):64-71.
79. Pawar HV, Tetteh J, Boateng JS. Preparation, optimisation and characterisation of novel wound healing film dressings loaded with streptomycin and diclofenac. *Colloid Surf B-Biointerfaces*. 2013;102:102-10.
80. Liu HW, Chaw JR, Shih YC, Huang CC. Designed hydrocolloid interpenetrating polymeric networks for clinical applications of novel drug-carrying matrix systems using Tris (6-isocyanatoethyl) isocyanurate and hydroxypropylmethylcellulose. *Bio-Med Mater Eng*. 2014;24(6):2065-72.
81. Kim J, Shin SC. Controlled release of atenolol from the ethylene-vinyl acetate matrix. *Int J Pharm*. 2004;273(1-2):23-7. Epub 2004/03/11.
82. Uslu I, Aytimur A, Serincay H. Preparation of PVA/PAA/PEG/PVP Nanofibers with HPMC and Aloe Vera. *Curr Nanosci*. 2013;9(4):489-93.
83. Ng KW, Achuth HN, Moochhala S, Lim TC, Hutmacher DW. In vivo evaluation of an ultra-thin polycaprolactone film as a wound dressing. *Journal of Biomaterials Science-Polymer Edition*. 2007;18(7):925-38.
84. Lam CX, Savalani MM, Teoh S-H, Hutmacher DW. Dynamics of in vitro polymer degradation of polycaprolactone-based scaffolds: accelerated versus simulated physiological conditions. *Biomedical materials*. 2008;3(3):034108.
85. Lei L, Liu X, Guo S, Tang M, Cheng L, Tian L. 5-Fluorouracil-loaded multilayered films for drug controlled releasing stent application: Drug release, microstructure, and ex vivo permeation behaviors. *Journal of controlled release : official journal of the Controlled Release Society*. 2010;146(1):45-53. Epub 2010/06/23.
86. Shahverdi S, Hajimiri M, Esfandiari MA, Larijani B, Atyabi F, Rajabiani A, et al. Fabrication and structure analysis of poly(lactide-co-glycolic acid)/silk fibroin hybrid scaffold for wound dressing applications. *International Journal of Pharmaceutics*. 2014;473(1-2):345-55.
87. Shemesh M, Zilberman M. Structure-property effects of novel bioresorbable hybrid structures with controlled release of analgesic drugs for wound healing applications. *Acta Biomaterialia*. 2014;10(3):1380-91.
88. Chen DD, Wu MD, Chen J, Zhang CQ, Pan TZ, Zhang B, et al. Robust, Flexible, and Bioadhesive Free-Standing Films for the Co-Delivery of Antibiotics and Growth Factors. *Langmuir : the ACS journal of surfaces and colloids*. 2014;30(46):13898-906.
89. Yoo HJ, Kim HD. Characteristics of waterborne Polyurethane/Poly(N-vinylpyrrolidone) composite films for wound-healing dressings. *Journal of Applied Polymer Science*. 2008;107(1):331-8.

90. Pritchard EM, Valentin T, Panilaitis B, Omenetto F, Kaplan DL. Antibiotic-Releasing Silk Biomaterials for Infection Prevention and Treatment. *Adv Funct Mater.* 2013;23(7):854-61.
91. Wang Y, Rudym DD, Walsh A, Abrahamsen L, Kim H-J, Kim HS, et al. In vivo degradation of three-dimensional silk fibroin scaffolds. *Biomaterials.* 2008;29(24):3415-28.
92. Ninan N, Muthiah M, Park I-K, Elain A, Wong TW, Thomas S, et al. Faujasites Incorporated Tissue Engineering Scaffolds for Wound Healing: In Vitro and In Vivo Analysis. *ACS Applied Materials & Interfaces.* 2013;5(21):11194-206.
93. Self S, Franzen L, Windbergs M. Overcoming drug crystallization in electrospun fibers - Elucidating key parameters and developing strategies for drug delivery. *International Journal of Pharmaceutics.* 2015;478(1):390-7.
94. Breitenbach A, Pistel KF, Kissel T. Biodegradable comb polyesters. Part II. Erosion and release properties of poly(vinyl alcohol)-g-poly(lactic-co-glycolic acid). *Polymer.* 2000;41(13):4781-92.
95. Xu X, Lee PI. Programmable Drug-Delivery From an Erodeable Association Polymer System. *Pharm Res.* 1993;10(8):1144-52.
96. Jeon JH, Thomas MV, Puleo DA. Bioerodible devices for intermittent release of simvastatin acid. *International Journal of Pharmaceutics.* 2007;340(1-2):6-12.
97. Sharath C. Sundararaj TDD, Mohanad Al-Sabbagh, Cheryl L. Rabek, Mark V. Thomas, David A. Puleo. Comparison of Sequential Drug Release In Vitro and In Vivo. [in revision].
98. Sundararaj SC, Thomas MV, Dziubla TD, Puleo DA. Bioerodible system for sequential release of multiple drugs. *Acta Biomaterialia.* 2014;10(1):115-25.
99. Sundararaj SC, Thomas MV, Peyyala R, Dziubla TD, Puleo DA. Design of a multiple drug delivery system directed at periodontitis. *Biomaterials.* 2013;34(34):8835-42.
100. Raiche AT, Puleo DA. Association polymers for modulated release of bioactive proteins. *IEEE Engineering in Medicine and Biology Magazine.* 2003;22(5):35-41.
101. Rabek C. VSR, Dziubla T.D., and Puleo D.A. . The Effect of Plasticizers on the Erosion and Mechanical Properties of Polymer Films. *Journal of Biomaterials Applications.* 2014;28(5):779-89.
102. Wypach G. *Handbook of Plasticizers.* Toronto, Ontario, Canada: ChemTec Publishing, William Andrew Inc; 2004.
103. Dittrich ESaM. Pharmaceutically Used Plasticizers. In: Luqman M, editor. *Recent Advances in Plasticizers: InTech;* 2012. p. 45-68.
104. Platzer N, Sears, and Darby. The Technology of Plasticizers. *Journal of Polymer Science: Polymer Letters Edition.* 1982;20(8):459-.

105. Cao X-L, Zhao W, Churchill R, Hilts C. Occurrence of Di-(2-Ethylhexyl) Adipate and Phthalate Plasticizers in Samples of Meat, Fish, and Cheese and Their Packaging Films. *Journal of Food Protection*<sup>®</sup>. 2014;77(4):610-20.
106. Zota AR, Calafat AM, Woodruff TJ. Temporal trends in phthalate exposures: findings from the National Health and Nutrition Examination Survey, 2001–2010. *Environmental health perspectives*. 2014;122(3):235.
107. Siegel SC. Overview of corticosteroid therapy. *Journal of Allergy and Clinical Immunology*. 1985;76(2):312-20.
108. USP Veterinary Pharmaceutical Information Monographs - Anti-inflammatories. *Journal of Veterinary Pharmacology and Therapeutics*. 2004;27:1-110.
109. Hawkey CJ. COX-1 and COX-2 inhibitors. *Best Practice & Research Clinical Gastroenterology*. 2001;15(5):801-20.
110. Cryer B, Feldman M. Cyclooxygenase-1 and cyclooxygenase-2 selectivity of widely used nonsteroidal anti-inflammatory drugs. *The American Journal of Medicine*. 1998;104(5):413-21.
111. Flora SJS. Structural, chemical and biological aspects of antioxidants for strategies against metal and metalloid exposure. *Oxidative Medicine and Cellular Longevity*. 2009;2(4):191-206.
112. Ratnam DV, Ankola D, Bhardwaj V, Sahana DK, Kumar MR. Role of antioxidants in prophylaxis and therapy: A pharmaceutical perspective. *Journal of Controlled Release*. 2006;113(3):189-207.
113. Rice-Evans CA, Miller NJ, Paganga G. Structure-antioxidant activity relationships of flavonoids and phenolic acids. *Free Radical Biology and Medicine*. 1996;20(7):933-56.
114. Hu Q, Noor M, Wong YF, Hylands PJ, Simmonds MS, Xu Q, et al. In vitro anti-fibrotic activities of herbal compounds and herbs. *Nephrology, dialysis, transplantation : official publication of the European Dialysis and Transplant Association - European Renal Association*. 2009;24(10):3033-41. Epub 2009/05/29.
115. Baowen Q, Yulin Z, Xin W, Wenjing X, Hao Z, Zhizhi C, et al. A further investigation concerning correlation between anti-fibrotic effect of liposomal quercetin and inflammatory cytokines in pulmonary fibrosis. *European journal of pharmacology*. 2010;642(1-3):134-9. Epub 2010/06/01.
116. Gomathi K, Gopinath D, Ahmed MR, Jayakumar R. Quercetin incorporated collagen matrices for dermal wound healing processes in rat. *Biomaterials*. 2003;24(16):2767-72.
117. Antoniu SA. Pirfenidone for the treatment of idiopathic pulmonary fibrosis. 2006.
118. Costabel U. Emerging potential treatments: new hope for idiopathic pulmonary fibrosis patients? *European Respiratory Review*. 2011;20(121):201-7.

119. Hewitson TD, Kelynack KJ, Tait MG, Martic M, Jones CL, Margolin SB, et al. Pirfenidone reduces in vitro rat renal fibroblast activation and mitogenesis. *Journal of Nephrology*. 2001;14(6):453-60.
120. Richeldi L, Yasothan U, Kirkpatrick P. Pirfenidone. *Nat Rev Drug Discov*. 2011;10(7):489-90.
121. Card JW, Racz WJ, Brien JF, Margolin SB, Massey TE. Differential Effects of Pirfenidone on Acute Pulmonary Injury and Ensuing Fibrosis in the Hamster Model of Amiodarone-Induced Pulmonary Toxicity. *Toxicological Sciences*. 2003;75(1):169-80.
122. Iyer SN, Gurujeyalakshmi G, Giri SN. Effects of Pirfenidone on Procollagen Gene Expression at the Transcriptional Level in Bleomycin Hamster Model of Lung Fibrosis. *Journal of Pharmacology and Experimental Therapeutics*. 1999;289(1):211-8.
123. Kaneko M, Inoue H, Nakazawa R, Azuma N, Suzuki M, Yamauchi S, et al. Pirfenidone induces intercellular adhesion molecule-1 (ICAM-1) down-regulation on cultured human synovial fibroblasts. *Clinical and Experimental Immunology*. 1998;113(1):72-6.
124. Shi-wen X, Eastwood M, Stratton RJ, Denton CP, Leask A, Abraham DJ. Rosiglitazone alleviates the persistent fibrotic phenotype of lesional skin scleroderma fibroblasts. *Rheumatology*. 2010;49(2):259-63.
125. Huxlin KR, Hindman HB, Jeon K-I, Bühren J, MacRae S, DeMagistris M, et al. Topical rosiglitazone is an effective anti-scarring agent in the cornea. *PLoS one*. 2013;8(8):e70785.
126. Sime PJ. The antifibrogenic potential of PPAR $\gamma$  ligands in pulmonary fibrosis. *Journal of Investigative Medicine*. 2008;56(2):534-8.
127. Daniels CE, Lasky JA, Limper AH, Mieras K, Gabor E, Schroeder DR. Imatinib treatment for idiopathic pulmonary fibrosis: randomized placebo-controlled trial results. *American journal of respiratory and critical care medicine*. 2010;181(6):604-10.
128. Daniels CE, Wilkes MC, Edens M, Kottom TJ, Murphy SJ, Limper AH, et al. Imatinib mesylate inhibits the profibrogenic activity of TGF- $\beta$  and prevents bleomycin-mediated lung fibrosis. *Journal of Clinical Investigation*. 2004;114(9):1308.
129. Distler JH, Jüngel A, Huber LC, Schulze-Horsel U, Zwerina J, Gay RE, et al. Imatinib mesylate reduces production of extracellular matrix and prevents development of experimental dermal fibrosis. *Arthritis & Rheumatism*. 2007;56(1):311-22.
130. Rosenbloom J, Mendoza FA, Jimenez SA. Strategies for anti-fibrotic therapies. *Biochimica et Biophysica Acta (BBA) - Molecular Basis of Disease*. 2013;1832(7):1088-103.
131. Breitbart AS, Ablaza VJ. Implant materials. *Grabb and Smith's Plastic Surgery, 5th Ed Philadelphia: Lippincott-Raven*. 1997:39-46.

132. Park H, Park K. Biocompatibility issues of implantable drug delivery systems. *Pharm Res.* 1996;13(12):1770-6.
133. Thummel KE, O'Shea D, Paine MF, Shen DD, Kunze KL, Perkins JD, et al. Oral first-pass elimination of midazolam involves both gastrointestinal and hepatic CYP3A-mediated metabolism[ast]. *Clin Pharmacol Ther.* 1996;59(5):491-502.
134. Thummel KE, Kunze KL, Shen DD. Enzyme-catalyzed processes of first-pass hepatic and intestinal drug extraction. *Advanced Drug Delivery Reviews.* 1997;27(2-3):99-127.
135. Chan LMS, Lowes S, Hirst BH. The ABCs of drug transport in intestine and liver: efflux proteins limiting drug absorption and bioavailability. *European Journal of Pharmaceutical Sciences.* 2004;21(1):25-51.
136. P. A. Glare TDW. Clinical Pharmacokinetics of Morphine. *Ther Drug Monit.* 1991;13(1-23).
137. Jeu L, Piacenti FJ, Lyakhovetskiy AG, Fung HB. Voriconazole. *Clinical Therapeutics.* 2003;25(5):1321-81.
138. Polisson R. Nonsteroidal anti-inflammatory drugs: Practical and theoretical considerations in their selection. *The American Journal of Medicine.* 1996;100(2, Supplement 1):31S-6S.
139. Yano H, Hirayama F, Kamada M, Arima H, Uekama K. Colon-specific delivery of prednisolone-appended  $\alpha$ -cyclodextrin conjugate: alleviation of systemic side effect after oral administration. *Journal of Controlled Release.* 2002;79(1-3):103-12.
140. Shelke NB AT. Synthesis and characterization of novel poly(sebacic anhydride-co-Pluronic F68/F127) biopolymeric microspheres for the controlled release of nifedipine. *Int J Pharm.* 2007;10(345):51-8.
141. Zhu Y MK, McGinity JW. Influence of plasticizer level on the drug release from sustained release film coated and hot-melt extruded dosage forms. *Pharm Dev Technol.* 2006;11(3):285-94.
142. Palmieri GF, Michelini S, Di Martino P, Martelli S. Polymers with pH-dependent solubility: Possibility of use in the formulation of gastroresistant and controlled-release matrix tablets. *Drug Development and Industrial Pharmacy.* 2000;26(8):837-45.
143. Kumar AR, Grewal NS, Chung TL, Bradley JP. Lessons From the Modern Battlefield: Successful Upper Extremity Injury Reconstruction in the Subacute Period. *Journal of Trauma-Injury Infection and Critical Care.* 2009;67(4):752-7.
144. Huang SJ SS, Feng TH, Sung KH, Lui WL, Wang LF. Folate-mediated chondroitin sulfate-Pluronic 127 nanogels as a drug carrier. *Eur J Pharm Sci.* 2009;12(38):64-73.



145. Tan Q, Liu W, Guo C, Zhai G. Preparation and evaluation of quercetin-loaded lecithin-chitosan nanoparticles for topical delivery. *International journal of nanomedicine*. 2011;6:1621-30. Epub 2011/09/10.
146. Elgindy N, Samy W. Evaluation of the mechanical properties and drug release of cross-linked Eudragit films containing metronidazole. *Int J Pharm*. 2009;376(1-2):1-6. Epub 2009/05/20.
147. Zheng X, Zhou S, Yu X, Li X, Feng B, Qu S, et al. Effect of in vitro degradation of poly(D,L-lactide)/beta-tricalcium composite on its shape-memory properties. *J Biomed Mater Res B Appl Biomater*. 2008;86(1):170-80. Epub 2007/12/29.
148. Baumgart F. Stiffness - an unknown world of mechanical science? *Injury-International Journal of the Care of the Injured*. 2000;31:14-23.
149. Bruggeman JP, de Bruin B-J, Bettinger CJ, Langer R. Biodegradable poly(polyol sebacate) polymers. *Biomaterials*. 2008;29(36):4726-35.
150. Lemperle G, Morhenn V, Charrier U. Human Histology and Persistence of Various Injectable Filler Substances for Soft Tissue Augmentation. *Aesthetic Plastic Surgery*. 2003;27(5):354-66.
151. Jeon JH, Puleo DA. Alternating release of different bioactive molecules from a complexation polymer system. *Biomaterials*. 2008;29(26):3591-8.
152. Wu L, Zhang J, Jing D, Ding J. "Wet-state" mechanical properties of three-dimensional polyester porous scaffolds. *Journal of biomedical materials research Part A*. 2006;76(2):264-71. Epub 2005/11/03.
153. Bodmeier R, Paeratakul O. DRY AND WET STRENGTHS OF POLYMERIC FILMS PREPARED FROM AN AQUEOUS COLLOIDAL POLYMER DISPERSION, EUDRAGIT RS30D. *International Journal of Pharmaceutics*. 1993;96(1-3):129-38.
154. Sastri VR. *Plastics in Medical Devices: Properties, Requirements, and Applications*. Burlington, MA: Elsevier Inc. ; 2010.
155. El-Gendy NA. *Pharmaceutical Plasticizers for Drug Delivery Systems*. *Curr Drug Deliv*. 2012;9(2):148-63.
156. Sevgi Güngör MSEaYÖ. *Plasticizers in Transdermal Drug Delivery Systems*. In: Luqman M, editor. *Recent Advances in Plasticizers: InTech*; 2012. p. 91-112.
157. Rahman M, Brazel CS. The plasticizer market: an assessment of traditional plasticizers and research trends to meet new challenges. *Progress in Polymer Science*. 2004;29(12):1223-48.
158. Finkelstein M, Gold H. Toxicology of the citric acid esters: Tributyl citrate, acetyl tributyl citrate, triethyl citrate, and acetyl triethyl citrate. *Toxicology and Applied Pharmacology*. 1959;1(3):283-98.
159. Kranz H, Ubrich N, Maincent P, Bodmeier R. Physicomechanical properties of biodegradable poly(D,L-lactide) and poly(D,L-lactide-co-glycolide) films in



- the dry and wet states. Journal of Pharmaceutical Sciences. 2000;89(12):1558-66.
160. Triethyl Citrate. [4/6/2012] Available from: <http://www.thegoodscentcompany.com/data/rw1012771.html>.
  161. Tributyl Citrate. [4/2/1012] Sciencelab.com. Material Safety Data Sheet; Available from: <http://www.sciencelab.com/msds.php?msdsId=9925302>.
  162. Béchard SR, Levy L, Clas S-D. Thermal, mechanical and functional properties of cellulose acetate phthalate (CAP) coatings obtained from neutralized aqueous solutions. International Journal of Pharmaceutics. 1995;114(2):205-13.
  163. Liu J, Williams lii RO. Properties of heat-humidity cured cellulose acetate phthalate free films. European Journal of Pharmaceutical Sciences. 2002;17(1–2):31-41.
  164. Chaibundit C, Ricardo NMPS, Ricardo NMPS, Muryn CA, Madec M-B, Yeates SG, et al. Effect of ethanol on the gelation of aqueous solutions of Pluronic F127. Journal of Colloid and Interface Science. 2010;351(1):190-6.
  165. Azeredo HMC, Mattoso LHC, Avena-Bustillos RJ, Filho GC, Munford ML, Wood D, et al. Nanocellulose Reinforced Chitosan Composite Films as Affected by Nanofiller Loading and Plasticizer Content. Journal of Food Science. 2010;75(1):N1-N7.
  166. Lee SB, Kalluri R. Mechanistic connection between inflammation and fibrosis. Kidney International. 2010;78:S22-S6.
  167. Margolis DJ, Allen-Taylor L, Hoffstad O, Berlin JA. Diabetic Neuropathic Foot Ulcers: The association of wound size, wound duration, and wound grade on healing. Diabetes Care. 2002;25(10):1835-9.
  168. Cierny GI, Byrd HS, Jones RE. Primary versus Delayed Soft Tissue Coverage for Severe Open Tibial Fractures: A Comparison of Results. Clinical Orthopaedics and Related Research. 1983;178:54-63.
  169. Guo S, DiPietro LA. Factors Affecting Wound Healing. Journal of Dental Research. 2010;89(3):219-29.
  170. M. Abercrombie MHF, and D. W. James. Collagen Formation and Wound Contracture during Repair of Small Excised Wounds in the Skin of Rats. J Embryol exp Morph. 1954;2(3):264-74.
  171. Vicentini FTMdC, Georgetti SR, Bentley MVLB, Fonseca MJV. Assessment of in vitro methodologies to determine topical and transdermal delivery of the flavonoid quercetin. Brazilian Journal of Pharmaceutical Sciences. 2009;45:357-64.
  172. Uhrich KE, Cannizzaro SM, Langer RS, Shakesheff KM. Polymeric Systems for Controlled Drug Release. Chemical Reviews. 1999;99(11):3181-98.
  173. Grassi M, Grassi G, Lapasin R, Colombo I. Understanding Drug Release and Absorption Mechanisms: A Physical and Mathematical Approach: Taylor & Francis; 2006.

174. ChamCarthy SP, Pinal R. Plasticizer concentration and the performance of a diffusion-controlled polymeric drug delivery system. *Colloids and Surfaces a-Physicochemical and Engineering Aspects*. 2008;331(1-2):25-30.
175. Medicott NJ, Tucker IG, Rathbone MJ, Holborow DW, Jones DS. Chlorhexidine release from poly(epsilon-caprolactone) films prepared by solvent evaporation. *International Journal of Pharmaceutics*. 1996;143(1):25-35.
176. Govender T, Stolnik S, Garnett MC, Illum L, Davis SS. PLGA nanoparticles prepared by nanoprecipitation: drug loading and release studies of a water soluble drug. *Journal of Controlled Release*. 1999;57(2):171-85.
177. Heller J. Controlled drug release from poly(ortho esters) — A surface eroding polymer. *Journal of Controlled Release*. 1985;2(0):167-77.
178. Heller J. Development of poly(ortho esters): a historical overview. *Biomaterials*. 1990;11(9):659-65.
179. Okarter TU, Singla K. The Effects of Plasticizers on the Release of Metoprolol Tartrate from Granules Coated with a Polymethacrylate Film. *Drug Development and Industrial Pharmacy*. 2000;26(3):323-9.
180. Kibria G, Roni M, Absar M, Jalil R-u. Effect of Plasticizer on Release Kinetics of Diclofenac Sodium Pellets Coated with Eudragit RS 30 D. *Aaps Pharmscitech*. 2008;9(4):1240-6.
181. Quality by Design for ANDAs: An Example for Modified Release Dosage Forms In: Administration FaD, editor. 2011.
182. Gutiérrez-Rocca J, McGinity JW. Influence of water soluble and insoluble plasticizers on the physical and mechanical properties of acrylic resin copolymers. *International Journal of Pharmaceutics*. 1994;103(3):293-301.
183. Triethyl Citrate [database on the Internet]. 2014. Available from: <https://scifinder.cas.org/scifinder/view/scifinder/scifinderExplore.jsf>.
184. Tributyl Citrate [database on the Internet]. 2014. Available from: <https://scifinder.cas.org/scifinder/view/scifinder/scifinderExplore.jsf>.
185. Pirfenidone [database on the Internet]. 2014. Available from: <https://scifinder.cas.org/scifinder/view/scifinder/scifinderExplore.jsf>.
186. Quercetin [database on the Internet]. 2014. Available from: <https://scifinder.cas.org/scifinder/view/scifinder/scifinderExplore.jsf>.
187. Walker EH, Pacold ME, Perisic O, Stephens L, Hawkins PT, Wymann MP, et al. Structural Determinants of Phosphoinositide 3-Kinase Inhibition by Wortmannin, LY294002, Quercetin, Myricetin, and Staurosporine. *Molecular Cell*. 2000;6(4):909-19.
188. Huang CL, Steele TWJ, Widjaja E, Boey FYC, Venkatraman SS, Loo JSC. The influence of additives in modulating drug delivery and degradation of PLGA thin films. *NPG Asia Mater*. 2013;5:e54.

189. Harte I, Birkinshaw C, Jones E, Kennedy J, DeBarra E. The effect of citrate ester plasticizers on the thermal and mechanical properties of poly(DL-lactide). *Journal of Applied Polymer Science*. 2013;127(3):1997-2003.
190. Jackson WJ, Caldwell JR. Antiplasticization. II. Characteristics of antiplasticizers. *Journal of Applied Polymer Science*. 1967;11(2):211-26.
191. Siepmann F, Le Brun V, Siepmann J. Drugs acting as plasticizers in polymeric systems: A quantitative treatment. *Journal of Controlled Release*. 2006;115(3):298-306.
192. Kunze C, Freier T, Kramer S, Schmitz KP. Anti-inflammatory prodrugs as plasticizers for biodegradable implant materials based on poly(3-hydroxybutyrate). *Journal of Materials Science-Materials in Medicine*. 2002;13(11):1051-5.
193. Li Y, Pang H, Guo Z, Lin L, Dong Y, Li G, et al. Interactions between drugs and polymers influencing hot melt extrusion. *Journal of Pharmacy and Pharmacology*. 2014;66(2):148-66.
194. Pongjanyakul T, Puttipatkhachorn S. Alginate-magnesium aluminum silicate films: Effect of plasticizers on film properties, drug permeation and drug release from coated tablets. *International Journal of Pharmaceutics*. 2007;333(1-2):34-44.
195. Paz Z, Shoenfeld Y. Antifibrosis: to reverse the irreversible. *Clinical reviews in allergy & immunology*. 2010;38(2-3):276-86. Epub 2009/06/24.
196. Wood KC, Boedicker JQ, Lynn DM, Hammond PT. Tunable Drug Release from Hydrolytically Degradable Layer-by-Layer Thin Films. *Langmuir : the ACS journal of surfaces and colloids*. 2005;21(4):1603-9.
197. Huang SJ, Sun SL, Feng TH, Sung KH, Lui WL, Wang LF. Folate-mediated chondroitin sulfate-Pluronic 127 nanogels as a drug carrier. *European journal of pharmaceutical sciences : official journal of the European Federation for Pharmaceutical Sciences*. 2009;38(1):64-73. Epub 2009/06/23.
198. Pinon-Segundo E, Ganem-Quintanar A, Alonso-Perez V, Quintanar-Guerrero D. Preparation and characterization of triclosan nanoparticles for periodontal treatment. *Int J Pharm*. 2005;294(1-2):217-32. Epub 2005/04/09.
199. Shelke NB, Aminabhavi TM. Synthesis and characterization of novel poly(sebacic anhydride-co-Pluronic F68/F127) biopolymeric microspheres for the controlled release of nifedipine. *Int J Pharm*. 2007;345(1-2):51-8. Epub 2007/07/10.
200. Sciencelab.com. Material Safety Data Sheet Tributyl Citrate. [3/1/2015]; Available from: <http://www.sciencelab.com/msds.php?msdsId=9925302>.
201. Meyers DB, Autian J, Guess WL. Toxicity of plastics used in medical practice II. Toxicity of citric acid esters used as plasticizers. *Journal of Pharmaceutical Sciences*. 1964;53(7):774-7.

202. Gerhardt P. Brucella suis in Aerated Broth Culture: III. Continuous Culture Studies. *Journal of Bacteriology*. 1946;52(3):283-92.
203. Paik MY, Bosworth JK, Smilges D-M, Schwartz EL, Andre X, Ober CK. Reversible Morphology Control in Block Copolymer Films via Solvent Vapor Processing: An in Situ GISAXS Study. *Macromolecules*. 2010;43(9):4253-60.
204. Simonsen AC, Hansen PL, Klösgen B. Nanobubbles give evidence of incomplete wetting at a hydrophobic interface. *Journal of Colloid and Interface Science*. 2004;273(1):291-9.
205. Ketoprofen. [3/1/2015]; Available from <http://www.drugbank.ca/drugs/DB01009>
206. Klose D, Siepmann F, Elkharraz K, Krenzlin S, Siepmann J. How porosity and size affect the drug release mechanisms from PLGA-based microparticles. *International Journal of Pharmaceutics*. 2006;314(2):198-206.
207. Berg MC, Zhai L, Cohen RE, Rubner MF. Controlled Drug Release from Porous Polyelectrolyte Multilayers. *Biomacromolecules*. 2006;7(1):357-64.
208. Kabiri K, Zohuriaan-Mehr MJ. Porous Superabsorbent Hydrogel Composites: Synthesis, Morphology and Swelling Rate. *Macromolecular Materials and Engineering*. 2004;289(7):653-61.
209. Reish RG, Eriksson E. Scars: A review of emerging and currently available therapies. *Plastic and Reconstructive Surgery*. 2008;122(4):1068-78.
210. Tidball JG. Inflammatory cell response to acute muscle injury. *Medicine and science in sports and exercise*. 1995;27(7):1022-32.
211. Cheryl L. Rabek TDD, and David A. Puleo. The Combined Effects of Drugs and Plasticizers on the Properties of Drug Delivery Films. [in revision].
212. Shientag LJ, Wheeler SM, Garlick DS, Maranda LS. A Therapeutic Dose of Ketoprofen Causes Acute Gastrointestinal Bleeding, Erosions, and Ulcers in Rats. *Journal of the American Association for Laboratory Animal Science*. 2012;51(6):832-41.
213. Lamon TK, Browder EJ, Sohrabji F, Ihrig M. Adverse Effects of Incorporating Ketoprofen into Established Rodent Studies. *Journal of the American Association for Laboratory Animal Science : JAALAS*. 2008;47(4):20-4.
214. Wallace\* JL, Bak† A, McKnight\* W, Asfaha\* S, Sharkey§ KA, MacNaughton§ WK. Cyclooxygenase 1 contributes to inflammatory responses in rats and mice: Implications for gastrointestinal toxicity. *Gastroenterology*. 1998;115(1):101-9.
215. Ziats NP, Miller KM, Anderson JM. In vitro and in vivo interactions of cells with biomaterials. *Biomaterials*. 1988;9(1):5-13.
216. Noh HK, Lee SW, Kim J-M, Oh J-E, Kim K-H, Chung C-P, et al. Electrospinning of chitin nanofibers: Degradation behavior and cellular response to normal human keratinocytes and fibroblasts. *Biomaterials*. 2006;27(21):3934-44.

217. Md. Mominur Rahman MSI, Nahid Sharmin, Jakir Ahmed Chowdhury, Reza-ul Jalil. Preparation and Evaluation of Cellulose Acetate Phthalate and Ethyl cellulose based Microcapsules of Diclofenac Sodium using Emulsification and Solvent-Evaporation Method. Journal of Pharmaceutical Sciences. 2010;9(1):39-46.
218. Reese ET. Biological Degradation to Cellulose Derivatives. Industrial & Engineering Chemistry. 1957;49(1):89-93.
219. Reese ET, Siu RGH, Levinson HS. THE BIOLOGICAL DEGRADATION OF SOLUBLE CELLULOSE DERIVATIVES AND ITS RELATIONSHIP TO THE MECHANISM OF CELLULOSE HYDROLYSIS. Journal of Bacteriology. 1950;59(4):485-97.
220. Göpferich A. Mechanisms of polymer degradation and erosion. Biomaterials. 1996;17(2):103-14.

## VITA

### PERSONAL INFORMATION

Place of Birth: Louisville, KY USA

### EDUCATION

University of Kentucky, Lexington, Kentucky, 2009  
B.S. Materials Engineering

### RESEARCH EXPERIENCE

National Science Foundation IGERT Graduate Trainee  
University of Kentucky, Lexington, KY, August 2009 – present  
Advisors: Dr. D.A. Puleo, Department of Biomedical Engineering, Dr. Thomas Dziubla, Department of Chemical and Materials Engineering

Graduate Research Assistant, Department of Biomedical Engineering,  
University of Kentucky, Lexington, KY, August 2009 – present  
Advisors: Dr. D.A. Puleo, Department of Biomedical Engineering, Dr. Thomas Dziubla, Department of Chemical and Materials Engineering

Independent Research, Department of Chemical Engineering  
University of Kentucky, Lexington, KY, August 2008 – December 2008  
Advisor: Dr. J. Zach Hilt, Department of Chemical and Materials Engineering

### AWARDS/HONORS:

NSF-IGERT Fellow (August 2010 – present)  
Graduate Certificate in Bioactive Interfaces and Devices (December 2011)

### PUBLICATIONS:

Rabek C., Van Stelle R., Dziubla T.D., and Puleo D.A. The Effect of Plasticizers on the Erosion and Mechanical Properties of Polymer Films. *Journal of Biomaterials Applications*. 2014; 28(5):779-89

Rabek C., Dziubla T.D., and Puleo D.A. The Combined Effects of Drugs and Plasticizers on the Properties of Drug Delivery Films in preparation for submission. *Journal of Bioactive and Compatible Polymers*. (2015)

Rabek C., Perry E., Dziubla T.D., and Puleo D.A. Mechanical Properties and Sequential Release from a Multilayered Drug Delivery Film in preparation for submission. (2015)

Sundararaj SC, Al-Sabbagh M, Thomas MV, Dziubla TD, Rabek CL and Puleo DA. Comparison of *In Vitro* and *In Vivo* Sequential Drug Release in preparation for submission. *Journal of Controlled Release*. (2013)

#### **PROFESSIONAL CONFERENCE PRESENTATIONS:**

Rabek C. L., Dziubla, T.D., and Puleo, D.A. "Sequential Release of Two Drugs from Flexible Drug Delivery Films". Presented at the Society for Biomaterials, April 2014, Denver, CO.

Rabek C. L., Dziubla, T.D., and Puleo, D.A. "Sequential Release of Two Drugs from Flexible Drug Delivery Films". Presented at the Pacific Rim International Congress on Advanced Materials and Processing, August 2013, Waikoloa, HI.

Rabek C. L., Dziubla, T.D., and Puleo, D.A. "How Different Drugs Affect the Mechanical Properties, Erosion, and Release Profiles of Drug Delivery Films." Presented at the Annual Meeting of the Society For Biomaterials, April 2013, Boston, MA.

Rabek C. L., Dziubla, T.D., and Puleo, D.A. "The Effect of Plasticizers and Drug on the Erosion and Release Profiles of Drug Delivery Films". Presented at the Annual Meeting of the Society For Biomaterials, October 2012, New Orleans, LA.

Rabek C. L., Dziubla, T.D., and Puleo, D.A. "The Effect of Plasticizers and Drug on the Erosion and Release Profiles of Drug Delivery Films". Presented at 4th Annual Biomaterials Day, September 2012, Lexington, KY.

Rabek C. L., Dziubla, T.D., and Puleo, D.A. "The Effect of Plasticizers and Drug on Drug Delivery Films", Presented at 3rd Annual Biomaterials Day, October 2011, West Lafayette, IN.

Rabek, C.L., Dziubla, T.D., and Puleo, D.A. "The Effect of Plasticizers and Drug on Drug Delivery Films". Presented at the Society For Biomaterials Annual Meeting and Exposition, April 2011, Orlando, FL.

Rabek, C.L., Dziubla, T.D., and Puleo, D.A. "Effect of Plasticizers on the Properties of Drug Delivery Films". Presented at the 2nd Annual Biomaterials Day, November 2010, Cleveland, OH.

Rabek, C.L., Dziubla, T.D., and Puleo, D.A. "Effect of Plasticizers on the Properties of Drug Delivery Films" Presented at the Biomedical Engineering Society annual meeting, October 2010, Austin, TX.